**TAL
TECH**

TALLINN UNIVERSITY OF TECHNOLOGY
SCHOOL OF ENGINEERING
Department of Electrical power Engineering and Mechatronics

SYSTEM SIMULATION OF AN ELEVATOR

LIFTI SÜSTEEMI SIMULATSIOON

MASTER THESIS

Student:	Diwakar Kumar Gupta
Student code:	194357MAHM
Supervisor:	Kari Tammi – Associate Professor Aalto University
Co supervisor:	Kristjan Pütsep – Lecturer, Taltech

Tallinn 2021

AUTHOR'S DECLARATION

Hereby I declare, that I have written this thesis independently.

No academic degree has been applied for based on this material. All works, major viewpoints and data of the other authors used in this thesis have been referenced.

"18" May 2021

Author: Diwakar Kr. Gupta ……………………………
/signature /

Thesis is in accordance with terms and requirements

"18" May 2021

Supervisor: Kari Tammi……………………………..
/signature/

Accepted for defence

" …..".………………….2021.

Chairman of theses defence commission: …………..…………………………………..
/name and signature/

Non-exclusive Licence for Publication and Reproduction of GraduationTthesis¹

I, Diwakar Kumar Gupta (date of birth: 22/05/1994)

hereby

1. grant Tallinn University of Technology (TalTech) a non-exclusive license for my thesis

"System simulation of an elevator'',

supervised by

Kari Tammi – Associate Professor, Aalto University,

(*Supervisor's name*)

1.1 reproduced for the purposes of preservation and electronic publication, incl. to be entered in the digital collection of TalTech library until the expiry of the term of copyright;

1.2 published via the web of TalTech, incl. to be entered in the digital collection of TalTech library until the expiry of the term of copyright.

1.3 I am aware that the author also retains the rights specified in clause 1 of this license.

2. I confirm that granting the non-exclusive license does not infringe third persons' intellectual property rights, the rights arising from the Personal Data Protection Act or rights arising from other legislation.

---

¹ *Non-exclusive Licence for Publication and Reproduction of Graduation Thesis is not valid during the validity period of restriction on access, except the university`s right to reproduce the thesis only for preservation purposes.*

_____ (*signature*)

_____ (*date*)

Department of Electrical Power Engineering and Mechatronics
THESIS TASK

Student: Diwakar Kumar Gupta 194357MAHM

Study programme,   MAHM02/18 – Mechatronics

Main speciality: Automation, Robotics and control Engineering

Supervisor(s): Kari Tammi – Associate Professor, Aalto University

Co supervisor: - Kristjan Pütsep –Lecturer, Taltech

Consultants: D.Sc. (Tech) Gabriela Roivainen, KONE Corporation

Thesis topic:

(in English)   System simulation of an Elevator

(in Estonian)   Lifti süsteemi simulatsioon

Thesis main objectives:

1. Design of a sample hoisting virtual model inside SimulationX.
2. Unknown Parameter estimation in hoisting model & its real time functioning.
3. Analysis of HIL deployment and stability of the model inside HIL.
4. Decrease the software testing time of drive and wider testing.
5. Hoisting Model validation.

Thesis tasks and time schedule:

No	Task description	Deadline
1.	Training of SimulationX software	April-June 2020
2.	Modelling of elevator model inside Simulation X	June-Sep.2020
3.	Determination of elevator parameter and sensitivity analysis	October 2020
4.	Testing of Model performance inside the Beckhoff	Nov-Dec. 2020
5.	HIL Model Deployment & stability of the model	Dec.-Jan 2021
6.	Validation of 1d model and thesis Writing	Jan- March
7.	Submission of the thesis	May 2021

Language: English   **Deadline for submission of thesis:** "18" May 2021

Student: Diwakar Kr Gupta   /signature/   "18" May 2021

Supervisor: Kari Tammi   /signature/   "18" May 2021

Co supervisor: Kristjan Pütsep   /signature/   "18" May 2021

Consultant: Gabriela Roivainen   /signature/   "18" May 2021

Head of study programme: Prof. Mart Tamre ....   "18" May 2021
/signature/

Abstract

Simulation is a powerful method for simulating the behaviour of nearly every system and it is increasingly being used in testing. Characterisation of physical testing involves the use of mechanical systems. However, in increasing cases, it is now possible to adequately describe portions of the test specimen using mathematical models. Consequently, test systems that divide the specimen into a physical and a virtual part, where the virtual part consists of real-time simulation, are used. One such powerful technique which connects physical hardware device and virtual prototype is HIL simulation. HIL simulation interacts in real-time and allows the possibility to interface MBS models with actual hardware in a virtual space. This provides the flexibility to test control parameters in a variety of operation settings without physical prototypes. This research aims to develop an elevator model inside the Beckhoff unit and using HIL simulation technique that improve the quality of software, and to reduce the testing time.

This paper highlights the operational Dynamics of an MBS elevator, which demonstrates how a system simulation is connected with MBS dynamics, and also how the modelling of a simple hoisting and a general framework for HIL system analysis is developed. The elevator model was created inside SimulationX, and their FMU was loaded inside the Beckhoff for HIL. The simulation model was looped with the drive then used in the HIL test rig using Jenkins and C.I for drive software testing. The elevator simulation has been done using HIL that improved the elevator's lifetime and has minimised its cost. Measured results of test rigs of the real-time capable synchronisation model were verified and compared with the real elevator.

Multibody dynamics is used to investigate the effect of incorporating non-linearity and discontinuity into a HIL system. The overall system simulation of the elevator using the HIL technique has increased the test accuracy, efficiency and has increased automated testing. The model provided realistic results with the time-step size of the HIL test rig. However, the results are good in the 1D model and, but investigation and stability of the 3D model are still being investigated.

Keywords- Multibody dynamics, Virtual prototype, Motion-Motor control, FMU, HIL, C.I, Software testing and Vibration analysis.

CONTENTS

LIST OF FIGURES

9

LIST OF TABLES

PREFACE

The idea for this project originates from the KONE oy Hyvinkää HIL Laboratory. KONE provided the opportunity to conduct this research and to present it as my master thesis. This project started during the COVID-19 pandemic, and it served as something to focus on and rely on the time of crisis. As in this time when work from home is next to normal, it would have been difficult to carry out my research but KONE provided all the necessary help required to complete this project. It gave me a chance to challenge myself and be responsible for difficult situations as well. The KONE never gave up their attitude, despite many obstacles and failures, which lead to the success of this project.

Not only does this project enhance my technical knowledge of mechatronics, signal processing, simulation, drives, and system engineering but it also taught me the importance of teamwork, the role of devotion to work, and self-discipline. I also understood the importance of diversity as a team working on this project has different backgrounds and expertise. This is something I am going to have to deal with every day in the workplace.

After many years of working with various professionals in different parts of India, I have made much strong decision so, when KONE offered me this project, I was delighted to accept the project. However soon the pandemic was all over the world, which proved to be the biggest obstacle. KONE's hard and dedicated team did not give up and accepted the challenge and started this project with twice as much as the same determination, which boosted my confidence to complete the project with sheer determination and hard work. I was optimistic and focused on my work with full dedication and commitment to thinking about the situation. All these difficulties and situations not only made me more independent and stronger than before and prepared me for any difficult time, but also made this project and research a success

My special thanks go to Gabriela Roivainen for her scientific guidance, versatile practical support, and her objective leadership on this research project. I would also like to thank head of System Engineering Team Viita-aho Tarvo for providing guidance and leadership on this project and for making me part of his hardworking and dedicated team. Further thanks go to the other members of the KONE HIL team, Salomäki Janne who always assisted me in HIL laboratory and collecting previous data, and several fruitful discussions that we have had during this period.

LIST OF ABBREVATIONS

- AIA- American Institute of architects
- CPU- Central Processing Unit
- C.I- Continuous Integration
- C.W- Counter Weight
- DOF- Degree of freedom
- DUT- Device Under Test
- DZS- Door Zone Sensor
- EBOi -Emergency Battery Operation (internal battery)
- EBDi - Emergency Battery Drive (internal battery)
- FBD- Free body diagram
- FPM- Feet per minute
- FMI/FMU- Functional Mockup Interface/unit
- GUI- Graphical user interface
- HIL – Hardware in the loop
- LBS- Pound
- LHS- Left-hand side
- MAP- Maintenance Access Panel
- MBS- Multibody System
- MIL- Model in the loop testing
- MSB- Main Safety Controller
- PCB- Power Circuit Board
- PI- Proportional Integral
- PID- Proportional Integral derivative
- PD- Proportional Derivative
- PLC- Programmable Logic Controller
- PMSM- Permanent magnet synchronous motor
- PWM- Pulse width Modulation
- RHS- Right-hand side
- RPM- Revolution Per Minute
- SE- System Engineering
- SD- Spring Damper
- SRT- Software Release Testing
- TTS- Trip Transfer Switch
- VFD- Variable Frequency Drive
- VTS- Vertical transportation system

LIST OF SYMBOLS

F_a Acceleration force

a   Acceleration

T_{mn} Actual load

ω Angular Velocity

m_g All moving linear equivalent masses

α Angle of wrap of the forces

σ_{B1} Bearing force at nominal speed

m_{c0} Compensation error

E   Elastic modulus

v_{nom} Elevator nominal speed

h_{nom} Elevator shaft height

σ_F Friction forces

Ws   Fundamental frequency

u   Model Vector

Q_R Rated load

h   Step size

t_a Start or stop (acceleration) time

m_n System imbalance

T_{mn} Torque

m_{c1} Unit mass of travelling cable

P_{out} Output power

Z   Vibration

σ_W Wind drag force at nominal speed

λ Eigen Value of stiffness

1 INTRODUCTION

The proportion of people living in cities is continuously increasing and, as a result, the demand for housing and elevators is also increasing steadily. Cities are growing, leading to high demand for living space within the city. The limited land area of these cities, especially the residential elevator, is quite expensive and needs affordable and long-lasting solutions. Buildings require a sophisticated vertical transport system, the backbone of which is elevators. KONE, one of the largest manufacturers of elevators globally, aims to provide efficient solutions for the smooth flow of people in buildings. So, this research aims reduce the software testing time by replacing manual testing with automatic testing runs, that is going to be possible through system simulation. A virtual prototype of an elevator model will be created and deployed in one of the testers for drive software testing.

The research includes creating an elevator system (Multibody) model using SimulationX software, and the dynamics of the multibody elevator system will be simulated. Currently, the model is hand-coded inside the Beckhoff elevator. The new model is optimised for action in real-time where experimenting with the model and its validation is most important part. This research involves potentially necessary model reductions and optimisation for real-time capabilities. It will help improve the elevator system as well as the automotive industry. The proposed elevator to be created will use new technology to enable the system's smooth flow, speed, and accuracy.

The elevator dynamics will be created with the aid of mechanical, electrical, and control systems. The model will be used for elevator development and testing, focussing on improving the test accuracy using hardware in the loop that will do more and more manual testing to be automatic by decreasing testing time using hardware in the loop(HIL), increasing the elevator lifetime by simulating and mitigating malfunctions.

This model should enable the developer to evaluate elevator car dynamics, the interaction of subsystems and their impact on product performance at an early stage. By collecting other parameters while simultaneously testing the simulation, the model fidelity will be high. Any additional effect can be examined during testing, reducing future errors and improving the elevator drive software testing. Moreover, the model will have lateral vibration, reducing the time taken to calculate the data. It is one of a kind of digital transformation in the elevator industry. After developing the elevator model inside the Beckhoff unit, more accurate software testing of the elevator drive has been possible, which will decrease the testing time of the drive from week to hours.

Also, it will cover more comprehensive testing, but the HIL testing will ensure the accuracy of the system and increase the lifetime of an elevator.

Problem statement

The simulated hoisting in the current systems is modelled through the Beckhoff programme code. It is not only expensive [1] but also tricky to change the physical elevator motor (PMSM) if one needs to increase the elevator's acceleration [2]. In addition, any software update of the drive would come at the cost of time as the drive software needs to be rigorously tested to establish its functionality.

This thesis will address the following research questions.

1) How to decrease the testing time of drive software.
2) How to enable automated testing and increase the lifetime of an elevator.
3) How to enable the testing of real-time elevator cycle while testing fault behaviour.
4) How to improve the previous elevator model.
5) How to change and test different parameters of the elevator shaft without changing the actual component
6) How to make the elevator safer for its use worldwide by accurate releveling after reducing the sag and bounce.

Objective of the research

The objective of this research is to increase the test accuracy of drives by using hardware in the loop, and the aim is to develop the elevator model inside the Beckhoff unit in order to deliver more accurate and broader software testing for the drive.

Subgoals:
- Find Unknown parameter estimation
- Designing of hoisting machine inside SimulationX software
- Stability of the Model and Real-time simulation of the Model
- Comparing the result of the Real model and Virtual prototype model
- Validation of the model
- Increase the lifetime of an elevator
- Decrease the testing time of drive software

Overview

The thesis deals with the model build-up, parameterisation, validation, calculation of relevant variables in different scenarios, model partitioning, and code generation. KONE is providing all necessary parameter data for modelling, testing and validation. KONE operates HIL systems for commissioning and testing motor; the test system contains an electric motor, Beckhoff system (Embedded Pc), shaft simulator, and frequency converter.

The thesis primarily focuses on understanding the theory, the validation of parameters, understanding the model project, Model preparation inside SimulationX, Sensitivity analysis, model running & its behaviour, and finally, validation of the model compared with the actual result.

The thesis is divided into two parts: the first part is about model preparation, and the second is about Model deployment inside the Beckhoff. This thesis is limited to building the model and its validation. However, as part of the project, it is the author's responsibility to thoroughly understand Beckhoff and implement it.

Thesis structure

The thesis is divided into eight chapters, which complies of many sections, item and sub-item. The first chapter begins with an introduction, problems, and objective. In chapter two, a literature review of past research has been done concerning the topic. In chapter three, the theory behind the elevator simulation and dynamics, their hypothesis, how electrical, mechanical component is connected and how it relates to SimulationX. chapter four covers the technical background that covers all technical details such as MONO 500, system simulation and HIL. The Elevator Model is defined in Chapter 5, along with all of the components that were created using SimulationX software. chapter six highlights the methodology and describe how the work has been finished, where it is discussed how the elevator model was deployed inside the Beckhoff. In Chapter seven, I have validated the model and compare the results between the original laboratory model and the virtual SimulationX model where The model has been validated with more than twelve cases. Finally, at the end, the summary and conclusion of the thesis are mentioned.

2 LITERATURE REVIEW

Existing Method

Before starting this thesis, the author went through the previous elevator model (MONO700) and its document where the model was prepared for the high-rise market segment. The author then went through many articles and scientific results related to system simulation/engineering, hardware in the loop, Modelling of Virtual elevators in various software, Modelling in SimulationX software, and Beckhoff. This section briefly describes the research work that is related to the topic.

- Hardware in the loop
- Multibody dynamics of an elevator
- Model deployment inside Beckhoff.
- Software/automated testing

The Project HIL team decided to prepare the Elevator model and simulate it using hardware in the loop. Earlier elevator simulation has been done using SIMIO software [3], SIMIO is a discrete simulation tool recently developed by the same authors as ARENA. Due to its similarity to ARENA-the most widely used general simulation tool globally, the SIMIO tool was preferred over others. High and low-intensity scenarios can benefit from lower dwell time. As a result, few clients or many other calls on other floors can attend. In medium-intensity scenarios, the longer the time of residence improves the performance of the system. Values enhance the importance of retrieving data from the site where the elevator system is being implemented to have a good customer demand idea.

In the Previous MONO 700 elevator has been simulated through the same SimulationX Software [4] in which the project involves the development of the elevator system model. This enables the user to evaluate the elevator car's dynamics, subsystems' interaction, and their impact on the product's performance at an early stage. Models created in SimulationX were linked to existing KONE models via various interfaces. The Functional Mock-Up Interface (FMI) as an independent model exchange and co-simulation tool was the most common approach that was being used. Other techniques, such as export as an S-Function for MATLAB / Simulink, are also available.

FEM models may be imported into SimulationX as reduced flexible bodies. The model was designed modularly, making it easy to exchange model parts for more detailed or simplified versions to increase accuracy or minimise computation time.

The real motion control algorithm has been implemented via the FMU to ensure the elevator's correct actuation by changing certain boundary conditions of the elevator's operation, and reasonable behaviour of the model has been verified. Thus, during development, the model was used to find the elevator's core parameters or test new system configurations. Still, there was a stability issue. Also, it was not tuned for real-time operation. In this thesis, the author will fix these limitations by finding the unknown parameter, repairing the stability issue, and adjusting it for real-time operation.

Multibody simulation has become a standard tool for the design process in the various automotive industry. Modern simulation packages like SIMPACK offer a wide range of modelling possibilities where railway vehicles' simulation has been done [5]. Current simulation packages offer modelling elements that are highly adapted for standard and unusual simulation scenarios. Where in the article gives an overview of state of the art in railway vehicle simulation. Calculation times are made short to allow complex examinations. The model was not stable.

In the Paper ¨Development of advanced driver assistance systems with vehicle hardware-in-the-loop simulations,¨ a full-scale ADAS-prepared vehicle is set up in equipment on top of its reproduction [6]. Climate case dynamometer is utilised to copy street collaboration and automated vehicles to speak to other traffic. The controlled climate helps in the presentation and dependability of the ADAS. This is tried to a severe level of unwavering and precision quality. The working standard and the additional estimation of VEHIL were shown by the test consequences of the versatile journey control and the forward crash notice framework. The situation of VEHIL in the ADAS advancement measure was delineated based on the 'V' chart. A new VEHIL idea for testing ADASs has been introduced in the paper, where an actual savvy vehicle is worked in a HIL climate. VEHIL is appropriate for different ADASs: ACC, 588 O. Giete link et al. stop-and-go, FCW, pre-crash frameworks, vulnerable side frameworks, and completely independent vehicles. The test results for ACC and FCW exhibit VEHIL that has an additional incentive in a few periods of the improvement cycle of an ADAS: sensor check, quick control prototyping, model approval, work level approval, adjusting of control calculations, creation close down tests, and readiness of test drives. For these purposes, VEHIL tests are acted in a reproducible, exact, and controllable approach to establish an agent test climate.

The tests can be performed proficiently as compared to external test drives. The test situations can be changed effectively because of the association with the fundamental re-enactment environment. With a higher trust in the framework, resulting test drives would then be able to be performed. This is possible as the ADAS has just been altogether tried in VEHIL. VEHIL is not intended to supplant MIL re-enactments, and test drives shape a productive connection between them. It was shown how to open FMI standards could accomplish the trading of models among the elaborate devices.

KONE had simulated an elevator model previously for an acoustic model of the elevator using a hybrid approach [7], The approach is based on a hybrid model, which mainly combines the finite element method for the elevator's deterministic parts, such as the sling, with the statistical energy analysis used in the modelling process. Both plates' behaviour with a large surface somewhat randomly reacts and affects noise Control treatments and leaks. The hybrid approach will also allow the simulation to cover relatively high-frequency areas above 200 Hz, which, in the present case, can be calculated by (FEM) only with unreasonably high computational effort.

Competitors work

KONE competitors like Schindler and TKE (earlier known as ThyssenKrupp) are currently using elevator simulation to improve elevator performance and to do the digital transformation in the elevator industry but there is not so much detail about their elevator simulation and HIL testing mentioned anywhere. As the competitors are working to improve the overall structure of elevator and automation testing, the company also do not want to lag in this field. In Figure 1, Schindler has presented their way of HIL testing, where they are trying to replace the test tower and engineer with one HIL simulator, as the way of testing is shifting from physical testing to a model-based approach where drives and all the mechanical component such as rope, car, etc is getting replaced by the virtual prototype. Virtual drive and the mechanical system allow changing any configuration.

Figure 1. Schindler HIL from physical testing to Model-based approach [8].

Recently TKE earlier known as ThyssenKrupp has also announced one such project, In Figure 2 where they are working on a rope-free elevator using system modelling, where they will do the performance evaluation, load calculation and also working on safety for overall better elevator performance for a better journey.

Figure 2. Thyssenkrupp- HIL System modelling for rope-free elevator [9].

Improving Existing Method through Technology

For the proper functioning of an elevator, there should be stability and accuracy in the power used in the system. The online method can identify power impedances to ensure that the system works normally to maintain this stability and accuracy. The new technology uses a system called Wideband System Identification (WSI) technique. This digital processing technique works differently from the current methods in the simulation of hardware. The current method involves the parametrisation of parametric impedance. Stability and accuracy in the power system are helpful as they can help the elevator system to work without failure. The digital technique helps improve accuracy as it helps in testing the actual DUT. Some of the benefits received from the digital processing technique include detecting delays, non-linearity, sensing errors, and preventing power amplifier [10]. The best method for accuracy and stability tracking in hardware simulation is the Damping Impedance Method (DIM).

The stability of power is an important aspect of hardware simulation. When delays are reduced in the functioning of hardware, the power stability will be maintained. The existing method uses continuous-time transfer functions to assess the stability in the PHIL system. However, this method is found not to be applicable in a real-life situation as it does not capture aspects such as numerical discretization and sample and hold effects [11]. As such, the digital method where new technology is used in maintaining the stability of power in the PHIL system is better. As mentioned above, using new technology is good as it helps in reducing time wastage and accuracy as well as power stability. Stability is enhanced when the DUT and Robot operating system (ROS) is connected. The connection should be at an angle of 180° for all the frequencies used in the connection [12].

The elevator models used in the other projects are not tuned for real-time operation. Potentially required model reductions and optimisation for real-time capability are part of this project. The project will be implemented for a MONO500 test bench, adapting models built for MONO700 in the previous high-rise building [13].

The model is reduced to achieve real-time. The created model in SimulationX has its own set of libraries or can be linked together with existing models at KONE via different interfaces. An essential part of the project is assessing the model performance and identifying performance bottlenecks; this may result in a project outcome that the existing Beckhoff hardware's performance is not adequate for the task [14].

Test model performance will be done outside of the test benches. Then the resulting draft models are deployed on-site together with engineers. In the future, the project

team intends to virtualise the test further, eventually replacing the motors in the test benches with HIL simulation models [15], [16].

The definition of a strategy and roadmap for this process is proposed in this document. When attempting to add rope elasticity and rope slip to the current hand-coded models. These problems could not be solved in the past.

Outlined below are areas the author seeks to improve the overall structure of the model.

- Balance and accuracy: In the article, the researcher was not able to put the balance between accuracy and performance [10], Here the author is going to set a shaft angle that will simulate the car in a particular position. It has been assured while modelling the elevator model in SimulationX.

- Stability: The stability issue has always been a major concern due to inherent delays within the interface devices [11],[12]. The time delay of HIL signal, lack of performance of hardware and the control signals was always getting some phase shift that leads to instability but here author will try to improve the stability by testing the model outside the test bench.

- Design of elevator model: In the other software model such as MATLAB and by other researchers [17], it was not that much computable; the earlier model has not so much actual physics component as much as SimulationX, this software has made it easy to design the MBS model.

- Real-time: Any previous elevator model was not tuned for real-time [18] and it was not fully feasible to achieve the HIL test with Real-time simulation l, but the SimulationX model has real physics element like spring and damper that will tune the model for real-time.

- Sag and Bouncing: Car sag and bouncing is one of the significant problems of customer around the world; that has always been a real issue for all the major elevator industries, and they have never overcome it, but here due to feasible real-time element, it is possible to get the exact re-levelling.

- Sensor Functionality: Sensor functionality at different part was not in the previous model. The sensor has been installed at different parts to record the behaviour early.

- Power consumption: In all the earlier project research, power was the critical question and power consumption used to be too much, but here in this research author is going to work on how to reduce the power consumption.

- Automating testing: In KONE many of the tests are manual that is very time consuming, it is the first time when it is targeted to do fully automating testing in place of manual testing.

- Parameter Variation: In the earlier project at KONE, and the research it was not possible to change the parameter in the middle of a test but here any simulation engineer can able to change the parameter while testing.

- Deployment of FMU (elevator model) inside the Beckhoff: It was not feasible to do in another project, other researcher used to do it on another test bench which is making this very costly. Previously available HIL equipment has some limitation on simulation performance

- Noise Reduction: In many kinds of research, the focus was to decrease the noise level but as It is known from [19], [20] The signal processing is associated with identification, structure as well as modelling, the resultant output of signal processing is mostly distorted and contain some noisy that is why noise reduction the removal of channel distortion are important parts of a signal processing system, in this thesis, the author only focuses on decreasing the vibration from the motor.

- HIL for High rise building: HIL for High rise building: It has not been done yet, but in the future, it might be possible to implement in high rise building too. High-rise building constructions are characterised by a small number of hoisting equipment and many construction resources to be hoisted. Therefore the configuration parameters should be more carefully planned with quantitative methods before being applied to high-rise building constructions [21].

- HIL Deployment- The overall structure of the HIL component and testing will be improved as the research has been focussed on each hardware and software component to improve the overall testing experience as this HIL technique so far has been used in automotive industry HIL, first-time HIL is going to be used in the elevator industry.

- Replacement of physical motor: it is not yet possible to change the physical elevator hardware motor through a virtual prototype motor, but the HIL technique will open the way to replace the motor too [22].

Amongst the problem mentioned above, apart from HIL for High rise building, the replacement of physical motor in the virtual prototype model, and Noise, the author will do work on everything in this research. Next, the theory behind the simulation will be discussed in the next chapter where it is shown the importance of elevator simulation and how the simulation works and how it has benefitted the elevator ride. The mathematical model of an elevator system and the equations of motion of the complete elevator system are derived and explained.

3 THE THEORY BEHIND THE SIMULATION.

The development of the elevator points out interest in elevator control a long time ago. The elevators' simulation is becoming more versatile and efficient, and elevator simulation styles have been evolving for several years. Complexity was written and implemented.

Simulation has been evolved from a control prototyping tool to a system modelling that has combines many advantages of both physical and virtual prototyping. The elevator aims to convert the motor's initial electrical power into mechanical power that the machine can use. Both the electrical and mechanical industries work together to make it easy and convenient to run elevators. Without electrical control, mechanical components are useless. The mechanical section of elevators includes service the mechanical parts to assemble components and installations. In contrast, the electrical section involves electric motor i.e., operate in close loop velocity control [23]. The electrical section of elevators includes electrical wiring of brakes and motors, wire the panel into a circuit board or machine that would provide instructions on how long and how easy it to run for an engine that powers the elevator mechanism.

The elevator purposes of transforming the motor's initial electrical power operate into mechanical power used by the machine. The elevator's most common design is the cable-driven elevator, where a car is raised and lowered by steel cables. The machines' muscle is mounted at the top of the elevator shaft. Its ropes are attached to the vehicle, and a pulley with grooves is looped around a sheave to grip the ropes linked to an electric motor. One way the elevator car goes up, turn the engine. As the motor turns the other way, it goes down. A traction elevator installation's critical component is the vehicle, cable elevator unit, control equipment, C.W(counterweight), hoistway, rail penthouse, and pin; more detailed description has been given in chapter 5.

Increasingly complex and detailed simulation models are becoming more difficult due to ongoing advances in software and computer technology. A virtual prototype of an elevator model can solve accurate simulations varying the parameters and evaluate the elevator behaviour. The multibody modelling of the elevator system will be created inside SimulationX, and it will be simulated. Here, all of the experiments are carried out with a 2:1 roping configuration. A general hoisting model of 2.1 rope ratio has been shown in Figure 3. The roping ratio with all the detail configuration has also been shown in Figure 28.
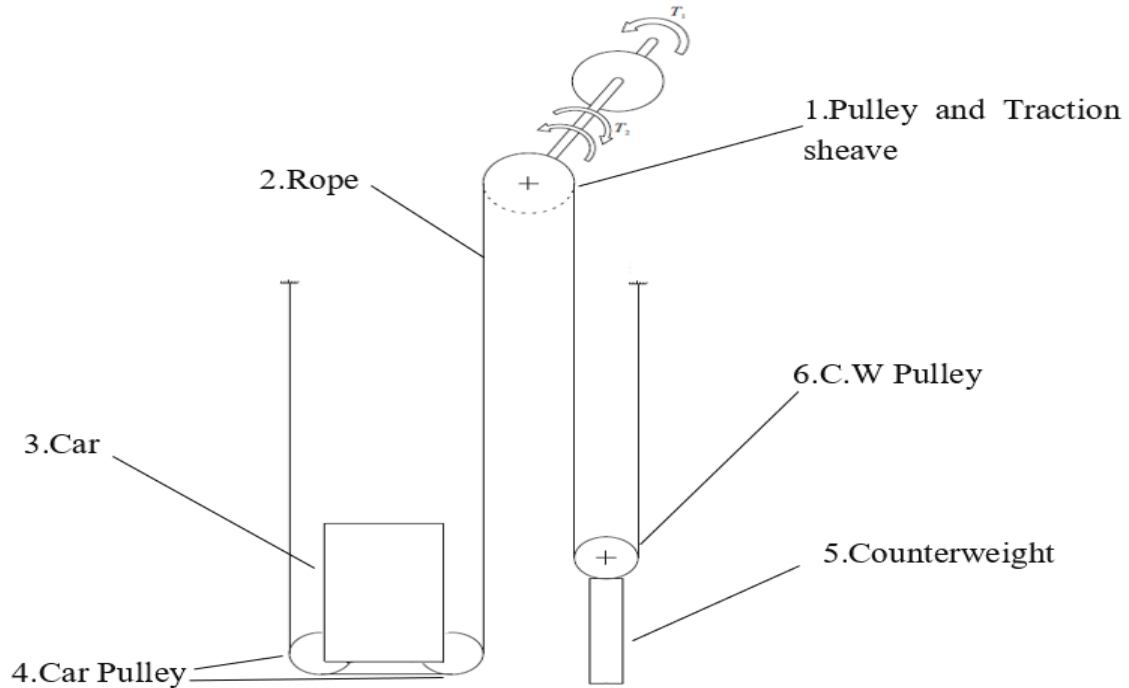
Figure 3. Current Hoisting Model of 2.:1 Ratio in HIL. 1)Pulley 2) rope 3) car Pulley 4) Car Pulley 5) Counterweight 6) C.W Pulley.

The engine for the elevator machine will be either an AC motor or a DC motor. To control the DC motor, strong starting torque and ease of speed are required. Due to its ruggedness and simplicity, an AC motor is used more often. The engine is selected depending on the design purpose for the elevator. Many factors that directly affect the elevator performance such as Rated load, rated speed, group size, acceleration, jerk and, Door type etc. Motor RPMs (Revolution per minute) are determined from the elevator's required travel speed. Rated speed is the speed of the elevator that decrease the travelling time. The information that is needed is

$$n = \frac{V_{lin}*Roping}{(\pi*Dtr)*60} \text{ [RPM]} \tag{3.1}$$

Where V_{lin} – Speed of linear movement, m/s

Roping- Roping ratio for Rope

Dtr   - Traction sheave diameter, r

n   -   Motor RPM speed

The power required to get the shaft in motion is equal to the power required to overcome static or stationary friction and accelerate the weight from rest to complete speed. The power output is calculated with the following data:

$$P_{out} = T_{mn} * \omega \ [W] \tag{3.2}$$

Where T_{mn} -   Torque output, Nm

   ω -   Angular Velocity, rad/s

The elevator consists of a motor and, most of the time, a worm gear reducer. A worm gear system comprises a worm gear, usually referred to as a worm, and a larger round gear commonly referred to as a worm gear. Rotational pulleys perpendicular to each other can decrease rotational pulley speed and change the rotational plane. By reducing the rotation speed using the gear reducer, the output torque is increased to lift larger objects for the diameter of a given pulley. Both ends of the elevator rope can be made in a possible arrangement to anchor to the overhead beam in a possible arrangement. In this case, the height of the elevator shaft/car can be calculated using the following formula:

$$h_0 = \frac{1}{2} h_{nom} \tag{3.3}$$

Where h_{nom} - Elevator shafts height, m

   h_0 -   Total Height

When the elevator is at its lowest, it means at the ground, than the height of the elevator shaft 'h_{nom}' become zero. Which leads the elevator torque also becomes zero.

A C.W is on the other end of the section to offset the weight of the car, usually approximately half of a fully charged passenger elevator so that on the average ride two of them are perfectly balanced. All the motors necessary to move the vehicle provide the impetus for switching one way to the other, consequently reduce the torque provided by the machine. The elevator car and the counterweight are attached to free moving sweaters. The pulley is attached to the tractor pulley. The traction drive is the way to convert the input mechanical power (in this case, a shaft) to useful mechanical power in the system (the vertical movement of the elevator). The friction between the cords and the sheave grooves, cut on the lid, initiates the force of traction between the traction drive and the rope. At this stage, the friction force can be expressed as

$$F_f(v) = v \cdot \sigma_F \tag{3.4}$$

Multiple friction forces oppose the motion of elevators. Such as wind force and bearing force. Wind and bearing force can be calculated, which is acting on elevators:

$$F_W(v) = v \cdot \sigma_W \cdot \left(\frac{v}{v_{nom}}\right)^2 \tag{3.5}$$

$$F_B(v) = v \cdot \sigma_{B0} \cdot \left(\frac{v}{v_{nom}}\right)^2 \tag{3.6}$$

Where v_{nom} - Elevator nominal speed, m/s

σ_W - Wind drag force at nominal speed, N

σ_{B0} - Bearing force at nominal speed, N

Combining all these forces, they form a combined frictional force that cannot be neglected during the evolution of ascent because the elevator will eventually fall if its factors are neglected. The combined frictional force is the sum of small friction, wind and bearing force can be expressed as.

$$F_F(v) = F_f(v) + F_W(v) + F_B(v) \tag{3.7}$$

Where $F_f(v)$- Friction force, N

$F_W(v)$ – Wind Force, N

$F_B(v)$ – Bearing force, N

$F_F(v)$ – Combine overall force, N

For the elevator, the first observer is kinetic, which estimates the angular positions, speeds, and acceleration of links by utilising the pellet's acceleration constraint equations, which play a role as a system model. An appropriate set of acceleration measurements to provide information on the acceleration of all connections used as model inputs.

The second observer, called a dynamic observer, estimates the excavation, the payload and the forces of action using dynamic model elevators as an inverse dynamic model. The kinematic estimate by the cinematic observer plays the role of the system inputs. The measurement or the known actuation force used to calculate the observatory corrections as the output variables.

While the kinematic observer is not dependent on the dynamic observer, it depends on the cinematic observer, and therefore must be operating simultaneously. The kinematic strength is observed as:

$$F_K(a, h) = \left(m_g + \frac{1}{2} \cdot (h - h0_1) \cdot m_{c1}\right) \cdot a \tag{3.8}$$

Where a - The acceleration of the shaft, m/s^2

        h - the height of the shaft, m

        m_g - moving linear equivalent masses, kg

        m_{c1} - a unit mass of travelling cable.

When one can observe the effect of kinematic forces on elevator movement. Then another force cannot be ignored. That force is Potential force can be expressed as.

$$F_P(h) = (m_n + (h - h0_0) \cdot m_{c0}) \cdot g \qquad (3.9)$$

Where m_n - System imbalance,

        m_{c0}- Compensation error.

        g - Gravity

        F_P - Potential force, N

When the traction drive is rotated, the power from the traction drive is transferred to the elevator and counterweight. Traction sheet power is required only to move the uneven load between the lift and counterweight. To calculate traction sheet torque before sheave power is using these formulae.

$$T_{TS} = (F_F + F_k + F_P) \cdot \frac{r_{TS}}{R} \qquad (3.10)$$

 Where F_k- Kinetic force, J

There is a transfer of power throughout the elevator system. Electrical power put into the motor is equal to:

$$P = \frac{VI}{\sqrt{2}} \text{ (For an AC motor)} \qquad (3.11)$$

Where V - Voltage

      I - AC source, A

This power is then transferred through the output of the motor shaft,

$$P = T\omega \qquad (3.12)$$

Where

$$\omega = v \cdot \frac{R}{r_{TS}} \qquad (3.13)$$

$$P_{TS} = T_{TS} \cdot \omega \qquad\qquad (3.14)$$

Where P_{TS} – Power of shaft, N/m

T_{TS} – Torque, N.m

ω – rotational speed of the shaft, (1/s)

The motor shaft speed is controlled to achieve good ride quality [23]. The power transmission via the gear reducer reduces the output speed and the torque is higher. The overall power will be slightly lower as the system is not 100% efficient. Tension on the rope from the elevator pulley is equal to its weight. The tension on the counterweight seam is W.C.

Generally, the efficiency of the geared machine for motor and gearbox assembly is 60 per cent. This efficiency was estimated at 2500 lbs(Pound)., which corresponds to a regular lift of 1.75 m/s. However, in this model, project estimation is to achieve 1m/s.

When the car moves the engines, it will only work for one object; both the car and counterweight will be fixed to guide the tracks inside the shaft. They will stop everything from swinging back and forth to take a backup set of wheels if something goes wrong with the hydraulic fluid and the brake will automatically be released. Technically, on the ropes of this steel, it is enough to hold both the car and counterweight and the remainder of it for back-up in case a snapshot is made. Next to the engine is a governor with his pulley and separate cable attached to the car. There are two spring-laden metal hooks called 'fly weights' inside the governor if a car falls freely and the governor spins over too quickly, centrifugal force spins out the hooks, stops hooks on a fixed inner band, stops the rope pulley on the governor's arm and locks brakes.

When the elevator starts or stops, the speed or deceleration force can be expressed with an equation of motion and the constant speed force.

$$F_a = m. \; (v_1 - v_0) \, / \, t_a \qquad\qquad (3.15)$$

Where F_a - Acceleration force, N

v_1 - Final velocity, m/s

v_0 - Initial velocity, m/s

t_a - Start or stop (acceleration) time (s).

The following analysis was done for continuous operation (no acceleration). The force on the pulley is equal to the difference in the two tensions exerted on both sides. This

force is equal to the user on the one side, and it is C.W on the other side. The net force on the pulley (the drive pulley) is, Therefore:

$$F = (W_e - W_c)/2 \qquad (3.16)$$

Where W_e- Force on one side of rope, N

W_c – Force on the C.W side, N

To find the required power to move the elevator, it must be known as either the rotational speed of the drive shaft (connected to the pulley) or the speed of the elevator. The power output is (assuming 100 per cent efficiency),

$$P = \frac{(W_e - W_c).V}{2} = \frac{(W_e - W_c). \, r\omega}{2} \qquad (3.17)$$

Where r - radius of the pulley, r

Force strain curve can be modelled by a 3rd-degree polynomial

$$F(\varepsilon) = k_1\varepsilon + k_2\varepsilon^2 + k_3\varepsilon^3 \qquad (3.18)$$

Where ε scalable variable calculated from $t \in [t_1 \, t_2]$

k is spring constant

The elastic modulus is the quantity that helps in measuring how an object can resist a given force that can deform it elastically. It ensures that a system usually operates with failure. As such, it can help an elevator maintain normal speed and accuracy during operations [24].

$$m_c\gamma_n\sin(\gamma_n l) - m\cos(\gamma_n l) = 0 \qquad (3.19)$$

$$f_n = \frac{1}{2\pi}\gamma_n\sqrt{\frac{EA}{m}} \qquad (3.20)$$

Rotatory stiffness,

$$k = \frac{E \, A}{l_{rope}} \cdot \frac{d^2}{4} \qquad (3.21)$$

$$k_{rot} = \frac{\widetilde{EA}}{l_{rope}} \cdot \frac{d^2}{4}$$

$$\text{Rotatory damping } b = \frac{b_s}{l_{rope}} \cdot \underbrace{\frac{d^2}{4}} \tag{3.22}$$

average value of EA = 10^6 N (Pa)

Where F_n- natural frequency, Hz

L- length of rope, m

E- Young's modulus, N/m²

A- cross-sectional area, m²

d- diameter. m

The properties of stiffness and damping, Maximum stiffness & damping used inside the elements, which are parameterized according to ropes: Rope elements, Spring Damper shaftSD, Slip inside traction sheave. The tension of the rope increases the value of EA increases as well [24].

Figure 4 shows the Rope parametrisation done in SimulationX, for real-time calculation, some additional parameter has been added in parametrization to limit the stiffnesses and damping in SimulationX. The parametrization is an example how the values are given in the SimulationX parametrization is done like python scripting has been shown in Appendix1 as it is easier to write in that way and understand it.

Ropes			
Elastic modulus (steel rope PAWO F3)	eSteelRope:	80000	N/mm²
Cross sectional area (complete rope)	crossSectionArea:	pi*8*8/4/1000^2	m²
Number of ropes	numberRopes:	4	
Axial Stiffness	EA:	eSteelRope*crossSectionArea*numberRopes	N
Maximum Effective Rope Stiffness	maxRopeStiffness:	3e6	N/m
Damping coefficient	coeffDamping:	1	-
Specific Damping	specificDamping:	150000000	Ns/m
Axial Damping	bRope:	coeffDamping*specificDamping*crossSectionArea*r	Ns
Linear Density (mi/l)	rhol:	0.28*self.numberRopes	kg/m

Figure 4. Rope parametrization.

The Hamilton principle [25],[26] to derive the equation of motion of the complete elevator system is stated as [27]

$$\int_{t_1}^{t_2} (\delta Q' - \delta\Pi + \delta W_{dc})dt = 0 \qquad (3.23)$$

Where δ' - Kinetic energy, J

   Π - Potential energy, J

   W_{dc} - Work due to non conservative forces acting upon the system, J

   T_1 and T_2 - Intial and Final time, s

The model is considered conservative when it is derived that is why work due to non-conservative forces is neglected between t_1 and t_2.

The following equation in a matrix form describes the vertical response of the car, compensating sheave and counterweight in terms of the modal parameters that have been transformed into model coordinates that correspond to three longitudinal modes of the system [27].

$$\vec{S} = [S_1 S_2 S_3]$$

$$\ddot{\vec{S}}(t) + [\dot{C}]\dot{\vec{S}}(t) + [P]\vec{S}(t) + [Y]T(\vec{\sigma}1 + \vec{\sigma}2) + [Y]T(\vec{F} + \vec{\eta}) = 0 \qquad (3.24)$$

Where $[Y]$ = mass normalised mode shape matrix

$$C = \begin{bmatrix} \omega_1^2 & 0 & 0 \\ 0 & \omega_2^2 & 0 \\ 0 & 0 & \omega_3^2 \end{bmatrix} \qquad (3.25)$$

$$P = \begin{bmatrix} 2\zeta_1\omega_1 & 0 & 0 \\ 0 & 2\zeta_2\omega_2 & 0 \\ 0 & 0 & 2\zeta_3\omega_3 \end{bmatrix} \qquad (3.26)$$

Longitudinal natural frequencies (ω_1, ω_2, ω_3) can be estimated by obtaining the eigenvalues with characteristics equation defined by 3.24. The coefficients ζ_1, ζ_2, ζ_3 represent the three longitudinal modal damping ratios of the system [27].

The state of a system in which an abnormally large vibration is produced in response to an external stimulus, which occurs when the frequency of the stimulus is the same, or nearly the same, is known as resonance; as the natural frequency is when a system vibrates when there is no force to drive it. It can be due to different thing sometimes, it is due to too much damping or may be due to coincide of different natural frequencies.

In the elevator, the natural frequency is become when the system moves without being driven by power. It depends on the stiffness of the system. Once the elevator has been

set in motion, it can make a natural movement without exerting force to push it. Apart from stiffness, the natural frequency depends on the mass of the system. It can be calculated from boundary value condition or eigenvalue problem. As In high rise building, there is an infinite number of natural frequency [28]. Here the residential elevator is considered so only till 150 Hz natural frequency has been considered. Usually, electromagnetic torque ripple exists around 90Hz and the main cogging torque frequency around 180 Hz [23]. Frequency would be lower than 150 Hz when the car reaches the nominal speed. However still, there are chances of a crash, where the two different natural frequency of different parameters like rope, that leads to large resonance and impact dynamic behaviour of elevator it can interrupt elevator service sometime even damage the component of an elevator. Usually, the car vibrates, particularly at those excitation frequencies close to the natural frequencies of the elevator system model, so it is important to analyze the natural frequency [29]. A number of discrete mass points can specify the number of degrees of freedom (DOF) of the system, the number of natural frequencies, and mode shapes that are being considered. The natural frequencies obtained from the eigenvalue problem can be expressed as[30]

$$\omega_n = \sqrt{\lambda_n} \qquad (3.27)$$

Where, λ_n is nth eigenvalue of the spectral matrix

The natural frequencies and mode shapes of the system have been calculated. the eigenvalues problem that determines the natural frequencies and mode shapes of the system is stated as

$$-K_u = M\omega^2 \, \mu \qquad (3.28)$$

Where u- the modal vector

$\quad$ μ - friction

$\quad$ ω – fundamental frequency, Hz

Longitudinal natural frequencies can be estimated by obtaining the eigenvalues with characteristics equation [27]

$$(K_M - \lambda I) = 0 \qquad (3.29)$$

Where λ – Eigenvalues of stiffness

$\quad$ I- $\quad$ Identity matrix

$$K_m = \begin{bmatrix} \frac{k^{u1}}{M_1} & \frac{k^{u2}}{M_1} & 0 \\ \frac{k^{u1}}{M_2} & \frac{k^{u2}}{M_2} & \frac{k^{u3}}{M_2} \\ 0 & \frac{k^{u1}}{M_3} & \frac{k^{u3}}{M_3} \end{bmatrix} \hspace{2cm} (3.30)$$

The most crucial phase of undertaking dynamic analysis includes measuring natural frequencies and their corresponding elastic-structured shapes in damp free, unforced vibration. Mode shapes and natural frequencies are needed for any type of vibration analysis. Various studies insist on increasing natural frequencies, and mass increase causes its decrease [31].
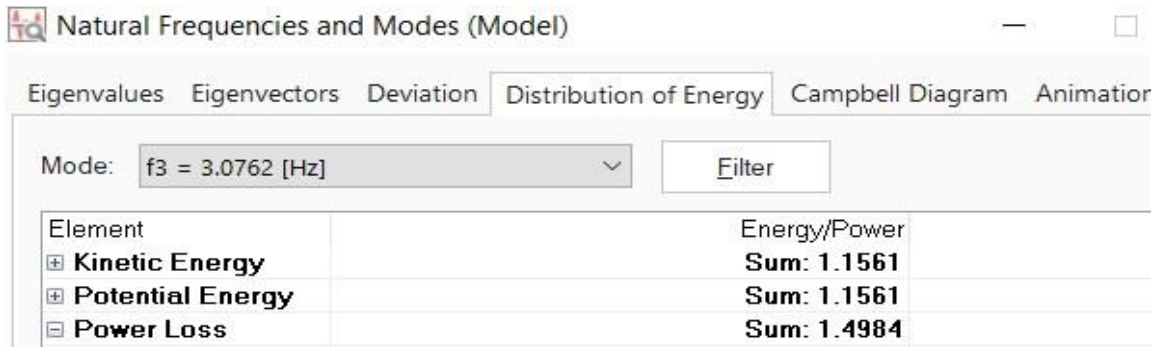
Figure 5. Natural Mode and frequency in SimulationX software.

The structure's deformed shape at a natural frequency is known as vibration mode. Figure 5 shows the natural frequencies and distribution of energy in SimulationX, where it is possible to calculate energy, including power loss of each component. The frequency of the first mode is a fundamental frequency abbreviated as f_0. Kinetic energy is due to load and C.W but P.E and power loss is mainly due to mounting motor, which are shown in Appendix 5.

Mass of travelling cable added as variable mass depending on the position; it has been used to balance the weight of a car, which is useful in calculating the vertical position of the car.

$$m_{comp} = \left(l_0 + \frac{y_{fix, \, elev}(t)}{2} \right) \cdot \rho_{l, \, cable} \hspace{2cm} (3.31)$$

With $\hspace{2cm} l_0 = \frac{l_{cable} - y_{fix, \, shaft}}{2} \hspace{2cm} (3.32)$

after putting the value of l_0 in m_{comp} in equation 2.18

$$m_{comp} = \left(\frac{l_{cable} - y_{fix, \, shaft} + y_{fix, \, elev}(t)}{2} \right) \cdot \rho_{l, \, cable} \qquad (3.33)$$

Elastic ropes & slip-on traction sheave pulley, where $F_{friction}$ is getting calculated by

$$F_{friction} = \min{(F_{K1}, F_{K2})} \cdot (\exp(\mu_i \beta) - 1) \qquad (3.34)$$

Where, $\beta = 180°$, Angle of contact (calculated internally)

$\mu = 0.19$, Static or sliding friction coefficient

Figure 6, shows the pulley where slip calculation between pulley and belt is shown
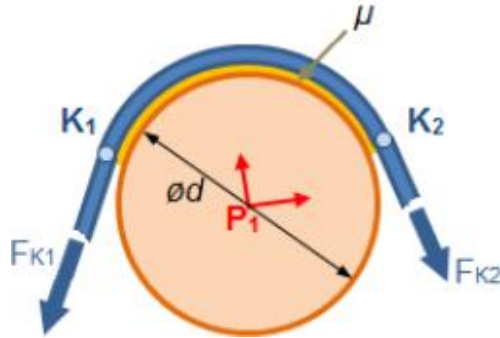
Figure 6. Pulley slip.

Slip is an action upon pulley and belt. Slip calculation between pulley and belt with Euler-Eytelwein approach [32],[33], shown in Figure 7 that has been considered while calculating friction torque:

$$T_{friction} = F_{friction} \cdot d/2 \qquad (3.35)$$

Where friction is acting at the circumference of the pulley.

According to the Euler-Eytelwein approach [33], there are two parameters of influence, one is friction coefficient μ and other is contact angle β. Slip shows a slight speed difference between rope and traction sheave, which is observable in the MBS model. Figure 7 shows the parametrisation of the belt and pulley. Figure 7 shows the parametrisation of rope where diffent value and formale has been used.
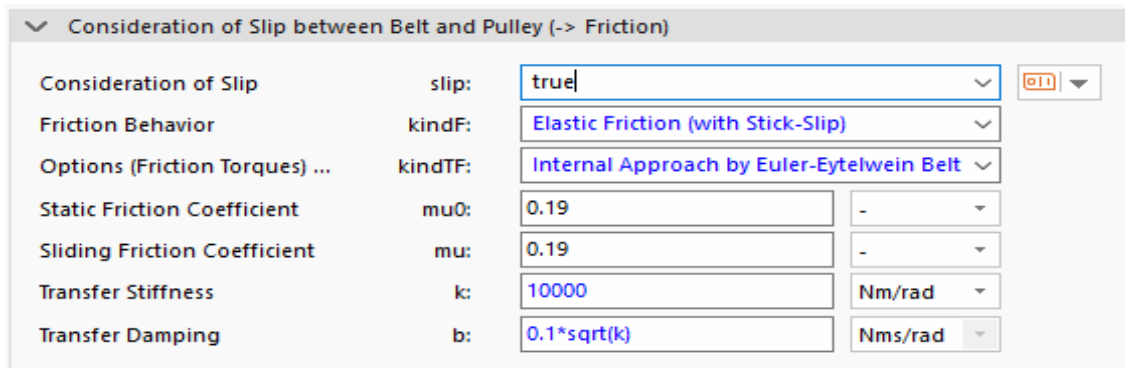
Figure 7. Parametrisation of slip between belt and pulley in SimulationX.

Traction drive systems are designed to operate across a range of system design parameters. Estimation of frictional charcateristics of traction system is one of the most important step in any kind of physical model of elevator [34] and the traction calculation can be possible via inequality formulae that has been originated from Euler-Eytelwein approach [33], [34] are applied.

For traction mentioned during normal condition or Car loading and emergency braking conditions

$$\frac{T_1}{T_2} \leq e^{f\alpha} \tag{3.36}$$

For traction to be lost during Car/C.W stalled conditions or resting on the buffer

$$\frac{T_1}{T_2} \geq e^{f\alpha} \tag{3.37}$$

Where α, angle of wrap of the ropes on the traction sheave

T_1 and T_2 forces in the ropes situated at either side of the traction sheave, N

f is the friction factor, which depends on μ , and geometry of Rope-sheave contact configuration.

In stalled condition, car and C.W resting on the buffers and the machine rotating in the ''down/up'' direction where protection against raising of the car or C.W is provided by limiting of traction.

Emergency braking condition; The dynamic ratio T_1/T_2 has to be evaluated for the worst-case depending on the position of the car in the well and the conditions (empty or with rated load). Each moving element should be considered with its proper rate of acceleration, considering the receiving ratio of installation.

In no case, the rate of acceleration to consider will be less than

0,5 m/s^2 for normal case

0,8 m/s^2 when reduced stroke buffers are used.

Car stalled condition; The static ratio T_1/T_2 must be evaluated for the worst-case depending on the position of the car in the well and the load conditions (empty or with rated load). Rated load, speed estimate of frictional characteristics of traction system, and maximum acceleration under normal and emergency conditions are among the most important parameters during the fundamental designing of a simple hoisting model.

Car Sag defined from the difference between unloaded and loaded car position. Traction between a sheave and the rope arrangement rendered by the elevator system allows for desired car movement. Damping, elasticity and the extended length roping characteristics drive an elevator to sag, oscillate or bounce based on a change in load, when the system's rise is sufficiently large when the elevator car is landing [35], [36]. Car sag acquired by measuring car position relative to landing door position before and after loading. Car bounce is measured using an EVA accelerometer. Vertical acceleration (Z) is used to analyse damping time and bounce frequency. Bounce is measured by stepping out from an elevator. Acceptance conditions for car sag and bounce have been declared as less than 2 mm is excellent and damping time is less than 1 second in order to ensure customer satisfaction. Car sag of more than 5 mm, and damping time of more than 3 seconds are considered as unacceptable. The car sag models use a specifically calculated axial stiffness EA for the ground floor position to account for rope non-linearity:

$$EA = 0.6 * eSteelRope * crossSectionArea * numberRopes \qquad (3.38)$$

Equation 3.38 has been shown in Figure 4, where this equation has been used during parametrisation inside thye software. The calculation of this adapted stiffness can be comprehended in the model using this approach; the EA value is changing depending on the position. The formula of mass excitation for a single passenger stepping in an elevator:

$$m(\mu) = \begin{cases} \frac{1}{2}(3\mu - \mu^3), \mu \leq 1 \\ m_c, \text{otherwise} \end{cases} \qquad (3.39)$$

Where $\mu = t/t_{sat}$

μ is the scaled time with force saturation time t_{sat} and m_c is mass of a single person. Saturation time (t_{sat}) used in is 0,5 seconds

The formula of mass excitation for a single passenger stepping out elevator calculated using Hermite interpolation [37]:

$$F(\xi) = H_1(\xi)m_1 + H_2(\xi)m_2 \qquad (3.40)$$

Where m_1 - Masses at time instances at t_2 , Kg

m_2 - Masses at time instances at t_1 , kg

Hermite polynomials H_1 and H_2 are written as

$$H_1(\xi) = \frac{1}{4}(2 - 3\xi + \xi^3)$$

$$H_2(\xi) = \frac{1}{4}(2 + 3\xi - \xi^3)$$

Where ξ - scalable variable calculated from $t \in [t_1 \ t_2]$

Excitation Mass is activation of Sagload for StepIn time and StepOut is the analogue behaviour for step out the case. Car sag has been validated in section 7.2.1

Radial magnetic forces at the machine air gap could be an addition of torque ripple [23] The radial magnetic force per unit area at any point of the air gap is obtained by using Maxwell's stress tensor theorem [38], [24] given a

$$\text{Prd}\ (\theta, t) = \frac{1}{2\mu 0}\{B_N^2(\theta, t) - B_t^2(\theta, t)\} \qquad (3.41)$$

Where θ – rotation angle w.r.t axis of symmetry of machine

μ0 - the magnetic permeability

t - the time, s

B_n- the normal components of the magnetic field around the air gap.

B_{tg} - the tangential components of the magnetic field around the air gap.

W_s- fundamental frequency, Hz

The machine torque ripple and the radial forces generated at the machine air-gap between the stator and the rotor [23]; It is possible to compute through FEM simulation. The drive system comprises a permanent magnet synchronous motor powered via an inverter that supplies a pulse width modulated (PWM) voltage [24]. The PMSM has 16 poles with a stator of 48 slots. The corresponding excitation frequency twice the fundamental one, $2W_s$, and it is the main harmonic of the radial force at constant pressure. For analysing the set-up of a three-phase synchronous machine, a mathematical transformation is known as direct quadrature zero(dq0) transformation is used [39], [23].

As the dq0 transform is applied to balanced three-phase circuits, the three AC quantities are reduced to two DC quantities. The inverse transform can then be used to recover the real three-phase AC effects using simplified calculations on these theoretical DC quantities [23].

According to reference frame transformation theory [39], The three-phase variables, currents and voltages, are converted to the dq reference frame, which rotates at the stator current frequency [23], The dq components of the currents and voltages are kept constant this way.

At the machine, friction and energy losses occur. The parameter C_{sh} accounts for viscous friction and other potential energy losses at the machine. A rough estimate of its value was obtained by using the following equation, which is satisfied during the constant velocity stage when $m_c = m_w$ and vibrations of the opposite inertial elements are neglected [29].

$$\frac{\tau}{r} - C_{sh} \cdot \theta r - C_w \cdot \theta r - C_c \cdot \theta r = 0 \qquad (3.42)$$

Where τ- the torque measured at the corresponding travel, Nm

θ - shaft velocity

C_{sh} – Friction and energy loss, watt

The value obtained is around 3 Nms.

Next, Elevator simulation is carried out by using software tools. Lumped-parameters discretization (spring-mass model), the Rayleigh-Ritz method [40] or nonlinear finite elements can be utilized for modelling rope inertia and weight [41].

All the equation mentioned above has been computed employing software SimulationX. Parametrisation in SimulationX described in Appendix 1. Getting the simulation result is easy just like MATLAB. One can get the simulation result just by dragging the cursor (drag and drop). The Following Figure 9, shows elevator Vertical direction, speed, Lateral Acceleration and change in kinetic energy respectively. The First graph in Figure 9 shows the relationship between displacement and time; displacement is maximum till t=14 s; after that it started coming down and at t= 35 s it reaches the ground floor. This vertical displacement is getting calculated with the help of equation 3.18 Second graph at right shows that vertical velocity is maximum at t = 0 to t = 15 s and 35 to 45 s when the car is on the seventh floor and the car is at the ground floor respectively. The velocity profile is composed of acceleration and deceleration stages and a constant velocity stage when the system travels at around 1 m/s, which is happening between t= 15 s to t= 32 s.
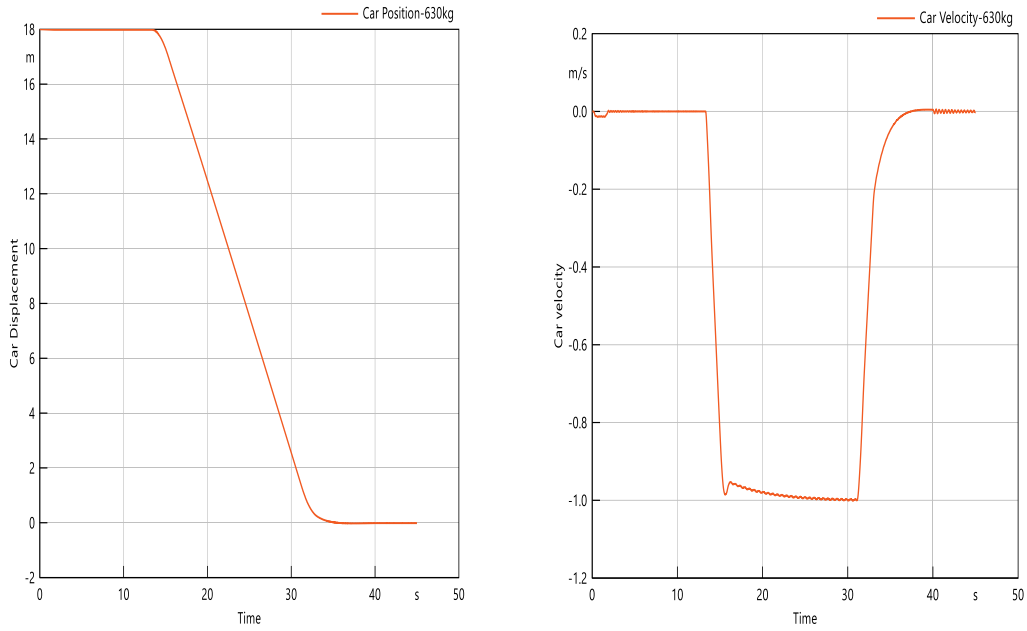
Figure 8. Simulation result of car position(left) and car velocity (in right).

In Figure 9, the left graph shows the variation of acceleration at the time axis. The acceleration is lowest at 14 s and maximum at 32 s and in right. The right graph shows the change in kinetic energy.
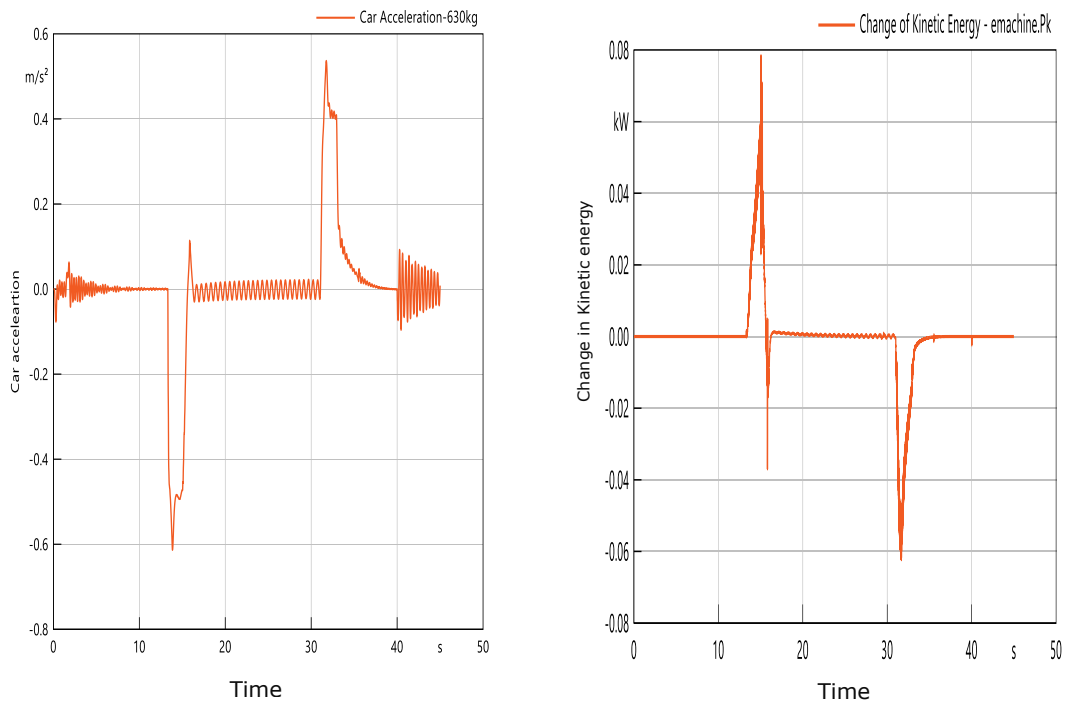
Figure 9.Lateral Acceleration result (at left) and change of kinetic energy (at the right).

42

In the second graph at right kinetic energy due to vertical movement is maximum at 15 s and minimum at 31 s. It requires the use of the kinetics formula from equation 2.8 as the acceleration and time given can be used in calculating the kinetics. It also involves the speed of the system which is calculated using the formula in equation 3.8 and 3.9. This is because the formula can help in determining the speed of the rotation of the system. Further Vibration analysis has been done more elaborately in chapter 9, where Validation has been done. It has been studied how different parameters affect vibration.

The formula for calculating the lateral acceleration is derived from equation 3.18 for fining kinetics. 'a' is the acceleration and h is the height which time in the figure above. Finding acceleration in this situation is as easy as the value of 'h' is given. The acceleration depends on the high or low value of h on the x-axis. The coupling between vertical and lateral vibrations is often assumed to be ignored because the lateral vibration amplitude is assumed to be small [23], as is the case when the rope tension is high, and hence vertical vibration is studied separately [42]. Following left Figure 10 shows elevator required torque and time relationship; torque is minimum at 13 s and maximum at 32 s. The machine torque has been estimated from
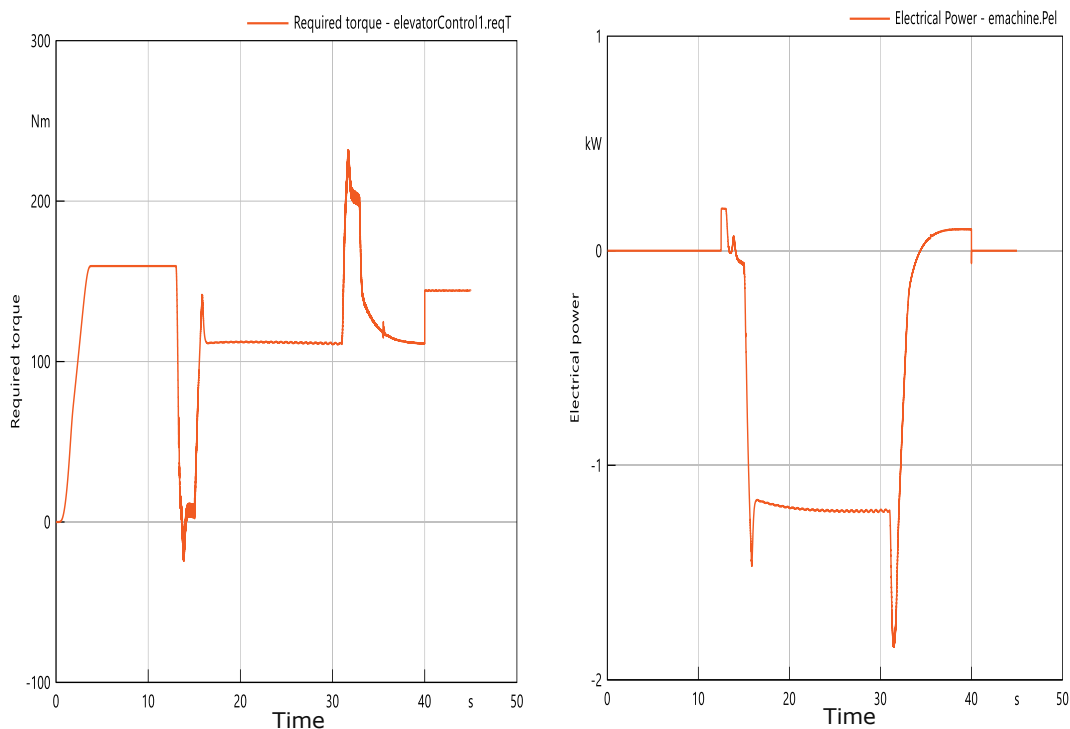
Figure 10. Required torque (at left) and electrical power (at Right).

43

The measured three-phase current intensities [43] employing the quadrature zero (dqo) transformation theory [39] that is being done with the help of PID controller. Figure 10 at right shows the electric power of the Car where it is maximum at 12 s when the car started coming down and minimum at 32 s when it started going up direction, the power loss of machine is maximum at 32 s and minimum at 0 to 12, 14 to 16 and 40 to 50 s that has been shown in Appendix 2.

It is necessary to evaluate the vertical motion of the compensating sheave during different emergency scenarios such as the brake activation and buffer strike to determine the maximum vertical displacement of the compensating sheave. Speed is getting controlled by VFD (Variable Frequency Drive) and it is mechanically controlled by breaks. Gear etc. It only shows how the parametrization of brake has been done in SimulationX to get the desired result, a more detailed description of modelling and parametrization has been done in Section 5.1 Components of an Elevator system.
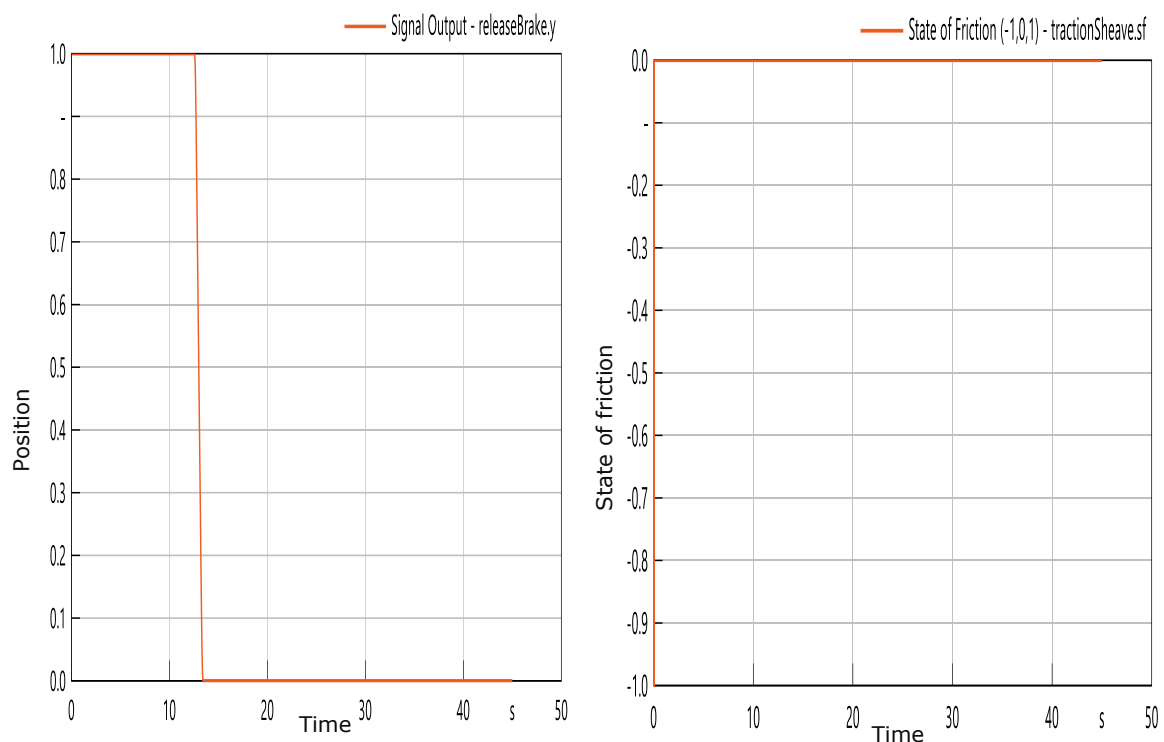
Figure 11. Signal output release brake (left) and traction sheave friction(right).

With the release of the brake in the software, the output signal is also observed. The signal output is one between zero to 12 s and minimum at from 13 to 45 s. The output signal can be found using the formula for finding the speed above. When breaks are released, the radius of the pulley must be considered to find the actual output. The formula for output is given by equation 3.17.

In this, the minimum and maximum range of time must be considered. By inspecting Figure 11, it can be seen how this method of speed control works successfully with this air gap torque and release the brake. It covers a wide range of control where low speeds are required at low torques but usually, this is not possible and the system becomes unstable [44] for these reasons. The performance of variable voltage systems at levelling is not as good and stable as more advanced systems [44]. However, here due to system simulation, proper braking has been applied, and it is possible to get the proper releveling. The Following Figure 12 shows internal force and external power due to eccentricity. It was important to consider eccentricity value, i.e. as eccentric load which can directly affect the system's vibration.
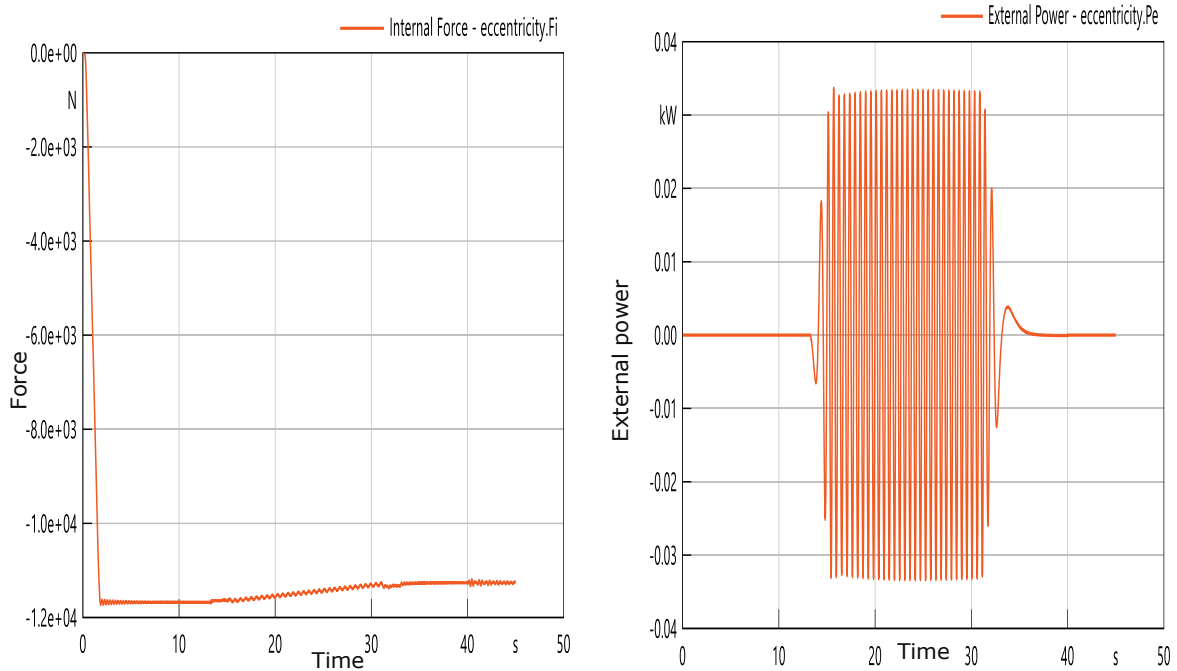
Figure 12. Internal force (at left) and External power (at right) due to eccentricity.

In the first graph, the force significantly decreases and then slowly increases from one to 45 s. Besides external power is constant between 0 to 12 s and 32 to 45 s, but there is too much resonance due to less damping between 12 to 32 s. In the above graph, the two formulas for force, and power are applied. When force increases and decreases gradually, the acceleration can be found as an increase and decrease in the movement of the elevator involves time and speed. When external power is exerted, the output formula can be used that can be used later to increase damping and to decrease vibration, as eccentricity can induce additional stress or forces at the joint.

In the end, some more parameter like power loss, air gap torque and angular acceleration has been illustrated in appendices and signal output remains constant irrespective of time. The angular acceleration and output are the same at the time of landing. F can vary from 0,15 to 0,19, it just has been ensured that deacceleration should always be less than equal to 0,5 m/s^2 as the friction is maximum at 0,19; As such in equation 3.33, 3.34 and 3.19.

In this chapter mathematical model of an elevator system is described. The theory and digital parts are linked here because this is a critical criterion for HIL simulation. It demonstrates how the elevator's theoretical formulae function in SimulationX. Experimental experiments were used to obtain device parameters such as the rope's modulus of elasticity, stiffness, and eccentricity estimates of their values, which were then used in simulations. It is essential to have a thorough understanding of the engineering principles and models used in order to perform the system calculations. This is essential for a correct understanding of the assumptions used in the formulae and parameters for safety standards, and for hoisting machine modelling and parametrisation.

This chapter also focuses on the maximum and minimum values that should be considered while putting an available general elevator stable and balanced. The theory section explains and justifies the sag and vibration during model validation after identifying all the elements. It will be applied during elevator modelling in the next chapter 5. The following chapter will go through all the technical terms, equipment, and their states of operation used during the testing of elevator drive software.

4 TECHNICAL BACKGROUND

4.1 Mono 500

Mono 500 is a new powerful, and long-lasting residential elevator that can accommodate eight or more passengers. This is a flexible elevator solution for new and existing low-to mid-rise buildings with a smaller motor than previous versions and minimum energy consumption [45]. It has a lightweight build with environmentally friendly technology.

Some silent features of Mono 500 include: -

1) Automatic wide screen doors for easy entry and exit
2) Smooth acceleration, deceleration, and accurate levelling for a comfortable ride.
3) A car and hoisting device that minimises noise and vibration
4) A pleasant, comfortable, well-lit car interior and easy-to-use signalisation
5) Millions of car interior material combinations to choose from
6) Mono 500 can cut electricity consumption when it is not in operation, leading to reduced maintenance costs [46].

Figure 13. Mono 500 elevator

Figure 13 shows the MONO 500 elevator where current improved drives software testing is going to be implemented in this model. The KONE MonoSpace 500 combines proven eco-efficient technology with ride-comfort and design innovations. Mono space 500 are a machine room-less elevator powered by KONE EcoDisc where the elevator's capacity will be approximately 2000 AIA(American Institute of architect), lbs(Pound) (800 kg) speed of the elevator will be around 150, 200, 350 fpm(feet per minute) or (0.75, 1.0, 1.78 m/s) Landings 2 to 15 [47].

The current drive software testing is going to be implemented inside the MONO 500 model. The parametrisation of the hoisting was done based on the previous hoisting Mono700 model. MonoSpace 700 was a previous hoisting model for a high rise elevator, and It is a fully customizable machine room-less solution. The Hoisting model was created and simulated inside SimulationX; this model was also Powered by KONE EcoDisc with specification; Capacity 2000 – 5000 AIA lbs (907 – 2268 kg) Speed 200, 350, 500 fpm (1.00, 1.78, 2.54 m/s) and a Landings 6 to 36 standard floors [47],[48].

''Monospace has been designed to take the quality of elevator experiences higher. These elevators come in themes that are fresh and energetic, representing the five elements of nature: Milky way (Space) SunGlow(Fire), Sandstone(Earth), DewDrop (Water) and ColdBreeze(Air)''[49]. It offers more flexibility to choose the ideal elevator that adds to the ambience, style and class of building interiors and exteriors.

4.2 System simulation

System Simulation is a set of techniques that use computers to simulate different real-world tasks or processes. Computers are used to generate numeric models to describe or display complex interaction among multiple variables within a system [50].

There are currently many software tools for system modelling and simulation to help eliminate surprises reactively, and the computer-based system is built. These tools are applied during the system engineering process. System Modelling is the process of developing abstract models of a system with a model presenting a different view or the perspective of that system. SimulationX software is one of those tools to model system modelling used here to model the virtual prototype of an elevator system.

Benefits of system simulation [51]**,** [52]**,** [53]:

1. Easy to design the model without programming knowledge
2. time-dependent of the entire system
3. Save time
4. Increase efficiency, precision and safety of the product
5. For an optimized product development
6. Meeting new standard and regulations

SimulationX: It is a software environment used to model the virtual prototype of an elevator. It is a software framework for technological system modelling, dynamic simulation, and analysis [54]. SimulationX encompasses complex behaviour as well as a simulated environment for the device. SimulationX is based on the design language of a non-proprietary model Modelica®. The individual parts, assemblies, and subsystems are being represented for the design component. It includes mechanical, electrical software (controller) and other physical behaviour [55]. It provides unique support for real-time simulation to support HIL.

Their physical behaviour is defined through differential equations or can be specified with characteristic curves. The software has been used in the industry for 15 years, and it is mainly known for its GUI for various computer-aided engineering solution and data formats.

Modelica: Modelica is a non-proprietary, object-oriented, multi-domain equation-based language to helpfully model complex physical systems [56]. In Modelica, mathematical models can represent any physical system, e.g., mechanical, electrical, electronic, and control. A library that contains more than 1600 model component and 1350 function of the different domain makes Modelica exceptionally proficient; a user can create a library without any knowledge of programming. It supports the C++ programming language [57]. Currently, software like SimulationX, Dymola, MWorks, AND MapleSim support the Modelica language. All the major automation and power industries like ABB, Siemens, Audi, BMW, Ford etc., are using Modelica.

Benefits of using SimulationX [58] **,** [55]**:**

1. Measurements could be done in the 3D system
2. Simulations are done with modelling in the diagram view
3. 3D visualization, 3D-Animations, 3D view of the models
4. Can import 3D cad files for visualization
5. integrated tool for macroing for multiple consecutive simulations
6. Intuitive user interface

7. sensors can be added almost anywhere to the model
8. Create a digital twin of the system
9. Save cost by using virtual prototypes instead of building physical prototypes
10. Shorten development time by using the model to test quickly

SimulationX has the immense potential to model, simulate and automate complex, technological systems where models can be built for custom applications. It real physics element, making it real-time capable. A vast majority of SimulationX applications where drive system, hybrid powertrains, mechatronics and vehicle dynamics are the most important [54]. Additionally, preparing the hoisting model(virtual prototype of an elevator), network modelling in SimulationX not only provides the user with a practical and modern engineering solution but is also time-saving and has a long lifetime. Also, software such as Microsoft Word, Excel, and COMSOL are compliant with this system. It is repeatable and can provide better mechanical testing for HIL. However, complex models take a long time to simulate; the software is not readily available and only qualified professionals in the fieldwork with it. While training entry-level engineers to use the software is essential, it is costly and time-consuming. Nevertheless, this program certainly has more benefits than drawbacks.

4.3 HIL (Hardware in the Loop)

HIL is used to develop and test a complex real-time embedded system. It provides an effective platform by adding the control plant's difficulty to the test platform [59]. HIL simulation is beneficial when testing the control algorithm on a real physical system that is costly or dangerous [60]. The plant's intricacy under control is included in the test and development by adding a mathematical representation of all related dynamic systems. HIL test bench is potent and very suitable for testing software automation [61].

These mathematical representations are referred to as plant simulation; the embedded system to be tested interacts with this plant simulation. A HIL simulation includes electrical emulation of sensors and actuators. In other words, HIL testing is a technique where accurate signals from a controller are connected to a test system that simulates reality, making the controller work as its assembled product. HIL simulations have provided the platform to perform otherwise costly, risky and as well as provided a means to perform experiments with marginal extremities.

Figure 14 shows one basic diagram of HIL testing. It describes how HIL testing works, how it is connected to other devices and how a tester can do some specific device testing using a real-time environment simulator.
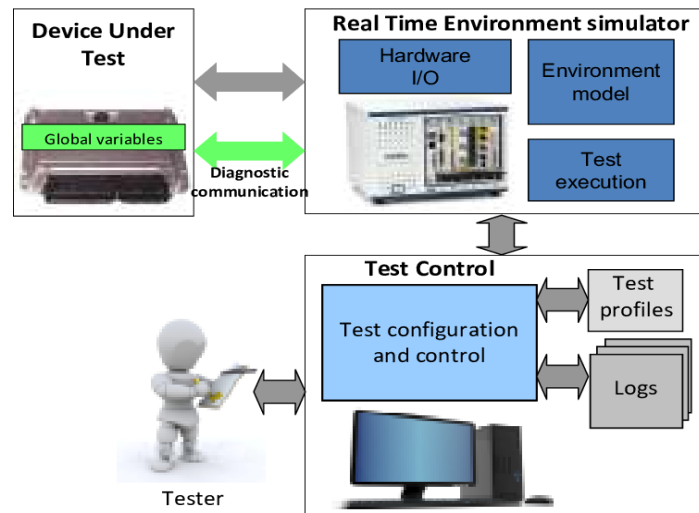
Figure 14. Basic diagram HIL testing[62].

The reason behind using the HIL simulator [63], [64], [65], [66], [67]:

1. To improve the S.W (Software) quality
2. To enable automatic testing
3. To enable the testing of real elevator cycle
4. To enable to test elevator commissioning /fault behaviour
5. To enable to test with different kind of elevator shafts
6. To enable to test of different elevator components and running parameters
7. To Increase the pace of drive software development
8. To reduce the testing time
9. To reduce the testing cost
10. To increase the reliability and repeatability

Figure 15 shows HIL systems; In general, It consists of 19-inch variable height racks and various programmable power supply units with varying capacities depending on the application. Powerful multi-core processors and a portfolio of modular I/O cards are combined here [68]. The real HIL simulator that is being used for the drive software tasting.

Figure 15. HIL Real-time simulation[18].

The things mentioned above can be achieved by using KCE(KONE controller and electrification) or using a test environment to run test cases or by using a shaft simulator to simulate shaft signal, or by using an elevator simulation model to simulate how load behaves like a car move in the shaft.

Benefits for drive teams:
  I.   Increase the coverage of automated testing
 II.   Enables fast feedback for SW(Software) development
III.   Enables specification based on real measurements EBOi(Emergency battery operation), EBDi(Emergency battery Drive internal battery), etc

The HIL simulation's main advantage is that it provides a repeatable laboratory environment for safe, flexible and reliable controller validation [6]. Controller Performance and stability can be systematically tested without interference from other unrelated systems, and reliability can be tested by controlled injection of disturbances and faults. HIL also allows validation of the real hardware in an early development phase without needing a prototype elevator because any missing elevator components can be simulated. For these reasons, HIL simulations are more efficient and cheaper than test drives.

Description for HIL Component

The aim of the thesis was to develop an elevator model inside the HIL main control unit. Here in this chapter, all the component of HIL testing is shown in Figure 16 that is being used currently has been described.
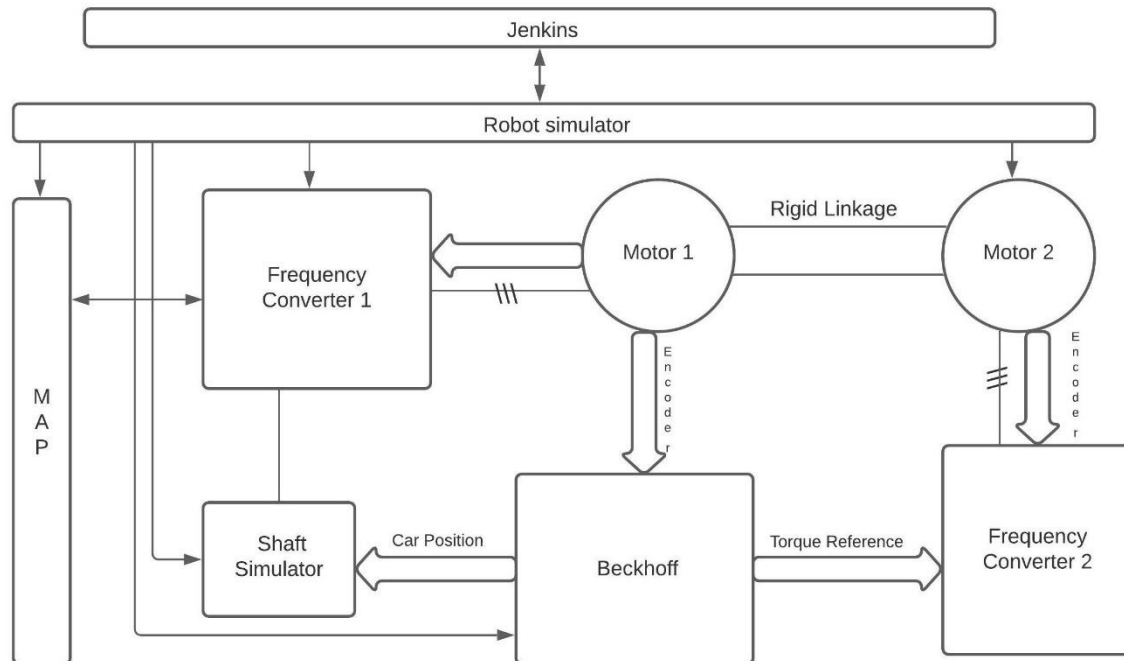
Figure 16. HIL layout.

HIL simulations consist of a combination of simulated and actual components in Figure 16. Alternatively, a real component can be emulated, i.e. replaced by an artificial component with the same input and output characteristics. Ideally, each component should be unable to distinguish between real, simulated, or emulated components are connected in a closed-loop configuration. HIL, therefore, offers the flexibility of simulation, where the use of real hardware offers a high level of reliability.

The key component of the HIL simulator are as follows:

Main Safety Control: Part of elevator electrics takes care of the safety. It cuts supply power for the frequency converter if the safety circuit is broken. It is connected to TTS BUS. The main safety control board cannot control the load frequency converter.

Elevator CPU: The main control board of elevator electrics. Collect car and landing calls and gives run commands to the motion control board. Typically, the CPU knows the state of the doors and which are simulated inside the shaft simulator.

Frequency Converter: Power electronics for power conversion and motor control. Control is divided into two main functions: motor control and motion control. (Drive is under test only the software, the current drive is being used in the HIL laboratory). Figure 17 shows the frequency converter with motion and motor control installed in that it controls the overall speed, position and torque of the elevator traction motor.

Figure 17. Frequency converter 1 with Motion and motor control in HIL Laboratory [59][60].

Motor control: It handles the speed and torque control of the motor. As the name indicates, this part controls the overall functions of the electric motor. The controller could be simpler or complex. The simple controller has simple functions such as the on/off function [69]. The Servo motor in Figure 17, shows the motor control part. The complex controller could control so many functions such as rpm of the rotation, direction of the rotation, speed of rotation and protection against errors. However, every controller does some common tasks, such as protecting the motor from overload by cutting the power supply. Motor starters, adjustable speed drives and stepper motor controllers that use microprocessors to control power are few examples of the motor controllers. The input for the motor control is the speed reference and the torque feedforward [69].

Motion control: Motion control is one of the most recognised terms in the field of mechatronics. It is responsible for more efficient and effective motion and automation. Controls come in different technologies, sizes and capabilities to suit demanding applications [70]-Control types such as ICs, PLCs, PACs, Industrial PCs. Figure 17 shows PCB that serves as baselines component of many internal systems in motion control, this board constitutes of SMD and socket component.

The PCB is a part of motion control. It calculates the speed reference according to the run command from the elevator CPU. It also provides the torque feedforward and controls the mechanical brakes [71], [70]. It calculates the car position according to the motor encoder and door zone sensors. The new motor and motion controller are coming with advanced and unique features such as heat dissipation, highly dynamic, excellent efficiency. It can be used for any application that makes this converter more valuable and easy to use for drive controller and protection. Table 1 shows the different features and characteristics of motor and motion control, as this device is under test.

Table 1. Comparison between Motion and Motor control.

S. No	Motor control	Motion control
1	Responsible for speed and torque control.	Responsible for motion.
2	The input for the motor control is the speed reference and the torque feedforward.	It calculates the car position according to the motor encoder and door zone sensors.
3	Controls generally manage the starting and stopping of the motor.	It provides the torque feedforward and controls the mechanical brakes.
4	Protection against any faults or errors.	It calculates the speed reference according to the run command from the elevator CPU.
5	Provides management to overall performance.	All motion control contains the power circuit board.
6	Controlled manually and automatically both way.	Available Control types are ICs, PLCs, PACs, Industrial PCs.
7	Each motor controller has some kind of protection, relays that cut the power if the motor dissipates too much energy.	Different size and technology are available.

Frequency converter 2**:** It is the Variable frequency drive used to control the speed, frequency and sometimes it uses an inverter. Figure 18 shows the second frequency converter, i.e. connected to the load motor and used to give the same torque as a rope

to load motor as in an actual elevator [72]. It is only being used for HIL testing in the laboratory, not present in a real elevator.

Figure 18. Frequency converter 2 [73].

Shaft Simulator: A simulator for shaft signals as if the car moved in the shaft. Shaft signals include car position in the door zone area (±130 mm) and final limit switches. The input for the shaft simulator is the encoder pulses [20]. It does not exist in a real elevator. The shaft simulator is connected to industrial PCs and Beckhoff through the signal. Shaft switches in real elevator provide the information of the elevator to the controller and, based on switch operation controller knows the exact location of the car.

Map (Maintenance access panel): MAP is the elevator user interface for the elevator technician. It can be used to run the inspection, and setup can be started. It is also used to reset MSC faults. The MAP contains the control board of the electrification system [74]. MAP is usually located near the entrance on the topmost or second topmost landing. MAP consists of a travelling cable, main safety controller, switch module, alarm board, and lightning switch. Map connection shows how different panel, controller and switch are placed inside the MAP. It is being used to give the command to the drive and Industrial PCs. one can give the command manually or automatically.

There are two types of MAP 1) Door Map, 2) Wall MAP.
As the name suggests, one is mounted in the wall and the other is like a box that has a door to cover usually, Door MAP is being used.

Elevator traction motor: It works as a motor for lifting. When moving downwards, it works as a generator and also generates power [1]. Nowadays, PMSM is used as an elevator traction motor. The use of a permanent magnet in the rotor in the rotor of PMSM makes it unnecessary to supply magnetising current through the stator for constant air gap flux. The stator current is needed to produce torque only.

As a result, the PMSM would have a higher power factor (due to the lack of magnetising current) and be more effective than the I.M [75] for the same performance. The traditional wound rotor synchronous machine, on the other hand, needs motor excitation, which is often provided by brushes and slip rings. This necessitates rotor replacement and routine brush cleaning, both of which necessitate downtime. The primary motivation for developing PMSM [2],[76] was to eliminate the SM's previous disadvantages by replacing the field coil, do power supply, and slip rings with permanent magnets. Figure 19, shows the elevator traction motor. If the car weight is more than C.W then it will go upward, power of elevator traction motor will be high, at the same time if C.W weight is more than car then it will go down and if both the weight of car and C.W are same then it will not move; usually, it is not true in the real elevator because there is always some friction and guides shoe rail.

Figure 19. Traction sheave motor [77].

Load motor: Load motor provides load torque for the elevator motor as if there were real traction sheave, ropes, car and counterweight. The load motor is controlled by its frequency converters such as ABB ACS880 or Danfoss as shown in Figure 18 The torque reference is provided by the HIL elevator model [78]. There is encoder feedback from the motor to the frequency converter [79],[80]. The traction sheave motor and load motor is connected mechanically, and this load motor is only for testing. it is not available in a real elevator, and it provides load during the testing.

Robot environment: It is an Industrial PC and it is used as a robot environment responsible for process control and data acquisition. It is one of the most powerful and easy to control device. Figure 20, shows the Industrial PC i.e. connected to the Jenkins server. There is an attached heat sink which is responsible for colling the box PC. It has higher dependability and precision standards.

It provides better reliability, expansion option, and long-term supply than embedded Pc, but It is costly than a typical electronics pc. It provides a controlled environment for the installed electronics; it also provides additional colling with air filtering [81]. It is dust and waterproof. It is a more robust and higher-grade power supply. It has a timer to reset the system automatically in case of software lockup [82], [83].

Figure 20.Industrial PC (Robot environment) [79].

It is available in several shapes and forms are at the centre of a good range of diverse automation tasks like control of machines, processes, networking of system components and data acquisition [83]. For traditional control tasks, PC-based control technology offers excellent scalability and adaptability and is hence progressively used in place of hardware PLC.

Here the TwinCAT software will be provided as a base level of programming to execute the software testing. The Industrial PC has one link port connected to the Jenkins server, and instruction sets are complex. Apart from these components, there is an emergency rescue battery connected with DUT to protect the equipment from any emergency shutdown and provides power for a rescue run in the case of power off. Earlier, the rescued battery was being used only once to open the elevator in case of an emergency; after that, one needs to replace the rescued battery, but nowadays it is also more powerful.

4.4 Beckhoff

It is New Automation Technology Beckhoff implements open automation systems based on PC Control technology. The product range covers Industrial PCs, I/O and Fieldbus Components, Drive Technology, EtherCAT and automation software [84]. Beckhoff is currently being used around the work in all Industries and plants for its different unique and trusted (Drive) product.

Embedded computer is a microprocessor-based system, it is specially designed to perform a specific task again and again, and it is a part of a more extensive system. It combines the hardware and software to finish the specified task and withstand different conditions. Embedded computers offer a smart alternative to PLC-based automation. Embedded PC is essentially any specialized computer system implemented as part of a larger device, smart system, or installation.

Characteristics of Beckhoff's embedded PC [85]**.** 1)Compact design, 2) Highly reliable 3) High efficiency, 4) Direct I/or Interface, 5) Modular options for extension and 6) Mounting of the DIN rail [85]. Nowadays, it is being used in varieties of application such as robotics engineering, heavy industries, process technology.

Configuration of CXxxxx Embedded PC
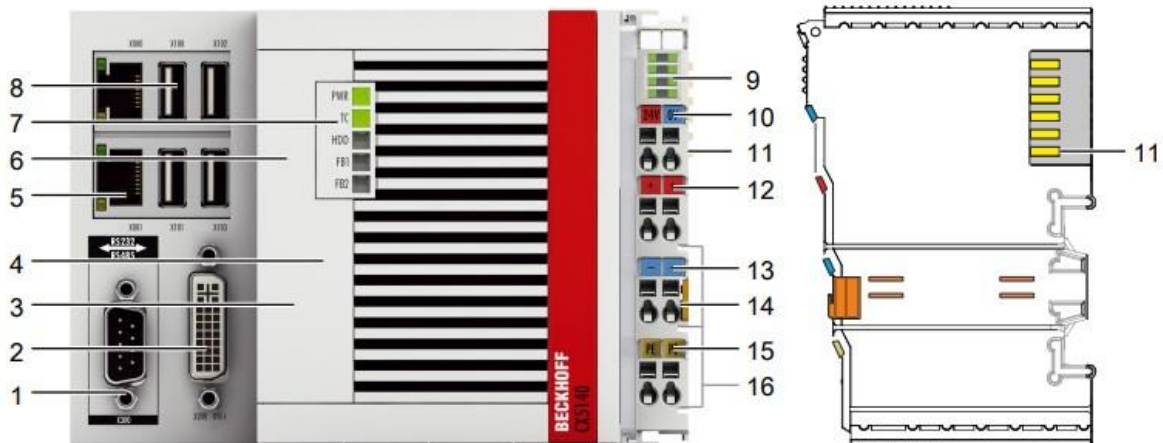
Figure 21.CXxxxx Embedded PC [84].

CX device series combines the features of Industrial PC and hardware PLC, making it ideal for all control tasks. The CXxxxx has an Intel Atom® multi-core processor with a clock rate of 1.75 GHz, making genuine multi-core technology possible in the Embedded PC segment [85]. It has Two independent Gigabit-capable Ethernet interfaces, four USB 2.0, and a DVI-I interface has been described in Table 2.

The CXxxxx is characterized by low power consumption and fanless design Figure 21 shows an embedded pc with its port and its characteristics. Table 2 shows all the port and their description of embedded Pcs, Elevator dynamics is modelled in this embedded PC. The input for the model is the elevator motor position (encoder). The load inside the elevator and elevator parameters are given via the user interface. The outputs of the model are the car position (encoder signals) for the shaft simulator and load torque for the loading machine.

Table 2. legend for the CXxxxx above configuration [85]**.**

S.NO	Component	Description
1	Optional interface	Space for interface such as EtherCAT, CANopen
2	DVI Interface	Interface for a monitor or Panel
3	Cfast card slot	Slot for industrial CFast cards
4	Micro SD card slot	Slot for Industrial MicroSD cards
5	RJ45 Ethernet interface	For connecting to the local network or the internet
6	Battery compartment	Power supply for the battery-backed clock for time and date
7	Diagnostic LEDs	Diagnostic LEDs for power supply, TwinCAT and optional interface
8	USB interface	Interface for peripherals Mouse, keyboard, or USB
9	Diagnostic LED power supply terminal	Diagnosis of power supply for embedded PC and terminal bus
10	Spring-loaded terminal +24v and 0v	Power supply for embedded pc
11	Terminal bus (kbus or Ebus)	Interface for EtherCAT Terminals or bus Terminals, Data exchange and supply
12	Spring-loaded terminal +24V	Power supply for bus Terminals
13	Spring-loaded terminal 0V	Power supply for bus Terminals
14	Terminal release	Release the power supply terminal and therefore the embedded PC from the mounting rail
15	Spring-loaded terminal, PE	Spring-loaded terminals for power contact PE
16	Power contacts +24v, 0v, PE	Power contacts for Bus Terminals

The elevator model can also be parameterized via an automatic tester interface. The model can control some switches in the primary safety control board. Inside the Beckhoff, there is a PC with an OS. Both the Beckhoff and the simulator is connected to a common point that is called a connector.

TwinCAT: It is a software platform and development environment for engineering and runs time, a type of PLC and Development environment produced by Beckhoff; it is considered Soft PLC and is one of the easiest PLC to use with Perspective. The Development software of this PLC generally allows the execution of up to four PLC on any PC without any cost; besides, it supports real-time, which is why it was advised to use this TwinCAT based PLC [86]. Depending on the installed TwinCAT runtime environment, the CXxxxx can be used for implementing PLC or PLC/motion control projects with or without visualization. The execution of motion control applications with interpolating axis movements is also possible. In combination with TwinCAT 3 automation software, The CX Embedded PC becomes a powerful IEC 61131-3 PLC that can efficiently execute the motion control task [85].

Beckhoff PLC processes the encode pulses to speed and position signal. All Beckhoff controllers are programmed using TwinCAT with TwinCAT 3, C/C++ and MATLAB/Simulink. Here in this research, TwinCAT plays a major role in importing FMU from SimulationX, described later in subchapter 6.2 FMU. TwinCAT automation software integrates real-time control with PLC [85], and CNC functions; here it will provide the base for tuning the Virtual elevator model for real-time operation.

The read/set parameters that are going to be used are:
1)Carload 2) Shaft speed 3) Rated load 4)Traction sheave radius 5) Roping Ratio 6) car and sling mass, 7) counterweight mass, 8) Rope and car cable weight in mass per meter 9) Sag at the bottom floor i.e flexibility of the rope. 10)Car guide rail friction force, and 11) Counterweight guide rail friction force

Beckhoff control technology is scalable from high-performance Industrial PCs to mini PLCs [84]. Beckhoff drive technology shows a sophisticated and complete drive system, the motion control solution offered by TwinCAT automation software. The drive system XTS (extended transport system) replaces classic mechanical systems with innovative mechatronics; that is why Beckhoff is extensively used with drives.

4.5 Jenkins

Jenkins is an open-source development platform and a Java framework with 100 + plugins built for continuous integration. This is used through continuous integration to automate software development processes and facilitates consistent distribution by sharing newly created codes [87], [88]. It is a stand-alone app, and that can be used on any Windows, Linux or Mac app. Jenkins is the most famous continuous integration and continuous delivery solution. To carry out continuous delivery, Jenkins introduced a new feature called the Jenkins pipeline. Figure 22 shows the Jenkins pipeline and how it executes and work.
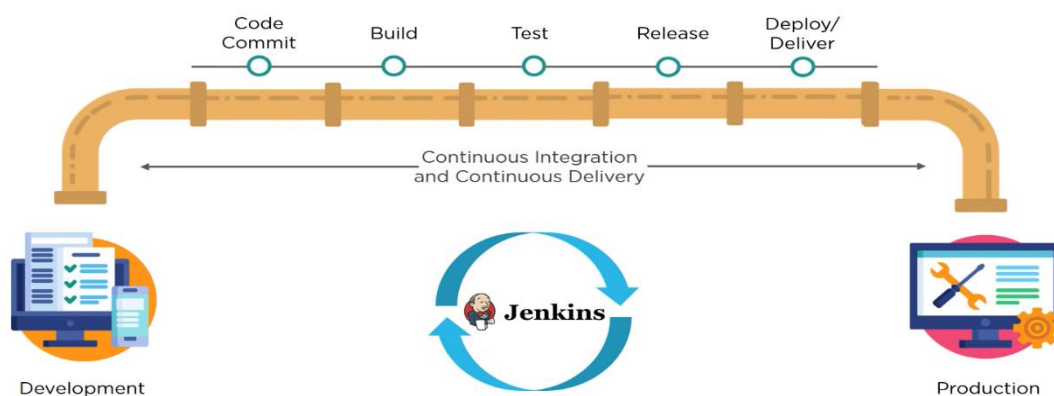
Figure 22. Jenkins pipelines [87].

Jenkins save time by triggering a built-in code as soon as any developer took the latest code as if there were any errors due to any commit as soon as any trigger help was notified to the developer. Continuous delivery can release software. It is a practice that ensures that the software is always in a production-ready state. There are five main Features of Jenkins that are namely 1) Distributed, 2) Easy configurable, 3) Easy installation, 4) Extensible, 5) plugin.

4.5.1 Continuous Integration

C.I (Continuous Integration) is a programming technique in which developers are expected to commit changes to source code multiple times a day or more regularly in a public repository [89]. Any commitments made in the repository are optimized, and this allows teams to identify the issue early on [89], [90].

Here, in this research, HIL deployment is being done using Jenkins and C.I as C.I enable the development teams to deliver a large number of software testing and deploying more frequently and reliably at low cost [91], [92]. C.I is seen as an essential

method for improving software quality while keeping verification costs at a low level[92]. Different developers change to commit the code, develop the code and check the code into a shared repository such as GIT / TFS. If it fails, it must be checked.

Earlier Integration used to be performed at the end of the cycle that was creating a lot of error and code rework. C.I is now being used in many organisations that create and test software; companies are using it to improve their product development. In this regard, it can be concluded that today entire computer farms are more or less working on building server and testing that perform intensive testing, and developer commit change frequently and C.I can solve an intriguing testing problem - Table 3 shows, how C.I save time, what has changed after the inclusion of C.I and how it is beneficial for testing and deploying.

Table 3: Difference before and after continuous Integration.

S.No	Before Continuous Integration	After Continuous Integration
1	The entire source code was built and then tested	Every commit made in the sources code is built and tested
2	Developers must wait for the test result	Developers know the test result of every commit made in the source code on the run
3	No feedback	Feedback is present

CI is related to the concept of automated test execution frameworks, in that a regression test suite automatically run before committing the code that ensures the stability of code. It should be performed consciously if some test fails, a developer should debug revealed by the test. This technique has reduced the timing and the code rework that was earlier needed in the later phase of development. Figure 23 shows the basic C.I workflow where it saves time by informing the developer about any error as soon as it finds the error, and It shows how C.I have improved the testing process.

Some of the Challenging task related to C.I are how to shorten the save compile cycle and move the checking additionally, test infrastructure should also be robust to work even at the time of code churn. The software testing is usually assigned to skilled professional. The basic idea behind CI is to commit, one or more times a day, all of the working copies of the software on which different developers or groups of developers are working.

The industry is facing huge challenges while developing software and its testing and Jenkins can help in automating the complete process, it checks the development at each step of software evolution by making the work easier for the developer [88], [90] Jenkins deploys the build application to the test server, so if the failure occurs, feedback would be transmitted to developers immediately [88].
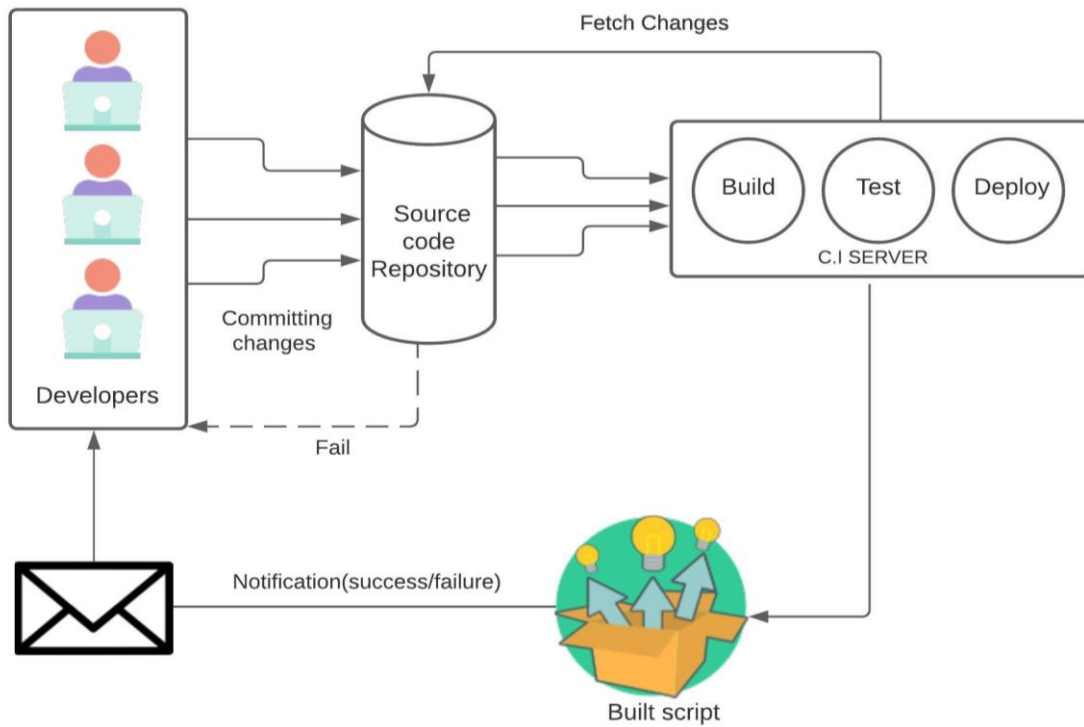
Figure 23.Continuous Integration workflow.

In continuous integration, the code can be pulled whenever there is a commit made in the source code and all the changes made to the source code are built continuously. C.I and C.D produce good quality software [93]. Knowing all of the components, their functions, and how they operate is vital because it aids in the procedure's implementation and ensures protection. After specifying all of the components of the HIL simulator and testing, the process and procedure for HIL testing are discussed in Chapter 6: State of the Art.

5 THE MULTIBODY ELEVATOR MODEL

This chapter explains the Multibody elevator system-the detailed approach used for modelling the virtual prototype of the elevator inside the SimulationX. The modelling of a multibody system is always a challenging task because it comprises several different details. The study of the complex behaviour of interconnected rigid or fluid bodies, each of which may experience significant translational and rotational displacements, is known as a multibody structure. Multibody systems include automobiles, cranes, and robots, etc. One such complex MBS is an elevator.

Figure 24 depicts a general multibody elevator system with all of its components, courtesy of Otis Elevator. It demonstrates how individual elevator components are connected to form a vertical transportation system (VTS). The entire elevator is depicted in the diagram; it is the most typical and common type of elevator, consisting of ropes that move through a pulley and are attached to the rope. The cable is wrapped around the top of the elevator car on a sheave at one end and connected to the C.W that moves on the guide rail at the other.

To avoid any vibration induced by dynamic forces as the elevator car moves along the hoistway, the elevator shaft walls are very well fixed to the guide rails. The roller guide and guide rails form the guiding interface between the building and the elevator car and counterweight. The directing guide ensures the relative position of the elevator car and counterweight, along with the height of takeoff. The elevator's control mechanism pushes the motor upward, while the sheaves turn around, causing the elevator car to travel upward. Similarly, the elevator car moves downward as the controller drives the motor in the opposite direction.

All of the elevator components, function and design, are described later in this chapter. Virtual models have begun to be used in laboratory research for the sake of safety and expense. In system engineering, models play an important role since they can represent any real-world structure or process and can solve any real-world problem. The model will verify the system and detect failures that are common in real MBS systems. The primary benefit of using a mathematical model is that it increases device performance, protection, accuracy, and technological attributes while also lowering total costs. The model should produce all of the necessary results in the same way that the actual system can.

Selector

Machine

Starter and controller

Electronic relay panel

Motor Generator set

Secondary sheave

Hoist ropes

Governor

Roller guides

Terminal stopping switch

Final limit switch

Door operator

Final limit cam

Car

Travelling cables

Car safety device

Roller guides

Counterweight guide rails

Terminal stopping switch cam

Counterweight

Car guide rails

Counterweight guide rails

Compensating cables

Final limit switch

Car buffer

Governor tension frame

Figure 24. A general hoisting machine [93].

So, To predict and analyse the system response, a mathematical model of an elevator is developed in Figure 25, which is similar to the general physical model as shown in Figure 3. It demonstrates how individual elevator components are connected to form a VTS [34], [94] also described in chapter 3. Where it is possible to vary any parameter without changing the actual component, which is safer and cheaper. It includes a detailed representation of the drive mechanism, as well as a 6- DOF lumped- parameter model of the actual component.

The multibody modelling of the elevator system has been created inside SimulationX ,and it will be simulated. Modelling of the car–building interface components has received more attention because it direct impact ride quality. In the mathematical model, a single rope is used to describe a multi-rope structure. For concentrated mass necessities, the CW, compensating sheave, and elevator car is used. It is inferred that the dynamics of the system have no bearing on the dynamics of the building structure.

Figure 25 shows the structure of the simple hoisting model inside the simulation, and the Virtual model should show the same behaviour as of real model. All the element Here has been shown in Appendix 3. Modelling of the car–building interface components has received more attention because it has a direct impact on ride quality. This model represents an event when the car is placed at a certain shaft height and the auto electric brake system is used on the system. As a result of car elevator restrictions, the relationship between compensating and suspension ropes is also investigated.

The proposed real-time synchronization model combines a rigid multibody system approach and a multiscale simulation approach [95]. The simulations of such multibody systems are computed to determine the kinematics and dynamics of the system. The multibody system approach is suitable for the describing the big motions for different electrical, mechanical and electronic components. The virtual prototype of the elevator model has been used in HIL test rigs, where data from a real system is used to validate the analytical results. The SimulationX model is divided into six parts that will be explained in detail in subchapter 5.1

1. Cabin incl. Guide Rails & Pulley Beam
2. Counterweight
3. Rope Fixation
4. Motor
5. Controller
6. Parameter block
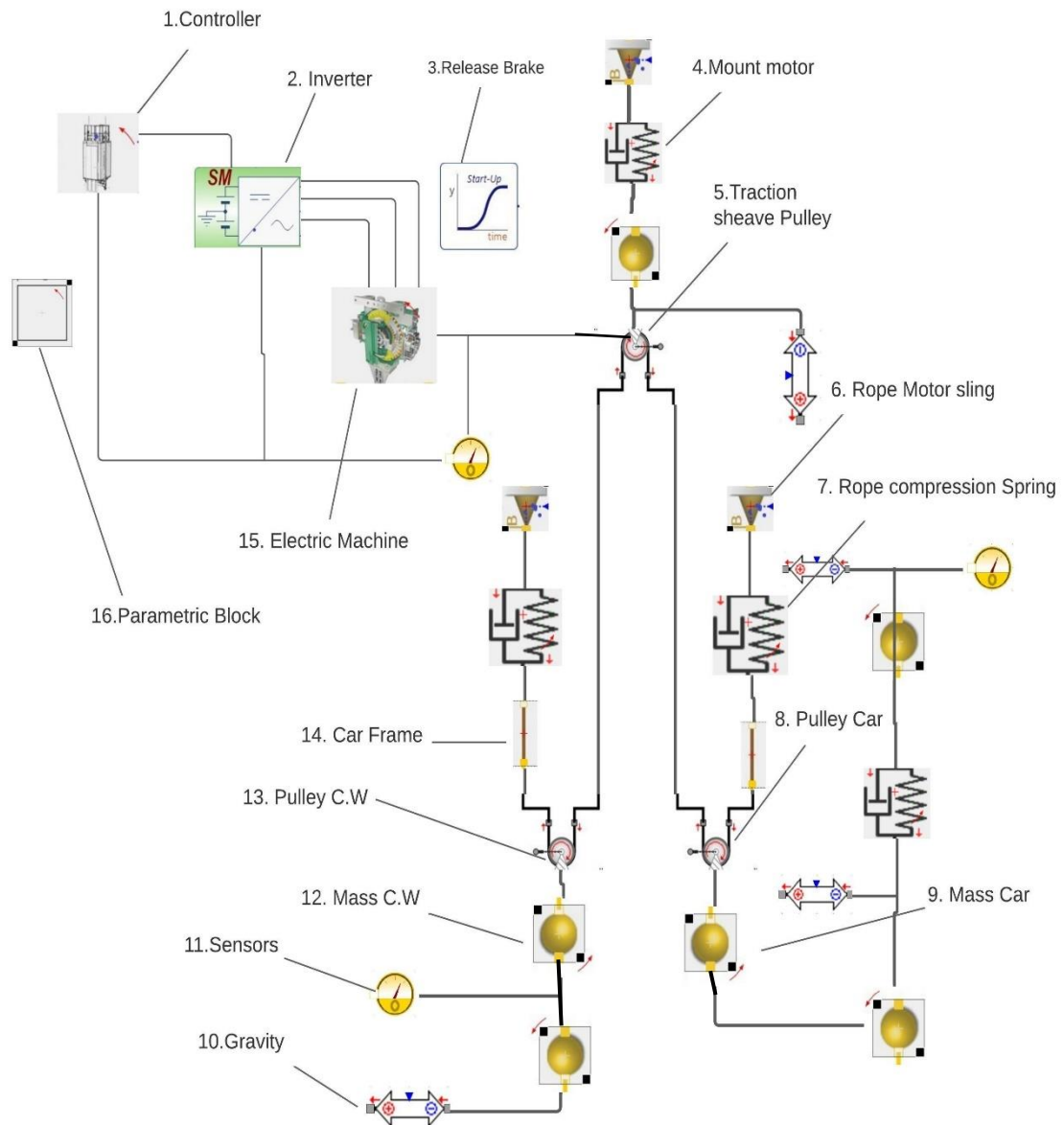
Figure 25. Simple Elevator model inside SimulationX 1) Controller 2) Inverter 3) Release brake 4) Mount Emotor 5) Traction sheave pulley 6) Rope motor sling 7)Rope compression spring 8) Pulley Car 9) Mass Car 10)Gravity 11) Sensors 12)Mass C.W 13) Pulley C.W 14) Car frame 15) Electric Machine 16)Parametric block 14) Gravity.

Table 3 Summarises the model components with the required parameters and possible results/outputs. The mechanical part of the model consists of Multibody system (MBS) elements with two spatial DOF.

Table 3. Model parts, parameter and output.

S.no	Model Parts	Parameter (Inputs)	Outputs (Result)
1	Param Mono 500	Motor position	
2	Car (including car suspension/car mount, guide rail/shoes)	Stiffness of rope coupling, Position, cabin-mounting stiffness, damping and air density	Cabin acceleration, velocity, displacement and twist, cabin-frame mounting forces and deflection
3	Counterweight (including guide rail and guide shoes)	The stiffness of rope coupling	Counterweight displacement, velocity, acceleration and twist
4	Sling/pulley beam	Mass, Position,	Centre of mass
5	Elevator ropes	No of rope, density & Elastic Modulus, position and Damping	Vibration
6	travelling cable	Variable mass depending on car position, Rope stiffness and density	Vibration behaviour
7	Electric machine	Datasheet motor, electrical equivalent circuit	Motor supply voltage, driving torque, rotation speed, energy consumption, losses, bus signals
8	Controller	controller structure, parameters and floor position	Acceleration, speed, Jerk, PID and O/P Gain

5.1 Components of an Elevator system

Car: A car that moves in a vertical shaft to carry passengers (people) from floor to floor in a multi-storey building is said to be the car of the elevator. Here In the Mono 500 model, the maximum weight is 630 kg that can carry at least eight passengers (can vary in Asian countries such as China and India). The car is one of the most essential parts of an elevator. The car and its connected component inside SimulationX consist of four important elements i.e. pulley, beam, guide shoes and car mount, that are discussed later. These four elements are interlinked with each other and support each other directly.

The inside of the car has been divided the car into two zones; The fixed values (mass of door, the mass of car without load, the mass of sensor and mass of balancing weight)

have been put in the zone while the values of variables (such as load that can be changed every time) have been shaded under the one box.

In-car Vibration

How different filter has been put for the different vibration in order to get desired reduce the vibration. Two different vibrations are present in the car e.g. horizontal and vertical. Because of the usage, the vertical vibrations were mainly focused. To get these vibrations, Low pass filter with 80 Hz frequency was applied to vertical vibration.

Pulley beam: A pulley is a type of machine with a rope that fits into the groove of a wheel. By pulling the rope, the wheel would turn. It is used to lift the car. There are three types of pulleys that are moveable, fixed, and compound pulleys. The compound pulley was used because it consists of two or more fixed and moveable pulley simultaneously. The ideal mechanical advantage of a pulley equals the number of rope segments pulling up on the load.

So let suppose, four rope with four pulleys were used, and it has a mechanical advantage of four, which means if a 100 N of force is applied to a pulley then with four mechanical advantage, the pulley would multiply the force by the factor four and apply 400 N of force to lift the car. Combining a beam with a pulley makes it a pulley beam which is used to reduce the amount of friction, which makes it easy to lift the car.

This was connected to the lower car mount**,** car, guide rail shoes and compensation rope of the car and C.W side**.** Car and pulley beam relate to frame elevator, which will decide the initial position of the car. In the modelling, the beam pulley is separated from beam mass, and there is elastoplastic mounting between cable and pulley beam. Guide rail shoes directly connected to cabin and reference frame from frame elevator. The pulley of a car similar to the real CW pulley and traction sheave. The Contact angle of the rope around the pulley is 180°.

Real pulley beam in 3D is shown in Figure 26. The Traction sheave and pulleys where the Internal transformation element belt was calculating the translational forces between two rope ends and the mounting. Forces on the rotational axis are calculated based on the rope running on the transformation element. Slip can be considered with static & sliding friction coefficient.
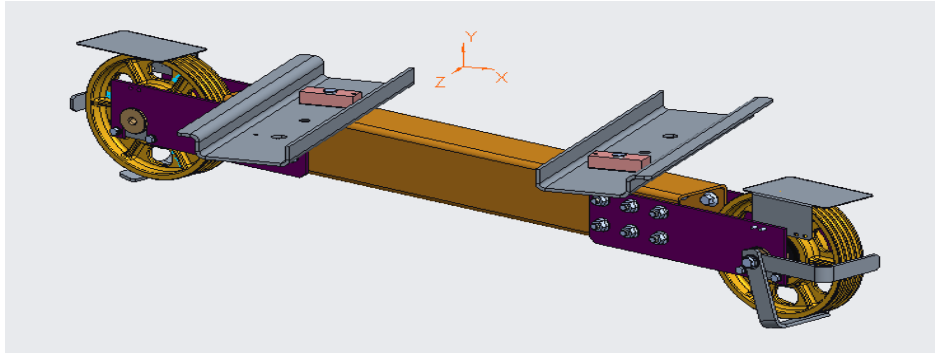
Figure 26. Pulley beam.

Car mounts: It connects car and pulley/sling, which is also referred to as car suspension. Here in this model, only using Lower car Mount was used. The inside of the lower car mount can be seen where the Cylindrical 3D spring element has been used while modelling Lower mounts that provide stiffness in both directions (axial and radial). In the configuration, three different symmetrical sets of springs per side have been used on both sides.

Earlier, these three springs on both sides were used but now started using four pads instead of the spring, two on the left side and two on the right side. The used mounting element was the same from the Mono700 (that was with six spring sets), and here in the Mono500, four elastomer pads are being used. Earlier, these three springs on both sides were used but now started using four pads instead of the spring, two on the left side and two on the right side. This behaviour can also (with neglectable deviations) be modelled with these spring sets. Therefore, only the four elastomers out of the six springs are being used in the model. A single spring was representing a set of springs before. In addition, now, one spring represents one elastomer pad. The middle ones are not active in the Mono500. Car Suspension on Sling Platform based on Coil Springs.

Counterweight: Counterweight is used to balance the elevator car, and at the same time, it provides safety to the car. C.W is like a catalyst to the motor that reduces the amount of energy motor need and it also decreases the amount of braking which produce less strain on the rope. Furthermore, this increases the life of the cable and makes the elevator safer. Figure 27, shows the C.W in the 3D view.

The frame of C.W define the initial position of counterweight based on car position, and it provides the degree of freedom to the counterweight. Both the MBS element C.W and compensationC.W define the mass, inertia, gravity and movement. Sensor CW is responsible for the movement and position of C.W, then the Pulley C.W, which depict the deflection of the pulley.

71
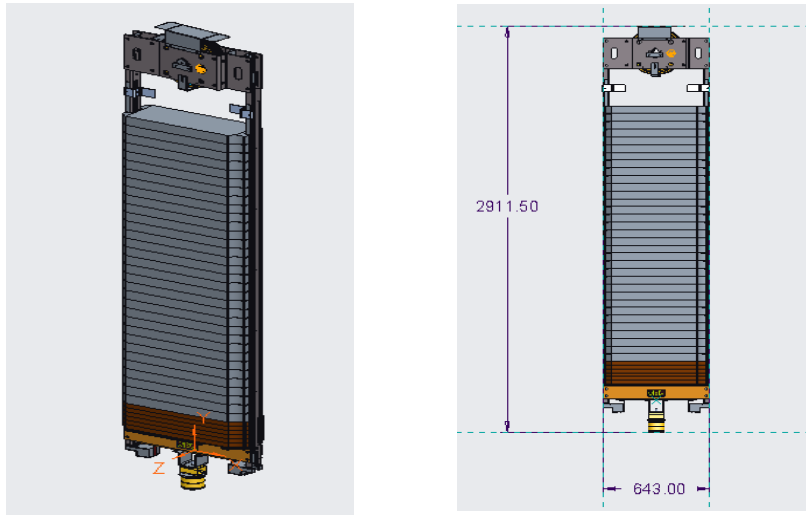
Figure 27. Front (left) and back of C.W (Right).

Rope: It connects the elevator car to all the other component of the elevator system, Cable is connected to the control equipment on top of the elevator and the elevator car, cabling relay power. Arrangement of hoist ropes in which one end of each hoisting rope passes from a dead-end hitch in the overhead, under a car sheave, up over the drive sheave, down around a counterweight shave and up to another dead-end hitch in the overhead. The car speed is one-half the rope speed. Figure 28, shows the 2:1 raping ratio configuration in a general elevator that has been used in this configuration. Flexibility of the rope and low internal damping characteristics largely determine the resonance in the system that leads to vibration [23].
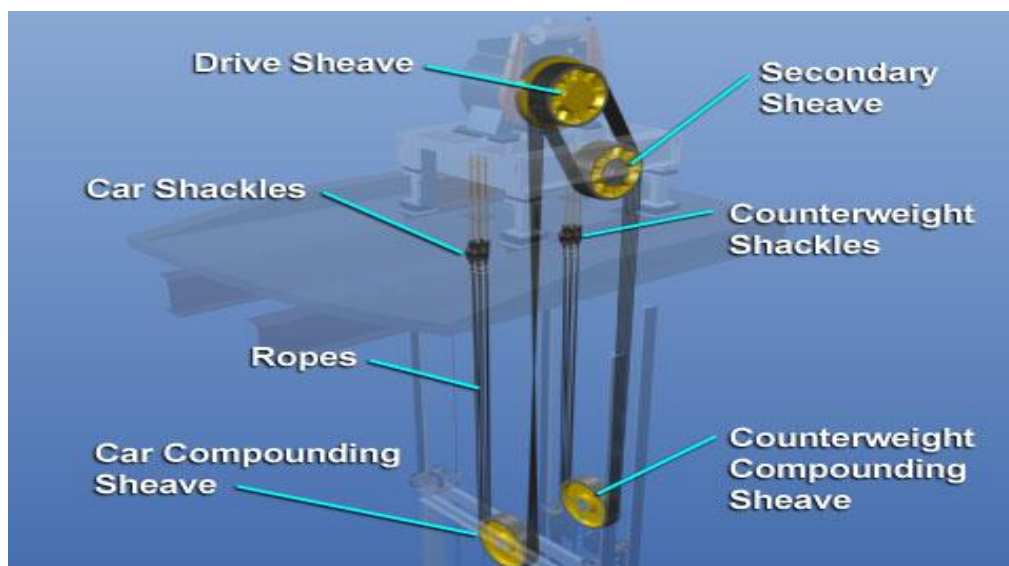
Figure 28. Roping Ratio 2:1[96].

In the modelling, the Rope length-dependent mass is split up into mass one and mass two. The Spring damper element has been used to represent the rope length dependent on stiffness and damping. Constraint one and two calculates the correct initial positions based on the connected elements. The element is directional. Positive force direction as indicated by the spring-damper element. Gravity is defined in the same direction.

Guide Rail and Guide shoes: The shoe is a sliding segment between the elevator guide rail and the floor, that is being said to be tracked. It mounts the car on the guide rail and makes the car move upward and downward. Oil cup upper lead shoe can reduce shoe line friction and lead the rail. The guide shoe installation method is to place it in the location of installation of the car frame's guide rail. After finding the right position, use the bolt to fix it on the rail frame of the car guide. The installation must comply with the following requirements:

1) Placing the upper and lower guide shoes in the appropriate position, they should be on the same vertical side.
2) No slant or deflection permitted. Both roller guide shoes and fixed guide shoes meet the same specifications.
3) Adjusted guide shoes are used mainly for FOVF systems, the clearance between the two sides should be compatible and the clearance between the inner liner, and the top of the rail should be inside O. Dimensions 5 ~ 2 mm.

The guide rail shoes connected to the cabin. There are two guide Rail shoes in the model, one is a for car and the other one is on the Counterweight side to support. The guide shoes that are mounted on the car will travel up and down along the mounted guide rail that is built on the wall of the building's well way to prevent the car from deviating or swinging. The guiding interface ensures the relative position of the elevator car and counterweight along with the height of travel [94]. Lateral vibration directly depends on Guide rail shoes, so it is important to provide a proper parameter to guide rail shoes in order to reduce vibration.

The inside component such as stiffness and guide rail misalignment and sensor that has been used for guide rail. There are four sets of guide shoes installed in each unit on either side of the upper beam and under the safety clamp seat at the bottom of the car, and four sets of counterweight guide shoes are mounted on the bottom and top of the beam.

Travelling Cable: A cable made up of electrical conductors providing an electrical connection in the hoist way between an elevator or dumbwaiter car and a fixed electrical outlet. Elevator travelling cable is vital to the link between the elevator car and controller [30] as shown in Figure 24 ,many of these cables are replaceable, with no serious consequences from any failure. The standard size of travelling cables are bare copper vest PVC made with the size of 0.5 mm^2 with PVC vest capable of withstanding temperatures up to 700° C. It can withstand the temperature up to 70 ° C. It will be put inside the car as some constant value like 0.8 kg/m. Travelling cable affect the lateral vibration of the system. The dynamics of a travelling cable and Natural frequencies has been discussed in chapter 3 and vibration and frequencies have been investigated and validated in section 7.1

Electric Motor: In an electric motor, PMSM is being used at both the motor as elevator traction motor and load motor. PMSM has numerous advantages over other motors such as I.M(Induction motor) [2],[75],[97],[98] that are conventionally used for ac servo drives. The stator current of an induction motor contains magnetising and torque producing components [22],[76],[99]. Investigation into the Electromagnetic Field Simulation of a Permanent Magnet Synchronous Motor As a result, for the same output, the PMSM will have a higher power factor (due to the absence of magnetizing current) and will be more efficient than the I.M. The standard wound-rotor synchronous machine (S.M) [100] on the other hand, one must need to do excitation on the motor, which is commonly supplied by brushes and slip rings.

This suggests rotor losses and regular brush maintenance, which means downtime. Note that the key reason for developing the PMSM [2],[75],[76] was to get rid of the preceding disadvantages of the SM by replacing its field winding, do power supply, and slip rings with a permanent magnet. The parametrisation of the motor has been done inside SimulationX.
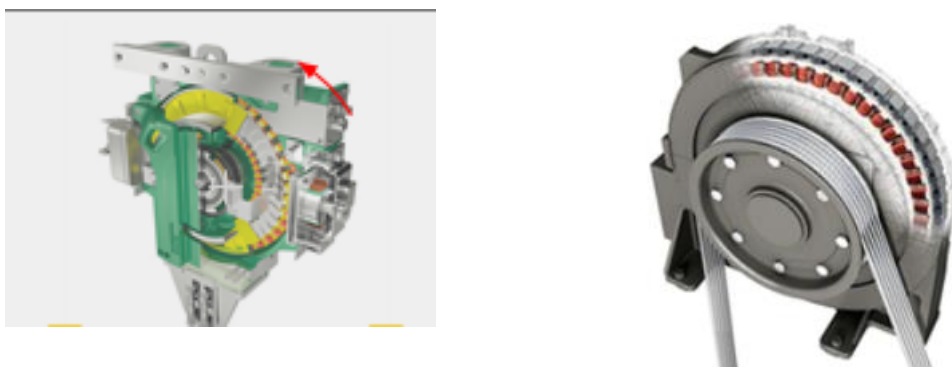
Figure 29. Virtual Motor (left) Real motor(Right) [101].

To achieve good ride quality, the motor shaft speed is controlled so that the car follows a specified velocity profile $\omega * m$ within the computer simulation, a well-known vector control technique directed to the magnetic flux has been applied [102]. Figure 29 shows the motor, it consists of a KONE eco disc, inverter, control model, protection and sensor in SimulationX. Since the inverter and the emachine (Electrical machine) are directly connected, the inverter will provide power to the motor in the event of a power outage. Sensors have been used to detect any damage or faults as soon as possible. Since the motor will not be changed at this time, only the motor has been installed; however, the author will work on this later. Motor (PMSM) powered via an inverter that supplies a pulse width modulated (PWM) voltage which will later help the model in providing high voltage.

Controller: The controller is a crucial part of any simulation. It is considered as the brain of the system [103], [104]; It contains the central operator logic of the elevator system. It is connected to every part of the elevator system. It monitors the elevator car and landing calls and allocates priorities to them. Various simulation models have been developed for the inverter, cable and motor; also different simplifications degrees were adopted to ease the simulation burden [105].

Most of the controller parts are still basic SimulationX models and these are not necessarily identical with the industry controller. However, it has worked very well so far, so it was decided to stay on this level for the controller part. A PID controller is used to regulate temperature, flux, friction, rpm, and other process variables in industrial control applications [104]. The system robustness of motion always requires very high stiffness in the controller [70]. Here in SimulationX, all the controller element has been collected inside one compound. In order to control process variables and to be the most reliable and efficient controller, PID controllers use the control loop feedback mechanism.

The overall control is cascaded:

1) The motion controller (FMU) sets the desired velocity for the PID controller based on the current position, velocity and requested floor.
2) The PID controller sets the required torque based on the difference between desired elevator speed (from FMU) and the current elevator speed derived from shaft speed.
3) The controlled inverter sets the currents for the electric phases of the machine firstly This control is based on a coordinate transformation of the machine into a $dq0$ representation [43]. Then the control consists of several parts, including a

PI controller for the current d and q with the mentioned gain estimated by the inductance L_{dq} and which has been mentioned in the parameter of the inverter.

Parametric Block: A new element is used multiple times has been termed as a parameter block (has been shown in Appendix 3) for hoisting machine (Param_HIL) in which the most common parameter has been collected like general(initial and desire floor, travel height), rope (stiffness, damping and linear density), drive(traction sheave and Nominal torque) and position (Fixation and traction sheave).

Reduced 1D Model (Code Export for Performance Check)

SimulationX application influences performance (i.e. by result windows, GUI, etc). The model has to be run without the application in order to have a good performance estimation; that is why code export has been done for performance check in which it removed all the necessary element [49], [50]. The code export defines the models, fixed-step solver (by using Euler forward integration method), calculation step size (0.05 m/s) and output step size (0.1 m/s). Only the output parameter has been used to check the quality of calculated results.

Features of Reduced 1D model:

1. Controller & Emachine part of the HIL are not needed inside model and it is substituted by torque source for a single run.
2. No animation and simple torque pre-set.
3. Stiffness of the ropes was limited to 3000 kN/m in the CodeExport models
4. Used for performance analysis & comparison.
5. Unnecessary elements got removed for the CodeExport to have a good performance approximation.
6. Model without signal connection to the tester.

An overview of different solver settings, as well as the available fixed-step solvers, available in the SimulationX help centre. The matter of choosing the best solver for the problem and the system is very complex; However In the final models running on the HIL, the Euler Forward method for fixed-step solver has been used because it has the best performance In the help for fixed-step solvers, Heun's method has a different stability domain (area) compared to the Euler method: It covers a wider range of the imaginary axis eigenvalues of the model. but it also comes with a longer computation time, which was not double anymore for real-time conditions on the Beckhoff system.

Stability for the solver method requires choosing the minimum step size such that the product $h * \lambda$ (step-size * Eigenvalue) lies inside the stability boundaries of the solver for all eigenvalues λ of the model. Using the SimulationX natural frequencies analysis, these eigenvalues for every model can be calculated in the post-processing tab of Natural frequencies under SimulationX. It means that a higher step size will not affect the real-time boundary but will lead to eigenvalues outside of the stability boundaries, leading to an unstable simulation. The model can collect multiple parameters while testing simulation. Additional effects can be examined directly at the time of testing. There are two models that has been prepared in order to check the performance and The 1D elevator model was built as a performance benchmark. After comparing the 1D and 3D model it can be seen that the 1D model is easy to use and takes less time to do the simulation but compared to the 3D model, the 1D model only provides the vertical movement and vibration which is enough for controller testing but still, it does not gives the vibration in all directions.

Table 4. Comparison Between 3D and 1D Model.

Comparison 3D vs 1 D model		
S.no	3D	1D
1	Masses of CW pulley and CW separated	The mass of CW pulley and CW are together and the pulley car comprises the inertia of the two pulleys
2	PulleySensorCW gives the position of the pulley	MassCar comprises the mass of cabin, doors, load & travelling cable massSling comprises the mass of pulley beam & two pulleys
3	Car and sling are connected	Car and sling are separated by spring-damper representing the mount elasticity
4	Guide rail interaction and It does not provide rail force over velocity	No guide rail interaction and Possibility to give a rail force over velocity (e.g. by measuring from MBS model)
5	It gives both the vertical and lateral vibration	Only gives only vertical movement and vibration. No COM positioning in the lateral direction (No of balancing)
6	More element inside the pulley, two-car pulley with 90° contact angle	Reduced pully element, two-car pulley with 180° contact angle
7	Length of dependent mass of complete rope is together	Length dependent mass of complete rope is split up to mass 1 and mass 2
8	Electric machine compound is together	In drives, electric machine compound is split off

Current, the 3D model is slower than real-time but it gives a simple and low-cost virtual prototype [106], [107]. Table 4 summarises the differences between 3D and 1D model.

The motor current step response test (setup a step of the desired motor torque and measured the motor current response) does not affect the motor, but it gives an inside view of the realizable dynamic using this load motor. The step-response time shows the limited frequency of the torque applicable with the load motor. Applying higher frequency effects to the motor-under-test would require a setup that allows for a higher dynamic. The executable model will also be created for all three models, elastic, elastic with slip and rigid. The executable model and load result will be loaded into the SimulationX curve set. Their FMU will be later put inside the Beckhoff then a performance check will be done where the time element gives the dedicated time for every single step. This model represents an event when the car is placed at a certain shaft height and the auto electric brake system is used on the system.

The system analysis and design of elevator tends to be relatively simple with this modern and advanced SimulationX software, i.e. equipped with relevant software programme Modelica and different library that's easily do all the calculation that is described in chapter 3.

This chapter described how the system simulation work, why a virtual model is necessary for simulation work, and how the model's virtual prototype possesses the same characteristics and behaviour as a real hardware system. How the elevator component has been designed. The virtual prototype of the elevator model has been used in HIL test rigs, where the analytical results are validated by data from a real system. The proposed real-time capable synchronization model combines the rigid multibody system approach with a multiscale simulation approach. The procedure related to FMU and methodology will be discussed in the next chapter.

6 STATE OF THE ART

The main aim of the thesis was to create a virtual prototype of an elevator model which and later it will be put inside the Beckhoff for HIL testing. After the replacement of hand-coded Beckhoff elevator behaviour and the load model by a code [108],[109] Functional mock-up unit, it could be possible that is a simulation generated out of elevator system models and It is possible by the use of hardware in the loop simulation [108]. This chapter consists of a description concerning the procedures related to improvement and drive software testing [110]. As stated above, the research was on to replace the physical Model with a virtual SimulationX model. In the past, the hoisting model in HIL was very simple because it only consisted of masses and inertia. The elevator industry consists of a digital transformation because it moves from a state of physical testing to simulation [109]. The research tries to improvise the previous Beckhoff system to promote the testing method [111].

A lumped-mass model of point masses joined by springs and dampers with the corresponding stiffness, and damping coefficients can be used to model the suspension rope. A series of ODEs is used to define those models [23]. The number of individual mass points refers to the system's degrees of freedom (DOF) and the number of normal frequencies and mode forms that are taken into account. Through updating the models at each time level, this method allows for the simulation of vertical vibration during flight [24]. The roping ratio is 2:1, which means that the elevator car goes twice as quickly as the cables. The machinery uses half as much energy to lift the elevator car, and the elevator's load capability is doubled [108]. Some specific features are desired for the HIL model. The considerations of elastic rope and rope slip play a very important role.

The research would result in a hoisting model with increased stability. The first phase in comparing results has been completed. The 35-second calculation time is reduced to 20-seconds, with the support of HIL or real-time emulation, the latest applications for the HIL main control unit should provide the old features, and, the hardware equipment will be replaced with virtual/digital components [110]. The Beckhoff computer code is used to model the virtual load in current systems.

The following features should be used in the elevator model: Rope flexibility (3 mass system), which considers damping and elasticity, although it will be built into a three-dimensional model in the future for greater versatility, the rope sliding through the traction sheave, and scripts for loading and unloading (predefined load change patterns)

Model accuracy will be measured outside of the test benches during model planning. Along with project engineers, the resulting draft versions are implemented on-site [110]. Previous efforts to use existing hand-coded patterns for elastic ropes and slides in the HIL bench resulted in instability issues. If these phenomena occur in Simulation X-based models as well, they will be investigated together. The HIL simulation models that result from the draft models will gradually replace the motors in the test benches.

The new model must work at least in the car Position control loop, which contains the shaft simulator. If the same model cannot be used in the load torque control loop due to stability problems, a different (rigid) model may be used. Another key move was to finalise the rope elasticity and slip value in the model. as a result, To begin, the old stiffness value from the previous model (MONO 700) was used, and other stiffness values were tested. Many Simulation was done to verify the model's stability and vibration.

6.1 HIL operation and its Function

Hardware in the loop simulation is increasingly emerging from a control prototyping technique to a framework for device modelling, simulation, and replication that therapeutically combines many physical and computational prototyping benefits. HIL technology is known as Hybrid testing or Model-in-the-Loop Simulation (MIL). HIL simulations are described in a variety of ways [59], [111], [112]. It mainly plays a role in acting as an interface between plant simulation and embedded systems under test [113] [114]. In this case, HIL testing is characterized as a test system that uses both a numerical model and a physical system to execute it.

HIL Simulator for Elevator Drive SW Testing

The purpose and testing of the HIL simulator for elevator drive software testing have been identified in this case. The goal was to design the elevator model within the Beckhoff machine. The mainstream implementation of emerging methods encourages shorter times in the testing process, such as continuous integration. The HIL simulator would explicitly delete research and measure a non-real-time simulation performed by the workforce, giving more test precision [115]. Figure 30 represent the HIL testing software and hardware component. The HIL consist of hardware devices that are brown and software devices of blue colour which are available in the device. A normal line means that it shows that the device is working normally because the signals are moving normally,

Therefore, a command can be executed. The motors are rigidly interconnected with each other. The second motor works directly with the frequency converter, and they are sure connected with an available three-phase wire and hardware and bus [114], [116]. The frequency converter plays the role of taking an incoming power and converting it to output power.
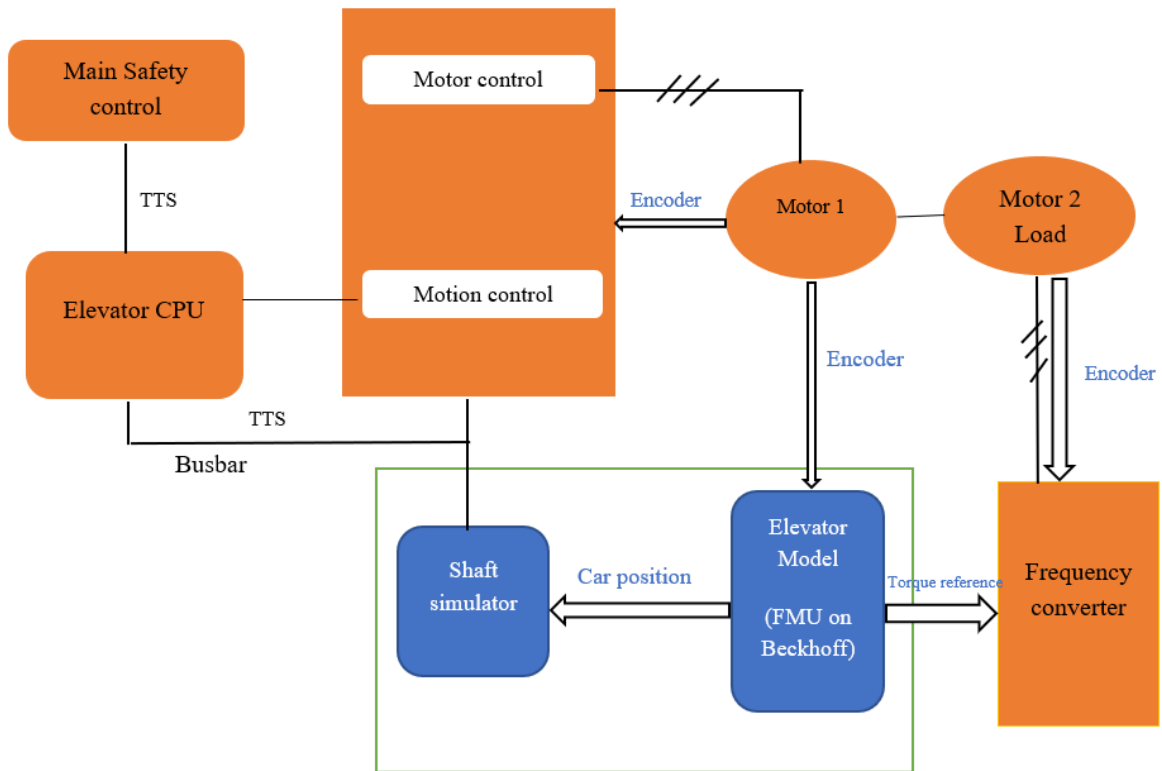
Figure 30. Description of HIL testing the drive software.

The frequency converter consists of motion and motor control (the drive-DUT) and hardware drive, together with the elevator model and simulator are in the HIL and it will be tested. The elevator motor (Motor 1) and the load motor (Motor 2) play a role in providing an encoder to both the frequency converter and the drive. TTS (Trip transfer switch) is a kind of trip switch that can be used when transferring load or protection from one bus to another. It plays a role in converting all the (safety) communication protocols in the elevator. MSC (Main safety control) is the master of TTS communication. The load frequency converter and the elevator frequency converter are under test since they play a variable voltage and power responsible for controlling the motor. The hardware in the loop of new models is used in cars as a control loop. It promotes the carrying out of automated testing in the vehicles. It is important to promote stability by using a rigid model in cases of load toque to promote equilibrium.

The real-time hardware in the loop simulators helps in improving the simulation analysis. The real-time simulator is interfaced to a type of prototype controller. In cases of real-time simulation, the simulation time has to be synchronized with the actual time. In the end, the computations for every stimulation time are completed within the same time as that of the real world [117]. It enables an individual to test an embedded code without the presence of a hardware system. The real-time computer hardware is one of the determinants of the performance of the hardware in the loop. The real-time behaviour can function well when the simulation sampling frequency is faster than that the expected switching speed of the existing system.

6.2 FMU

Functional Mock-up Unit data is a file that consists of functionality that can be invoked through co-stimulation or model exchange. It is a form of a ZIP archive that contains a file that can be edited after generation from SimulationX by the Modelica [118]. It is an open standard for exchanging dynamic simulations between different tools in a standard format. It is an open format in which simulation models can be imported and exported using different tools while maintaining the same Model.

Function of FMU

1. It plays a role in costimulation in the presence of an elevator model in the Beckhoff, which has more details.
2. Function mock-up unit encodes different signal inputs. Intense development of SimulationX's FMU functionalities to be compatible with Beckhoff's TwinCAT FMU import [118].
3. FMU acts as an input of the parameters, which can be changed in the case of the Beckhoff system.
4. FMU provides the means of model-based development for designing different functions.

SimulationX code export

The overall simulation model stop functionality that is transferred to the FMU by use of StimulationX code. The Model consists of solving a fixed step in addition to calculating the step size. It plays a role in defining the inputs and outputs which are needed for analysis. The stimulationX code export ensures that the safety and correct behaviour are maintained with no critical behaviour.

It is important to properly choose the real-time environment as a form of simulation setting before the exportation of code. The process of accessing model parameters is easy. It involves double-clicking into an empty region of the structure view. Through this, an individual can get access to use the FMU through the parameter; simulation X can lead to coming up with an FMU because of the availability of the post-processing option. The generation of FMU is possible SimulationX through the Post-processing option. MS Studio Express 2015 was used to modify the compiler in this study. When optimizing, there should be no errors. If anything does not function, there is always the option of inserting a value to test the outcome. The created FMU can be found in the file path specified previously.

TwinCAT FMU Import

A TwinCAT import importation can be possible with Microsoft Visual Studio, Beckhoff TwinCAT, Beckhoff TC3 Target for FMI. Before the actual importation process, it is crucial to ensure that creating a user certificate with and activation of test signing is in place. Execution of the FMU is done in the TwinCAT. It is vital for fulfilling the environmental requirements that are in place with Beckhoff. The available hardware determines the possibility of making changes in a file.

A backup should always be ready and available. The backup consists of any hardware or installation process to avoid various damages that result when a system fails. The most useful things that should be confirmed for functioning include the functionality of the FMU and expected torque level during the operation of the FMU on the HIL.

Start of TwinCAT FMI module via menu TwinCAT; It involves choosing SimulationX as Generation Tool and COSIMULATION as Solver (Only FMUs with included source code can be imported)

The FMU is unpacked, and a C++ project is created after pressing Start the source code located beside the FMU. TwinCAT attempts to create a C++ project. It is critical to conduct sufficient model validation before developing the FMU to avoid any build failures and delays in receiving quick feedback by using the technique of Regression testing in C.I.

Import of the C++ project and object

The FMU can be included in the TwinCAT project tree, and the C++ object can be inserted as well so that it is accessible at the top. The TwinCAT signing, TC certificate name, and certificate password should all be saved in the project's property. The cycle

time should be modified to match the step size of the FMU. Based on the priority, the assignment should be changed. The parameter should be changed from UseTaskCycleTime to phase size after FMU is activated from the result table. The TwinCAT project is deployed onto the desired target using the activate configuration command. The FMU will be used and executed if the C++ object is included in the project tree.

6.3 Testing of HIL simulator

Hardware in the loop simulator test has been adopted widely to improve the quality of different software. Different researches have been done over the years, and HIL research has been used successfully in various applications. Compared to conventional human-based testing, a HIL running testing framework is simpler and more impartial. Multibody dynamics is used to explore the effect of integrating nonlinearity and discontinuity into a HIL structure. Also, it was determined that the actuation system delay frequency should be 20 times greater than the system natural frequency to maintain the system simulation steady during HIL testing [111].

To commission and measure motor controls, HIL systems are applicable. The main Physical hardware elements of these test systems include that has been shown in figure 33:
1. Electric drive motor for an elevator type
2. Electric motor for emulating the load of the complete elevator (connected to the drive motor)
3. Drive motor controls
4. A Beckhoff system runs the load simulation of the elevator and sets respective torques to the load motor

A PMSM is used in the drive mechanism, and it is a drive that is widely used in a wide variety of motion control applications. It is operated by a pulse width modulated (PWM) voltage supplied by an inverter. In Figure 30 the two frequency converters can confuse; two prefixes will differentiate between the elevator components: one for installation at the elevator user site and the other for load side emulation in the HIL test. In the load drive, the torque comparison filter is used. Elevator CPU sends run commands to the elevator motion frequency converter controlled by two independent control boards. It would be more beneficial to first consider the workings and functionality of Beckhoff as the Virtual porotype of the elevator model to be placed within Beckhoff.

Beckhoff currently performs three functions:

1) Contains an elevator model that will be replaced by a new MONO 500 MBS SimulationX Model.

2) Makes related modules, such as the Load Frequency Converter and the Main Safety Control, work quickly and efficiently.

3) Adjusts input/output values according to the interfaces' specifications

These parts only include Beckhoff detail, which entails how the Beckhoff will be configured for the current hoisting model. Beckhoff is not related to the elevator model. Manual and automated tests are presently being conducted out in the HIL laboratory. While more than 100 cases are also being tested in manual testing, only approximately 15 cases are focused on in HIL primarily. Driving-only situations will be put in place in the future to save time. The elevator model can be parameterized with the automated tester, and it is still needed, but the interface must be changed.

The major types of errors currently being tested in the HIL laboratory are communication error which mainly consists of delay in communication time, an encoder that causes signal problems wire, fault code, and elevator setup.

The pulse will increase by 16000 per turn and will also increase inside the PLC. The Beckhoff code will be included inside the Model. At the start of the elevator simulation, only the shaft simulator parameter can be modified or edited in the GUI. Since there is no actual car, counterweight, cables, or tube, much of the elevator circuitry and elevator motor is present. Since there is no actual vehicle going inside the shaft, the elevator must be simulated using a shaft simulator. A gadget called a door zone sensor (DZS) reads magnets mounted on floors in a real elevator. DZS and magnets are not found in simulators that are not in operation. The DZS and the shaft simulator both have the same signal for elevator motion control.

The various shafts can be simulated by adjusting the floor positions within the shaft simulator and that can quickly shift the shaft from a three-story apartment building to a 100-story skyscraper, for example. It runs on a PCB that is identical to that of the elevator CPU but with different applications, Since the elevator model (inside the FMU) depicts a damped structure, the simulated car can be stable in a specific location for a given shaft angle. There is verification of the behaviour in the case of modelling in SimulationX.

That could happen because of HIL system time delay and insufficient hardware performance of the FMU signals, and instability results from the shift of the control signals. Both these cases can result in the increased oscillation of the output torque or the HIL control signals, prevent the instability of the result by testing the model performance.

To view fault codes and control elevator parameters, a special software programme has been used. It's even been used to call the elevator from a vehicle or a landing. This tool can also be used to adjust the elevator settings. The torque, strength, and torque of the elevator traction motor can all be seen.

HIL Deployment

Deployment refers to installing, checking, and then running the program, and it is the last step before testing. Some things needed to be developed before HIL implementation, such as how the components are linked and their functionality which has been described in section 4.3 HIL (Hardware in the Loop), and the safety and security function [119]. Through this, great improvements can be made to the system. The overall system outline was addressed and investigated,
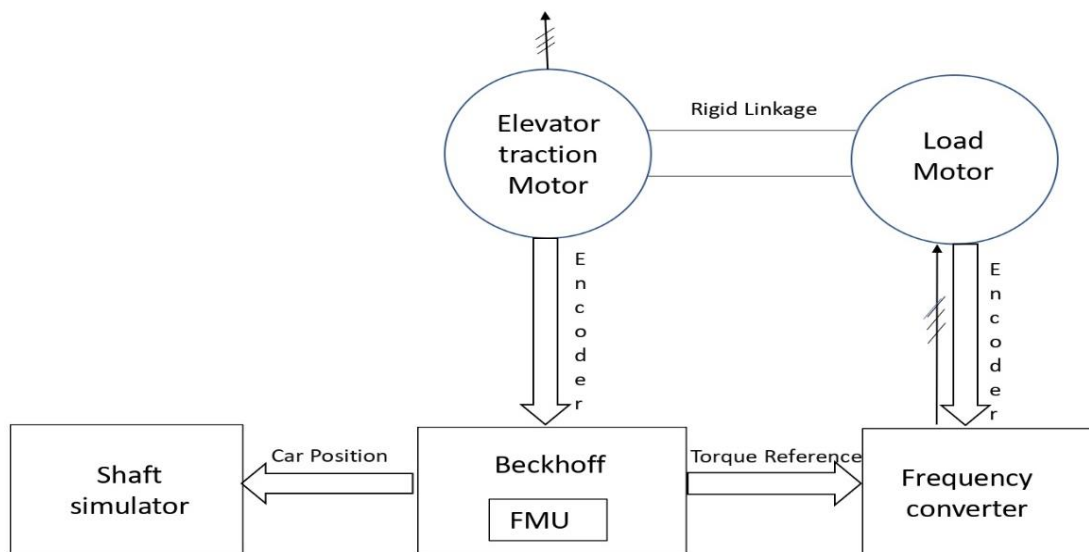
Figure 31. Detail Schematic diagram of HIL Tester.

and the estimated torque level in FMU preparation, after which adequate explanation of backup and restore management was given. Figure 31 describes the HIL testing, in which the research team uses HIL testers for a simple elevator model; the simulation model has been improved using a SimulationX model. The model is going to be installed on

Beckhoff, reducing the testing time of the software from four weeks to 20 hours. Where position will be controlled by shaft simulator simultaneously Torque and speed of car will be given by frequency converter. If the current manual testing in a real elevator is replaced with HIL based automatic testing, Jenkins and SimulationX models able to reduce the error and aid in automating testing.

The elevator model's interface can be modified, and the shaft simulator can be parameterized and monitored using PC tools. Since the Beckhoff elevator model and the shaft simulator are not related, the shaft length must be set independently from the Beckhoff elevator model and the shaft simulator. The response of the traction motor to the torque reference step (via load motor) must be set up. There must be no delay in the torque output if the rope versatility is modelled and the response is inputted as a load torque to the elevator motor. The method becomes unreliable if the delay is too long, so the phase reaction test is performed.

During the software update, an analysis of the adapted TwinCAT project was carried out by replacing the original hand-coded model code with interfaced FMU, followed by offline testing of various PLCs using plausibility checks, FMU with test signals stimulated elevator FMU and stimulation of the Model with the measured signals. The following instruction set was used to quantify shaft speed, torque, direction, and velocity in the standard configuration (closed loop) where, the ABB torque relation set to zero / open loop.

1. AbbInterface.rSpeedAct – Shaft speed measurement (ABB output)
2. AbbInterface.rTorqueAct – Torque measurement (ABB output)
3. AbbInterface.lrSpeedRef – Shaft speed reference (ABB input)
4. AbbInterface.lrTorqueRef – Torque reference (ABB input)
5. MAIN.uiFreq – Encode input frequency
6. MAIN.lrH – Current position measured from bottom
7. GVL.yc – Cabin position
8. GVL.yw – CW position
9. GVL.vc – Cabin velocity
10. GVL.vw – CW velocity

The system was optimized for the model test by doing a backup of the entire HIL system, including the PC and PLC, to prevent any potential damage due to malfunction, and, Beckhoff PLC was updated to TwinCAT Beta software includes the installation of a TC3 target for FMI. Following the system description and Model evaluation, the HIL Model was deployed, where tests comprise functionality and plausibility tests in the project context. TwinCAT was prepared for the performance of a test model with no in-and-out

connections, and a performance model was tested in which execution times and PLC workload were observed and analyzed to see what the predicted results were met.

The HIL Deployment can be subject to risk reliability issues and computational efficiency bottlenecks. To address these issues, a simplified model would be created by omitting some dynamics features or reducing some DOF only for performance testing.

• The Beckhoff system's performance bottleneck

For this purpose, a new different PC has been used, and since the complex MBS model has more DOF, the existing Model of execution must also be prepared to use the latest version of the TwinCAT program. Model computing complexity can be reduced by omitting dynamic functionality and reducing the number of six DOF model components. Due to a cost problem, the alternate test bench was not used. Furthermore, the latest Model of execution must be prepared to achieve real-time operation, which necessitates using the most recent iteration of TwinCAT software.

• Stability problems in the closed-loop control for load motor

The use of a torque sensor on the motor shaft, which is not mounted in the HIL tester, will be a more powerful and stable version. It can be done using the virtual testbench model. There would be no need for the time-consuming evaluation of this alternate solution if there were no stability problems with the new installation. It could be one of the options if there are stability problems and the possibility of installing a torque sensor.

6.4 Functionality Test

It is a type of software testing that ensure the system is operating as intended by the business document's functionalities. This research and testing aim to see if the device is fully functioning. Functional verification mainly involves black-box testing and is not concerned with the application's source code. This testing examines the application's user interface, APIs, database, security, client/server communication, and other features. testing can be carried out manually or automatically [120].

For the HIL test, the functional characteristics of information systems should be checked. However, there is little support for non-functional testing of MBT methods, and non-functionality testing research is still ongoing by different researchers. As a result, only the functional testing is carried out here. The test necessitates performing the device design twice: once during implementation and then during testing.

As the accuracy-test was carried out in the validation phase using ride comfort based on car sag, bounce, and vibration levels, and the real-time capacity based on off HIL and on HIL was carried out during the performance phase, all of these techniques were used to achieve the best balance between accuracy and performance. Jenkins' C I. The environment allows functional and output tests to be automated. For verification of the results, measurements were taken both on and off HIL. Torque, position, velocity acceleration, and vibration will be investigated with proper input and output during the functionality evaluation. Functionality checks on a step-by-step basis

1. FMUs for testing from the FMI project [121]

2. On the Beckhoff system, the first models of the elevator model FMU

3. on the Beckhoff system at HIL [9]

Beckhoff specific

The Beckhoff embedded PC's two 1,75 GHz cores as described in section 4.4 Beckhoff aren't quick enough to run both the PLC project and the FMU object on a single core. A more powerful CPU is recommended for potential applications.
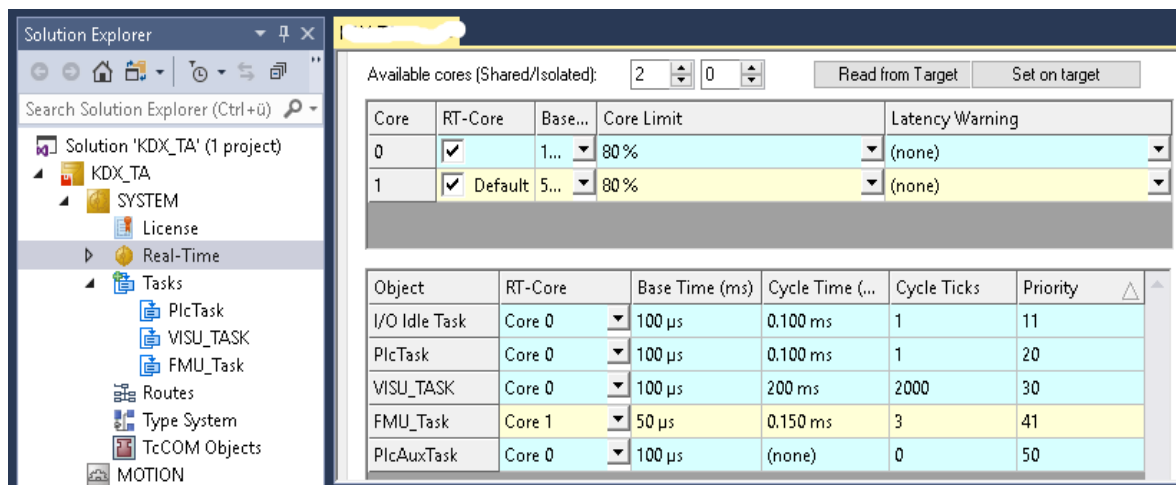
Figure 32. Beckhoff importing of TwinCAT.

Beckhoff TwinCAT importing is seen in Figure 32. TwinCAT was able to use the second core (shared, 80 per cent) as Windows could formerly use this core entirely and 20% of the other core. Windows now have access to just 20 % of both cores as a result of this update. According to a survey, the remaining unutilized TwinCAT CPU time is immediately provided to Windows. Then secondly the second centre is only responsible for the FMU mission. The maximum stack size value was changed to 4096 KB on the same tab.

FMU object to PLC connections

Connections between a PLC project and an FMU object do not exchange data immediately after Activate Configuration with the used beta version of Beckhoff's TE1420. The FMU importing in TWINCAT PLC is seen in Figure 33. The exchange begins after the PLC instance is manually switched to the OP→PREOP→OP state in the TcCOM Objects node. Some FMU parameter inputs, such as ratios and masses, do not allow for zero values depending on the model structure.
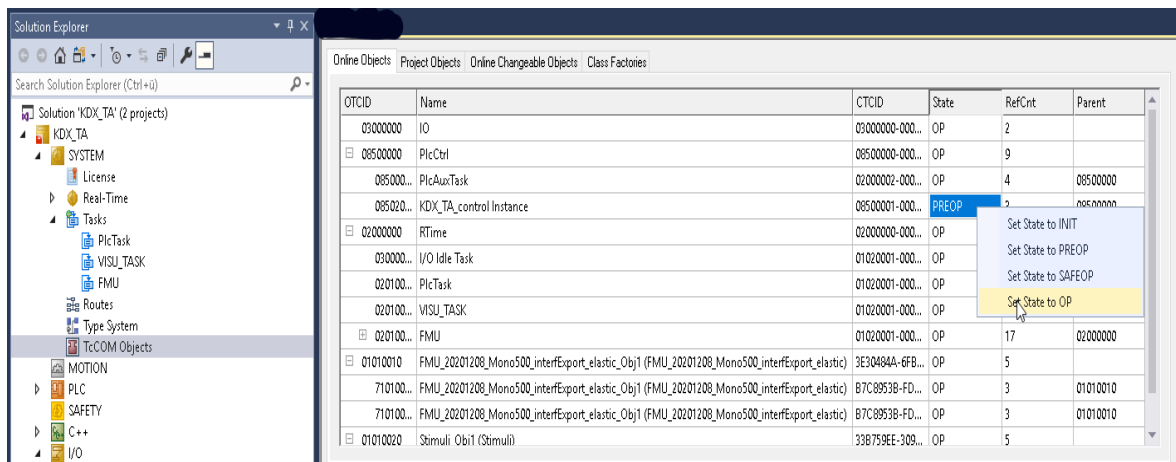
Figure 33.FMU importing in TwinCAT PLC.

Such inputs cannot be used with PLC outputs because data sharing begins only after the OP→PREOP→OP state transition seen in Figure 33 Both the inputs will be set to zero before the state transition, and the simulation (FMU model) will come to a halt immediately. The number of modified inputs for current FMUs can be reduced in the C++ project's.cpp file under TwinCATClasses. The number is defined by the third parameter of the... fmi2SetReal function in rows. For example, reducing the number of inputs to "3" allows only the first three to be modified cyclically. The other variables remain at their initial values during simulation. PLC code change is possible when any signal from and to the FMU has shared directly with the PLC code and only the PLC code. Value changes are made in the PLC code if necessary. There are only four sections of code changes; look for bFMU UseModel in the search bar.

1. In the declarations, a separate section

2. Calculation/setting of FMU parameter inputs, based in part on known variables.

3. From the FMU, retrieve the car's direction and speed.

Since the velocity is still used for security functions, this is only inserted as a comment. It is not advisable to use the values from the FMU here, and if there are issues with the

PLC-FMU link, the velocity could be 0 m/s, causing these security functions to fail. Before uncommenting, either the FMU connection should be monitored, or the security functions should use the calculated values more explicitly from the encoder input card.
4. Torque is given to the ABB frequency converter by inserting the shaft torque into the elevator model selection section.

There is KONE model introduced in the PLC code, with the FMU variant being the third. Some of the visualized effects (Velocity) are used in defence functions as well. Another KONE model is used explicitly in GUI controls, where reuse is impossible. A more generic approach to model collection and data visualization in the GUI would be preferable. After parameters, such as position, velocity, acceleration, jerk and torque, were investigated on HIL, with the ON HIL test bench providing the better results.

Since the elevator model (inside the FMU) depicts a damped structure, the simulated car should stabilise in a specific Position for a given shaft angle. While modelling in SimulationX, this behaviour was verified. However, due to two factors: first, the HIL system's time delays (for example, in electronic components of the feedback loops) or inadequate hardware efficiency, the FMU and control signals can experience a phase change, resulting in instability. There will be increasing oscillation of the output torque or either of the HIL control signals in each of these situations. The second scenario can be avoided by testing the model on its own, after that various testing level has been performed to check different scenario. Where verification, validation and defect analysis has been investigated as shown in process chart in Figure 34.

Test level
There are three levels of testing: unit testing, integration testing, and regression testing, all of which are conducted after the platform has been deployed to further boost the software testing.
Unit testing, also known as component testing, is a testing method in which specific units/components of the software are evaluated. It is the first and most critical stage of checking after the coding has been completed [120].
Integration testing is the process of testing a unit without having complete control over it and by relying on one or more of its actual dependencies, such as time and database [122], [123].
Regression testing is a black-box testing methodology that involves re-running experiments that have been affected by code updates. These checks should be run as often as possible [120].

It is being reviewed after a thorough understanding of the system and how it impacts current features. The tests are chosen based on the frequency of defects and the importance of the functionality. Many organisations automate GUI-based systems to automate the tester. Still, it was not feasible because changing the script for each modified GUI and then verifying was time-consuming, so this HIL and CI. has become the nucleus of the test bench for both automation and software testing, combining test sensitivity and robustness in most cases. Continuous integration is supported by test code (script) (unit testing and regression testing). The HIL simulation was chosen as It can reduce the time it takes for the production device to stabilize because it can detect and correct most mechanical and electrical failures [124]. Functional checks are used to validate the performance of software testing by supplying enough data and comparing it to the functional specifications.

Velocity, acceleration and jerk have been investigated on and off HIL. On and off HIL. The SimulationX model will eventually replace the hardware motor and load. The entire testing process is summarized in Figure 34 where the dotted line shows the data and result while the dark line shows the testing procedure, which includes parameter selection, a virtual prototype of the model, code export and TwinCAT import of the FMU, a HIL test bench, and functionality testing. To find the best balance between accuracy and performance, performance has been investigated on and off HIL and ride comfort of car sag, bounce and vibration, the wide range of assessment modalities available, as well as sources of artefact and prejudice that can significantly skew data obtained from a measure has been discussed and validated in the next chapter. Performance has been examined on and off HIL, and ride comfort of car sag, bounce, and vibration has been addressed and tested in the next chapter to find the best compromise between accuracy and output. Multibody dynamics has been used to investigate the effect of incorporating non-linearity and discontinuity into a HIL system. Real-time modelling of an elevator using HIL has been placed that is providing wider software testing and has decreased the testing time of drive simultaneously.

Figure 34. Flow chart of complete Testing Process.

7 VALIDATION

Validation of the model is vital during any research related to modelling as mistakes performed during modelling lead to errors in test generation that can damage the equipment and can be costly. the study includes seven sensitivity analysis. sensitivity analysis is a systematic procedure for investigating how reported results vary along with changes in the key assumptions on which the results are based [125]. In this chapter, Sensitivity analysis of the model has been done, where the author has done the numerous time simulation by changing different parameters such as load (No of passengers), No of rope, stiffness of rope, Elasticity, Travelling cable etc. and have analysed the effect on Rope force, car vibration (Vertical and lateral) - Vibration Peak to peak value, Damping, car position/velocity and sag. As it was necessary to fix the parameter, while there are different 1D model Variant elastic, elastic with sag and rigid and 3D model has been prepared during the research, but here the author has validated only the elastic with slip model as it was the most complex 1D model due to most no of the parameter. Herein all the model some value was standard like there is four Rope, the maximum load is 630 kg, the elastic modulus is 80,000 N/mm^2 and travelling cable is 0,487 kg/m, but all these parameters have been changed to validate the model.

Here for validation, firstly, the data of a real elevator has been collected and measured at the R&D site of KONE hyvinkää that was considered as base value and author goal was to achieve that same value from the virtual elevator prototype that prepared in SimulationX. The author measures the real elevator velocity and vibration in all direction and investigated it. Where the Low pass filter of 12 Hz has been used to remove external noise. The vertical velocity and vibration in the X, Y and Z direction of a real elevator have been investigated, where peak to peak value was approx. 55 Gal.

7.1 Sensitivity analysis of the model

Sensitivity analysis of the model has been done by changing the various parameters to validate the model; by identified simulation parameters, the car's lateral vibrations are investigated by changing several elevator parameters such as load, no of rope, travelling cable, elastic modulus etc. All the simulation results match the experimental ones precisely [126].

Vibration comparison between virtual elevator SimulationX model and a real elevator.

Figure 35 indicates a comparison between SimulationX and general elevator data obtained in terms of vibration against the duration with which the elevator car moves. The green line shows Car vibrations at 630 Kg, and the red line shows off-scale real data.
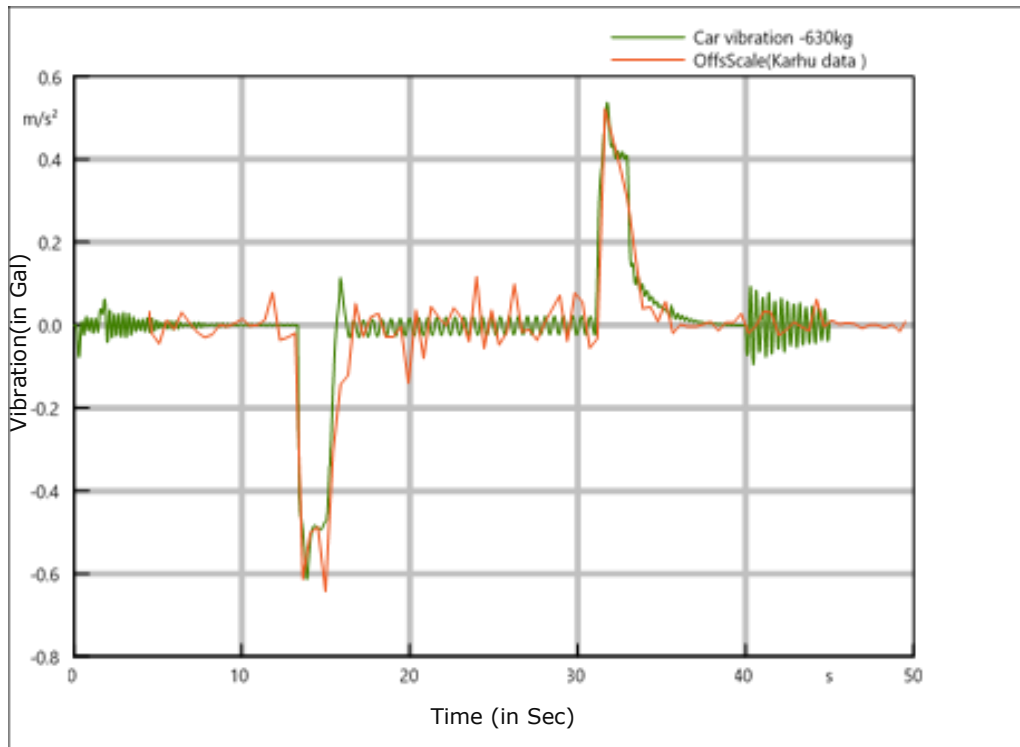
Figure 35. Comparison Between Simulation and general elevator data.

On the x-axis and y-axis, time and acceleration are mentioned, respectively. The value in the graph of simulation and off-scale elevator data are simultaneous to each other means very close to one another. Specifically, at approx 15 s, the elevator accelerates downwards with consistent speed and becomes a free body for nearly at t= 3 s at approximately 16 s and 31 s [127]. car vibrations go up to -0.5 m/s², which is quite good and in both upward and downward. The net force is pointed towards the downward direction, indicating the elevator's acceleration is towards the downward direction. In this context, the force of tension applied to the system is less than the elevator's overall weight. The elevator then accelerates upwards in a constant period

The free-body data indicates a consistent vibration to the right, implying that the forces subjected to the car elevator are equal [127]. During the 31st second mark, the elevator accelerates upwards at varying velocities between 0.0 m/s² and nearly 0.5 m/s²

95

before descending downwards at a constant speed. The vertical vibration is normally caused by torque ripple at the PMSM, which is transmitted through the car's suspension rope [23]. Then at last between approximately at t- 31 to 33 s, the net force is pointed upward implying that the acceleration is towards the upward direction. Therefore, the tension force is more significant compared to the weight of the elevator. The off scale signifies that the real elevator's data has been delay by some second in SimulationX to remove the human error.

In the following graph in Figure 36, the overall effects are defined as the changes in car displacement in comparison to the actual displacement. Offs Scale shows that the author has delayed the signal for some seconds to remove human error. Initially, In the virtual model, the car displacement is consistent between 0 to approximately 15 s at a maximum height of 18 m as opposed to the real elevator displacement that remains only consistent between zero and ten seconds [127]. The car displacement rapidly falls from 18 m to 0 m between 15 and nearly 33 s, while the real elevator falls between approximately 10 and 28 s seconds from 18 m to 0 m, where they both remain constant for twelve seconds and seventeen seconds, respectively. Therefore, the data indicates that the car displacement rate is more rapid than the general displacement, which is relatively slower. Nonetheless, the average displacements for both systems are relatively equal. The variance between both the car displacement is due to the late measurement of a real elevator, i.e. just a human error.
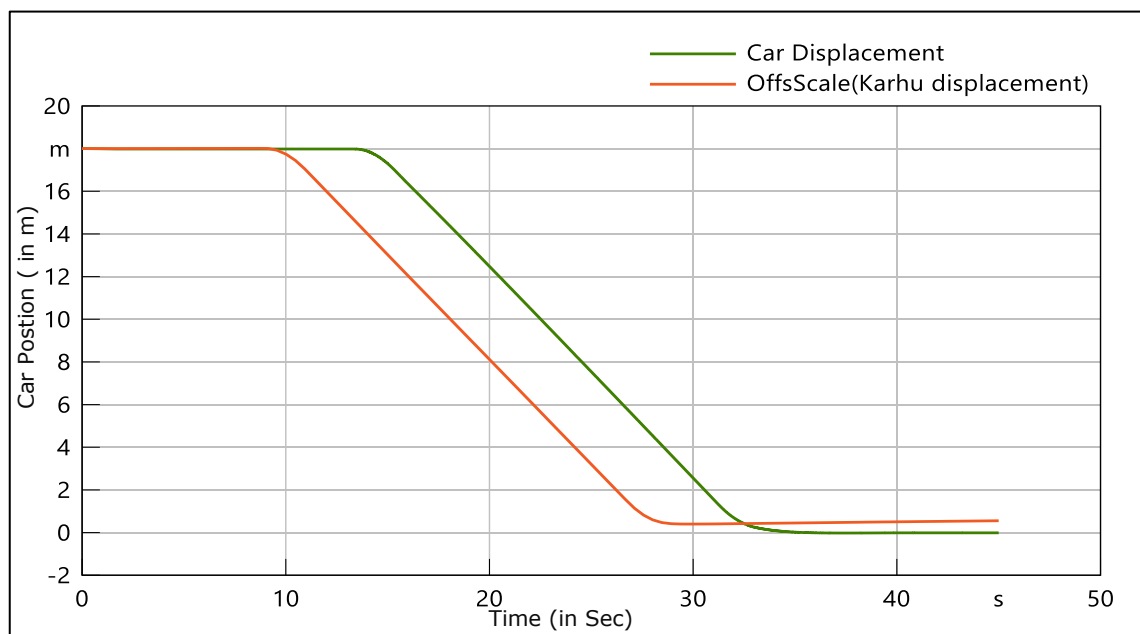
Figure 36. Comparison of Car Displacement and Off scale general elevator displacement.

Case 1) Effect on car vibration due to change in load 80,240, 400, 630kg

The mass of load and passenger number often changes during elevator system operation. The vibration behaviour is expected to change due to the varying elevator load [128], so vibration due to weight variation has been done and good result has been obtained from the virtual model. Figure 37 illustrates the impact on a typical elevator vibration based on the changes associated with distinct loads subjected to the car: 80, 240, 400, and 630 kg, respectively. Generally, it is essential to initially consider that guide rail shoes chiefly affect the lateral vibration of the car elevator while vertical vibration predominantly occurs due to the flexibility of guide rail shoes and the rope. The vertical vibration caused by torque ripple in the drive system, which is transmitted to the car through the suspension ropes [23].
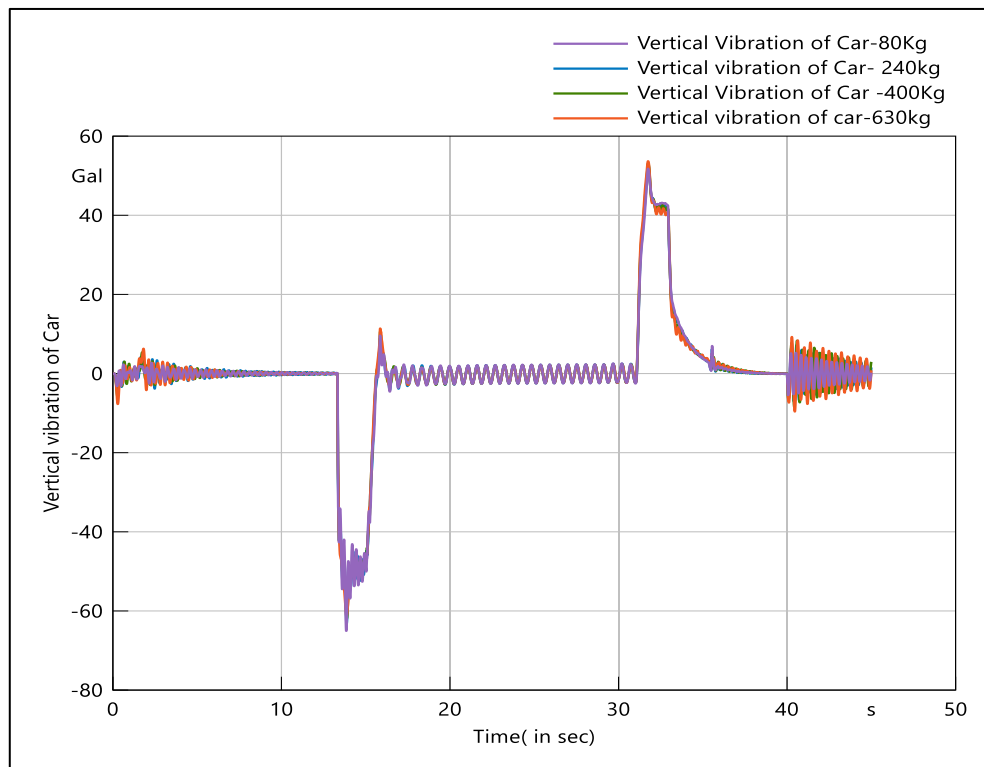
Figure 37. Vertical Vibrations at different loads.

Figure 37 shows that the elevator car's vibration amplitude is comparatively large when the exiting amplitude force is near zero and at t - 40 s (at the time of starting and landing the elevator) vertical vibration scale. The elevator's vibration amplitude due to different load does not vary much with the carload when the exiting force is near the zero marks [129]. In fact, in the whole travelling time, there is slightly more peak (vibration) at full load, but overall, it was a good result in order to validate the model.

The following graph in Figure 39 shows peak to peak value for 630 Kg load. Also, the highest peak value for 630 kg load is 11,24 Gal, and the lowest peak value is -2.881 Gal. So, the peak to peak value at 630 kg load in Gal is 14,221 Gal. In a real elevator, it was 55 Gal, there is quite a difference, but work is going on to increase the peak to peak value.
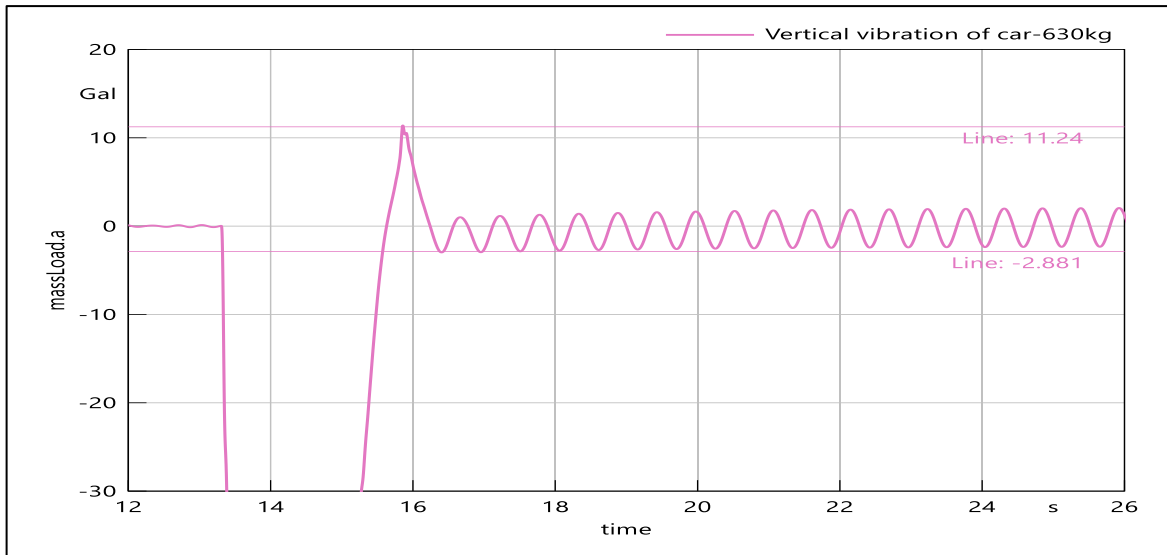
Figure 38. Vertical Vibration of the car at 630 kg load.

Case 2) Effect in-car vibration due to changes in the number of ropes

According to a recent study led by Qiu et al. (2020),[127], the number of ropes has a significant impact on the elevator car's vibrational acceleration based on the peak-to-peak gal values obtained from the system [127]. As the weight of the compensation sheave, which gives tension to the compensation ropes affects the lateral vibrations due to ropes [126], so it is important to analyse the effect of rope on vertical vibration. The next graph shows the effect on car vibration due to the change in the number of ropes specifically, vibrations of the elevator car are measured based on simulations involving two, six and eight ropes. Figure 39, illustrated while the vertical vibration of the car is almost the same with four, six and eight ropes, but the least number of ropes has a more sharp peak value throughout the journey in both the downward, as well as upward movement of the car elevator [129]. The graph mainly reflects the effect on car vibration based on the number of ropes subjected to the elevator.
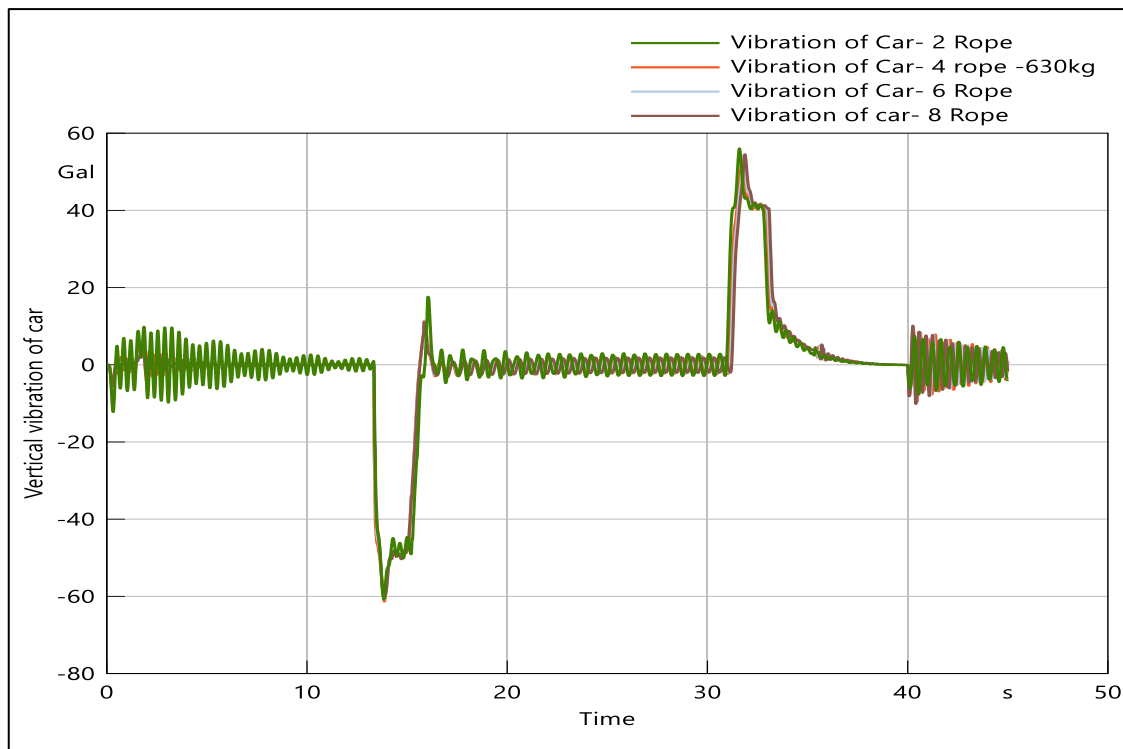
Figure 39. Effect of Number of ropes on Vertical Vibration of car.

Considering the lateral axis at approximately 32 s indicates a downward motion movement of the elevator car from the seventh position to the first position. In this context, the ropes indicated the highest Gal value of approximately 53 whereas eight ropes showed a slightly lower value of nearly 51 Gal. The number of ropes has a significant effect on the car's vibration. Specifically, the least number of ropes produces more vibration compared to the increased number of ropes. The stiffness of the car's main rope is greater than the counterweight side; however, the car can follow the traction sheave's motion, although the rope stiffness prevents the counterweight from moving in a similar pattern as the traction sheave. The counterweight assumes an upward acceleration increasing the counterweight side's rope tension, hence increasing the vibration intensity.

Both Figure 40, presents data indicating the peak to peak value on different ropes, which results from different vibrations of the car elevator. The first left Figure 40 involves two ropes that indicated a peak line value of 19,915 Gal. The second simulation process involved eight ropes that indicated a peak line value of 14,221 Gal, while the last process involved eight ropes subjected to a car vibration which produced a peak to peak value of 13,895 Gal.

99
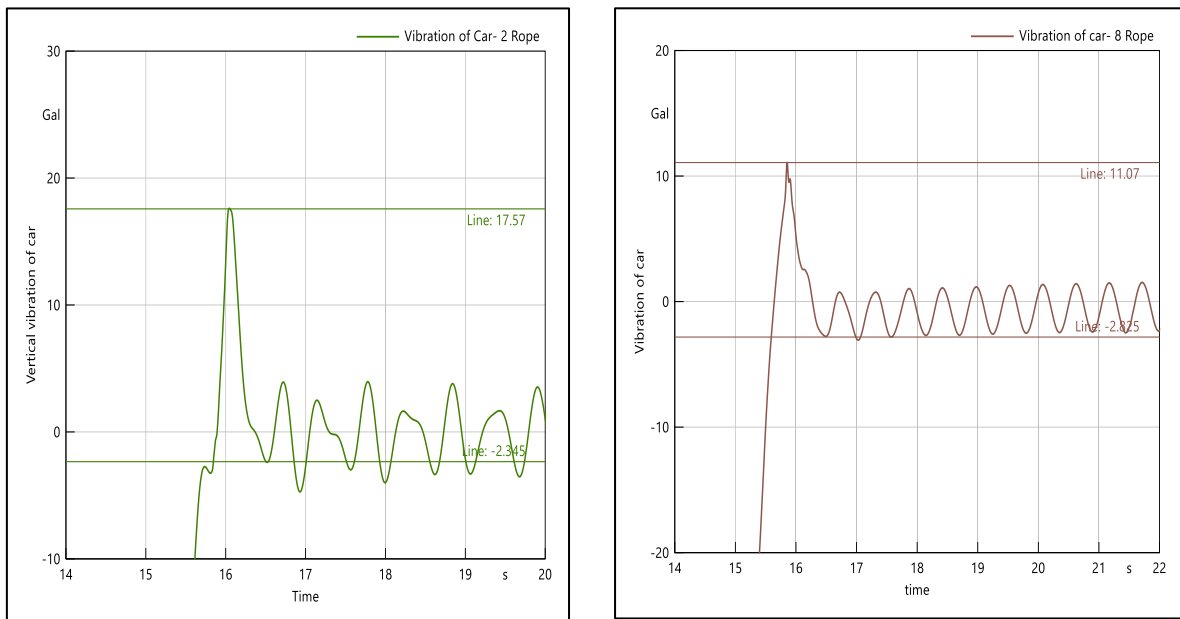
Figure 40. Peak to peak value of vertical vibration at 2 and 8 Rope in Gal.

The peak-to-peak value is also highest in the car vibration subjected to the least number of ropes. These measurements indicate that the highest vibrations both in the upward and downward movement of the elevator dependent on the least number of ropes subjected to a given weight within the car. According to Watanabe et al. (2013), the height and number of ropes of an elevator cause variation in the stiffness of the ropes resulting in varying vibrations of the car [129]. Considering the graphical representation above, the less the number of the ropes subjected to the car elevator the more the peak-to-peak value of acceleration. Specifically, a downward peak represents an upward motion movement of the elevator from the seventh to first floor. According to the research led by Watanabe et al. (2013), [129] such a result is crucial in analyzing the vertical vibration of an elevator based on its compensating sheave.

Case 3) Effect on car vibration due to travelling cable.

The cable length decreases with an increase in stiffness as a fully loaded elevator climb. The major causes of a car vertical vibration include wire rope load misalignment, securely fastened tractor bottom with bearing beam, nonuniform traction motor and worm gear reducer misalignment between axes, gear meshing vibration within a speed reducer and vibration experienced from running a tractor [130]. Moreover, the following Figure 41, shows the effect on Car vibration due to travelling cable 0,435 kg/m, 0,87 kg/m. where It shows sheave vertical vibration due to different travelling cable. The zero value in the Y-axis indicates the initial vibration at the time of starting the car.

100
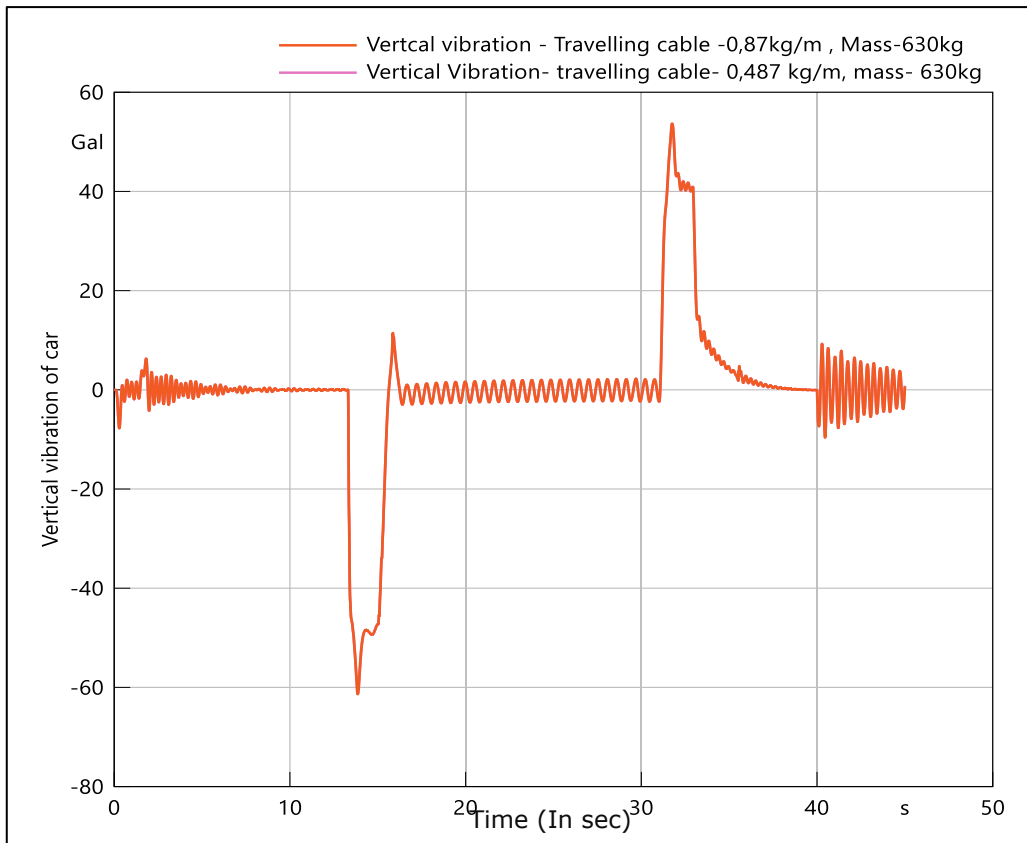
Figure 41. Effect on Car Vibration due travelling cable.
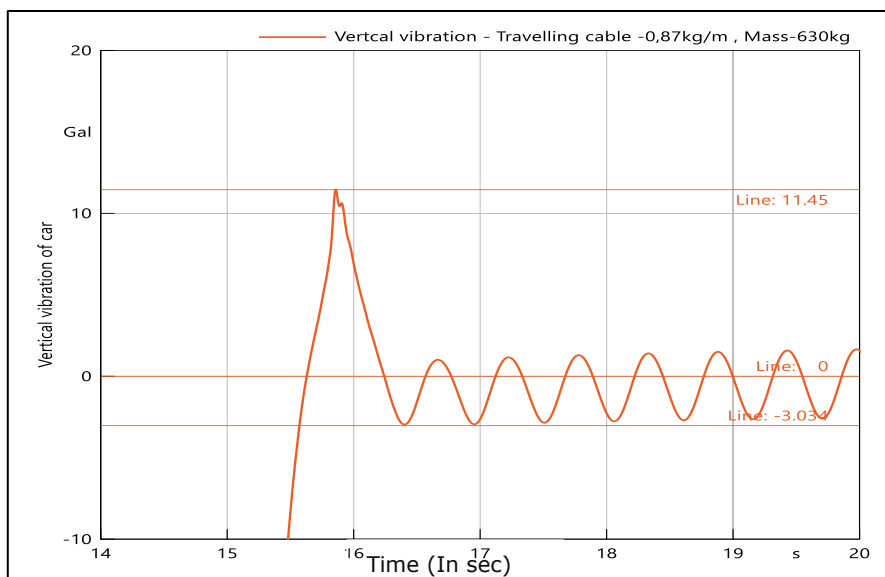
Figure 42. Peak to a peak value at 0.87 kg/m travelling cable.

Car acceleration takes place from 0 to 14 s before attaining a constant speed [131]. It then decelerates from 33 to 40 s. The following graph in Figure 42 shows the peak values of vertical vibration due to travelling cable 0,87 kg/m. The highest peak values are

101

11,45 Gal and the lowest peak values -3,034 Gal. So, the peak to peak value for 0,87 kg/m travelling cable is 14,484 Gal.

Case 4) Effect on car vibration due to suspension rope elastic modulus.

Further, the effect on Car vibration due to suspension rope elastic modulus is shown in the following Figure 43. Where Sky blue, Green line, Red line and shows the car vibration at 80,000, 60,000 and 100000 N/mm² respectively. It is essential to clarify the relationship between the compensation sheave weight and the rope's lateral vibrations, so it is essential to check the effect of rope and its stiffness on vibration by simulation.
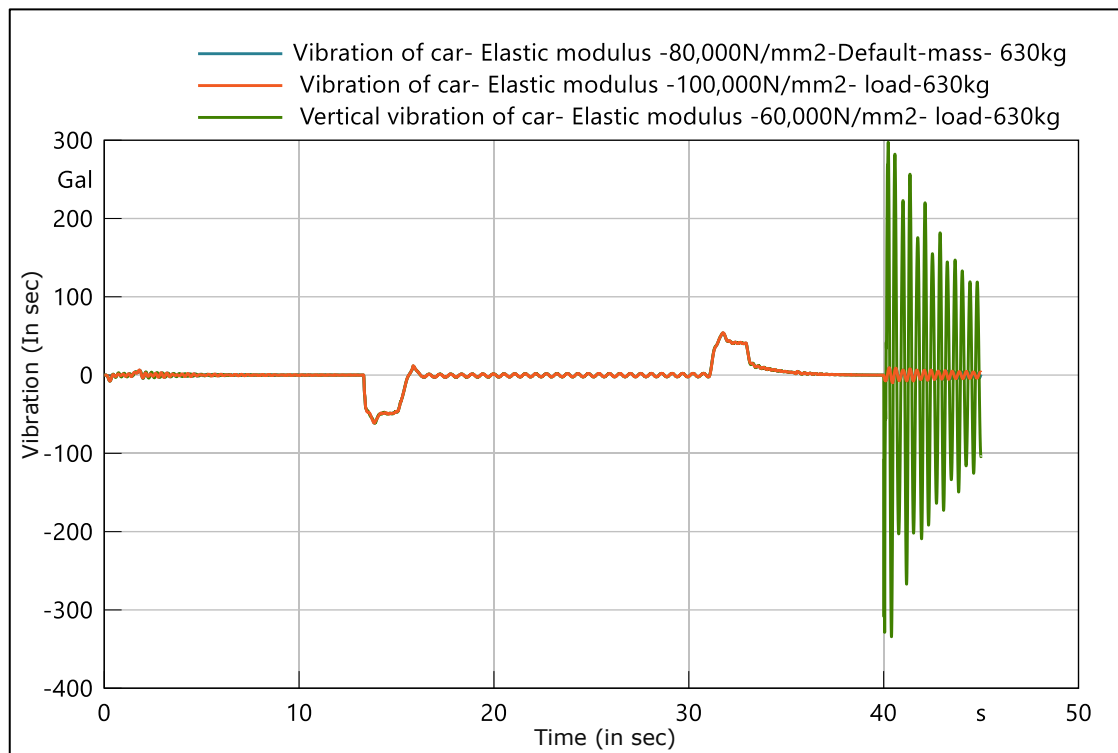
Figure 43. Effect on Car vibration due to suspension rope elastic modulus.

The effect on car vibration at 80000 N/mm² and 100000 N/mm² suspension rope elastic modules is almost the same irrespective of different elastic modulus, but when elastic modules decrease to 60, 000 N/mm² vertical vibration of the car abruptly increases at the end (t = 40 s). at the time of reaching the lift on the ground, the car is facing the sudden vibration, and the author is working on the model to remove this sudden vibration. Sudden large vibration due to flexibility in hoist rope, that has low internal damping characteristics that usually determine the resonance in the system.

The peak may be also caused by the traction sheave and the mount motor. Since the peak occurs at low elasticity, the tension on the rope is reduced. Stress may be the cause of the high vibrations at the end. At t = 40 s, there is an abrupt loss of control, but it stops after a few seconds. Furthermore, the high peak of vibration affects rope

powers that are shown in Appendix 4 and the author is working on an electric machine parameter to suppress this high oscillation peak that appears suddenly.
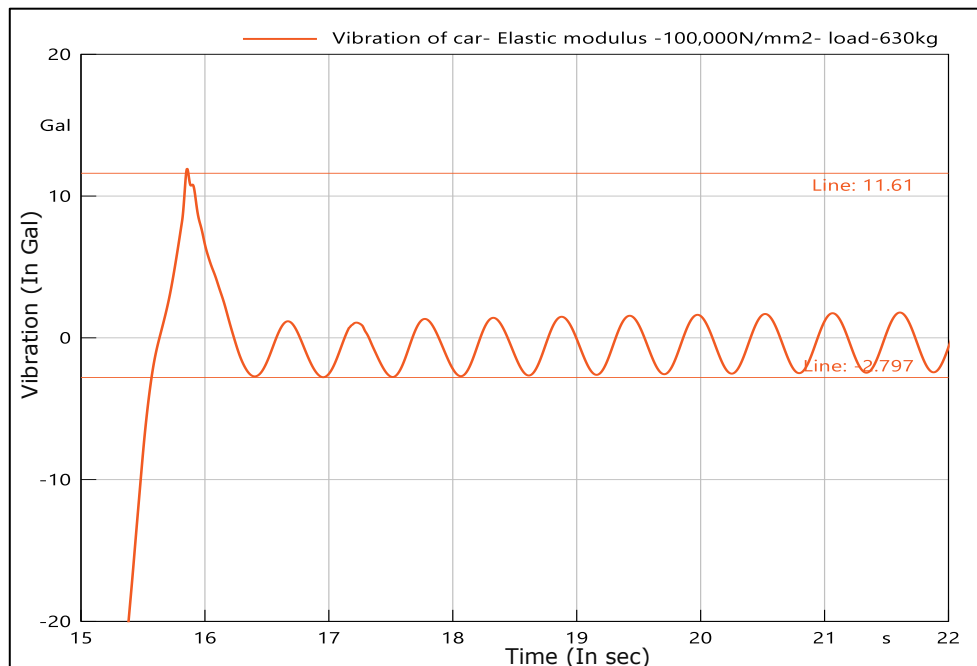
Figure 44. Peak to peak value at 10000 N/mm² elastic modulus.

Following Figure 44 shows the peak to peak value at 100000 N/mm² suspension rope elastic modulus. When the value of the suspension rope elastic module is 60000 N/mm² then the peak to the peak value of car vibration is 14,772 Gal, and when the value of the suspension rope elastic module is 80000 N/mm² and 100000 N/mm² so the value of peak to peak car vibration are 14,221 Gal and 14,407 Gal respectively. Here in this case peak to peak value is very slightly increasing.

Case 5) Effect on car vibration due to the change in mounting motor stiffness.

After observing the car vibrations at different elastic modulus, vibration has been investigated due to different mounting motor stiffness. Figure 45 shows the effect on car Vibration due to different Mounting Motor stiffness. The light green line shows the default motor stiffness is 1040 N/mm. While Camel, Ocean blue and orange colour line shows the vibration at 642 N/mm, 321 N/mm, and 1284 N/mm respectively. An analysis of Figure 45 can help one identify that There is sudden excitation at t= 40 s at the time of landing because of eMachine and velocity difference as shown in Figure 45, where There is too much oscillation due to low damping. The car vibrates the most at 321 N/mm motor stiffness.

103
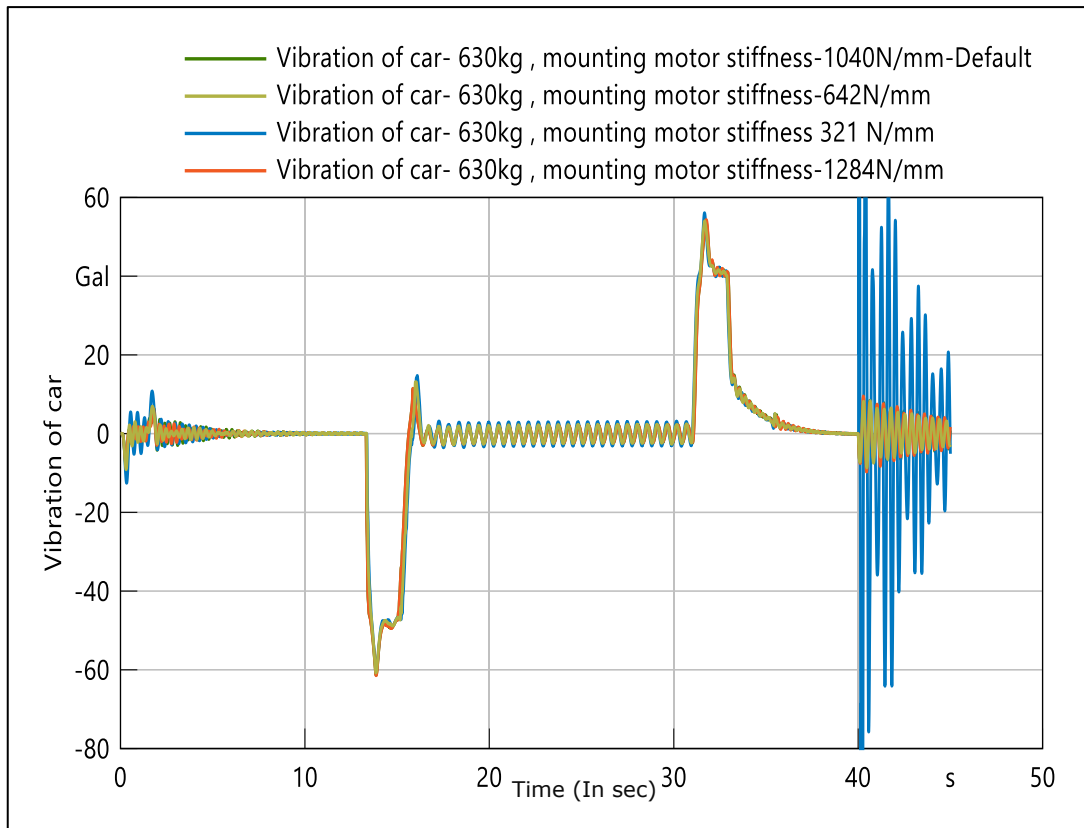
Figure 45. Vibration of Car at different values of mounting motor stiffness.

The vibration is induced by the ropes, electrical drive, and motors, which results in a high-power loss. High tension at rope velocity varies after t = 40s, and rotor acceleration varies from -1200 to 600 m/s^2 as shown in Appendix 5.
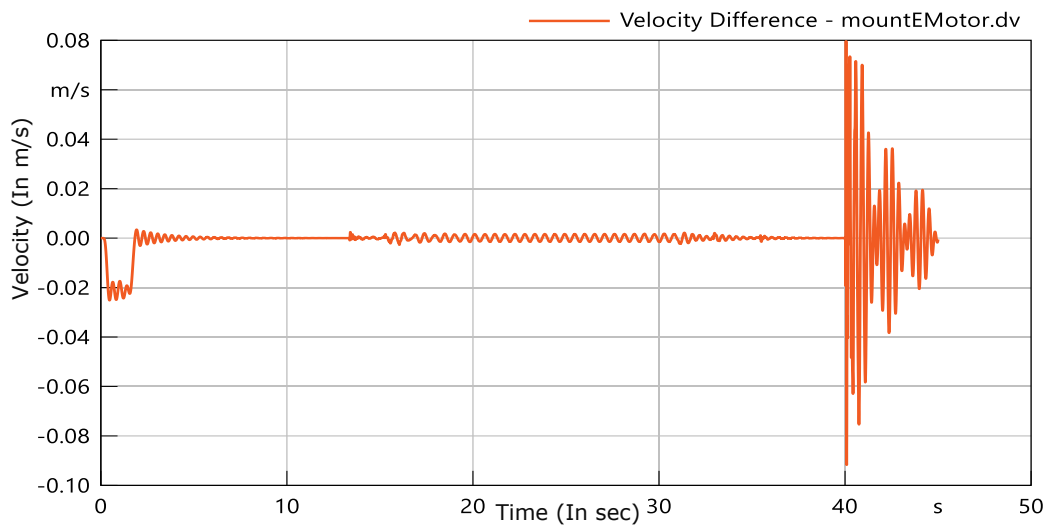
Figure 46. velocity-difference.

104

Motor imbalances, suspension rope motions, and mismatched guide rail profiles are all common causes of structural vibrations, which can be very uncomfortable.

Figure 46 shows the velocity difference when mounting motor stiffness is 321 N/mm. The peak to peak values that directly decide the jerk and sag on the car after the starting of motor due to mounting motor stiffness 321 N/mm, 642 N/mm, 1040 N/mm and 1284 N/mm are 17,417 Gal, 15,462 Gal, 14,221 Gal and 14,285 Gal respectively, So peak to peak value is decreasing while increasing the mounting motor stiffness.

Case 6) Effect on car vibration due to change in rope fixing sling stiffness.

Typically, cable deformation causes oscillatory suspension cable motions to decelerate continuously. Since continuous deceleration reduces the acceleration variance due to cable elasticity, dynamic cable solicitations are smaller [132], but here even after changing the sling stiffness, it does not vary much. The effect on car vibration due to change in Rope fixing sling stiffness is observed in Figure 47.

The rope fixing sling stiffness 102(default) N/mm change to 204 N/mm. The following graph shows the vibration of a car at different Rope fixing stiffness values. Where orange line shows the vibration at 204 N/mm while the green line shows vibration at default stiffness that has been used in the model. Where the result is quite the same and there is not so much effect on vibration due to different sling stiffness, that shows virtual elevator model is giving good result and it is ready to use. The orange line, which shows the vibration at high sling stiffness has a narrow higher intensity as compared to low sling stiffness.

Figure 48 shows when rope fixing stiffness is 102 N/mm then Peak to Peak Value is 14,121 Gal. The following image shows Peak Values of car vibration at 204 N/mm. the highest peak to peak value is 11.24 Gal and the lowest peak Values -3,113 Gal, so the peak to value is 14,353 Gal, which is quite lower than the real peak to the peak value of 55 Gal. However, it has been observed that peak to peak value is decreasing while increasing the sling stiffness.
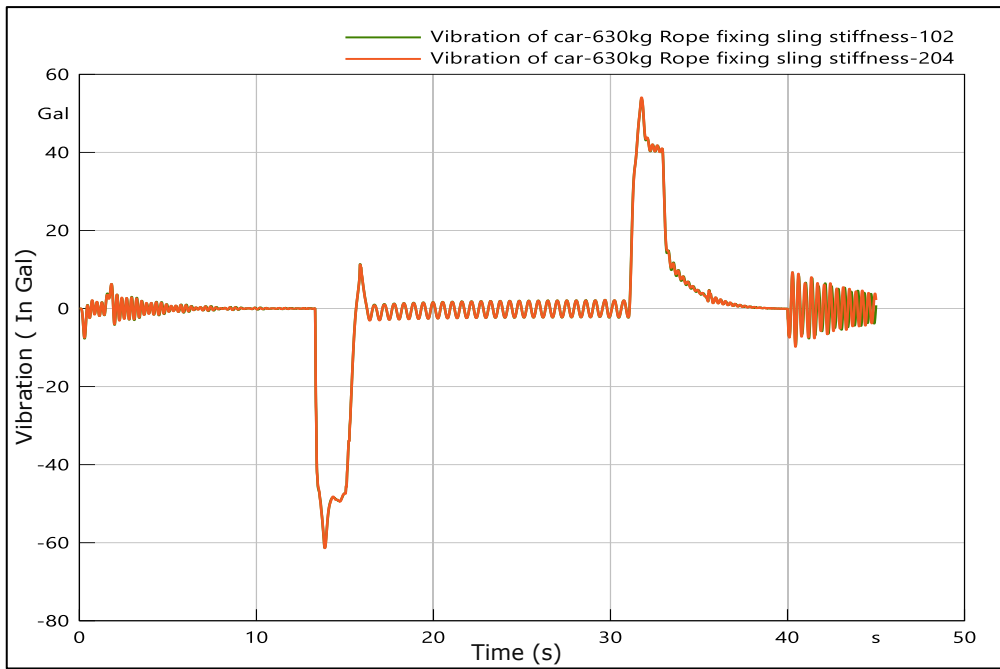
Figure 47. Vibration of Car at different Rope fixing sling stiffness.
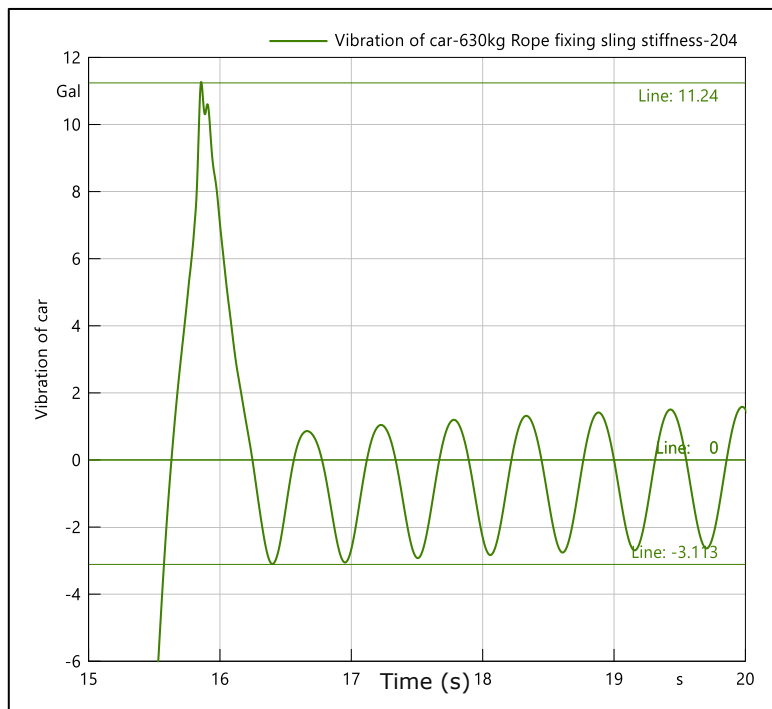
Figure 48. Vibration of Car at 204 Rope fixing sling stiffness.

Case 7) Effect on vibration due to change in max rope effective stiffness

Further, the effect on car vibration due to max effective rope stiffness is explained. The graph in Figure 49 shows the effect of different rope stiffness on car vibrations. The green line, orange line and blue line show the default maximum rope stiffness is 3000(default), 6000 and 1500 kN/m respectively.
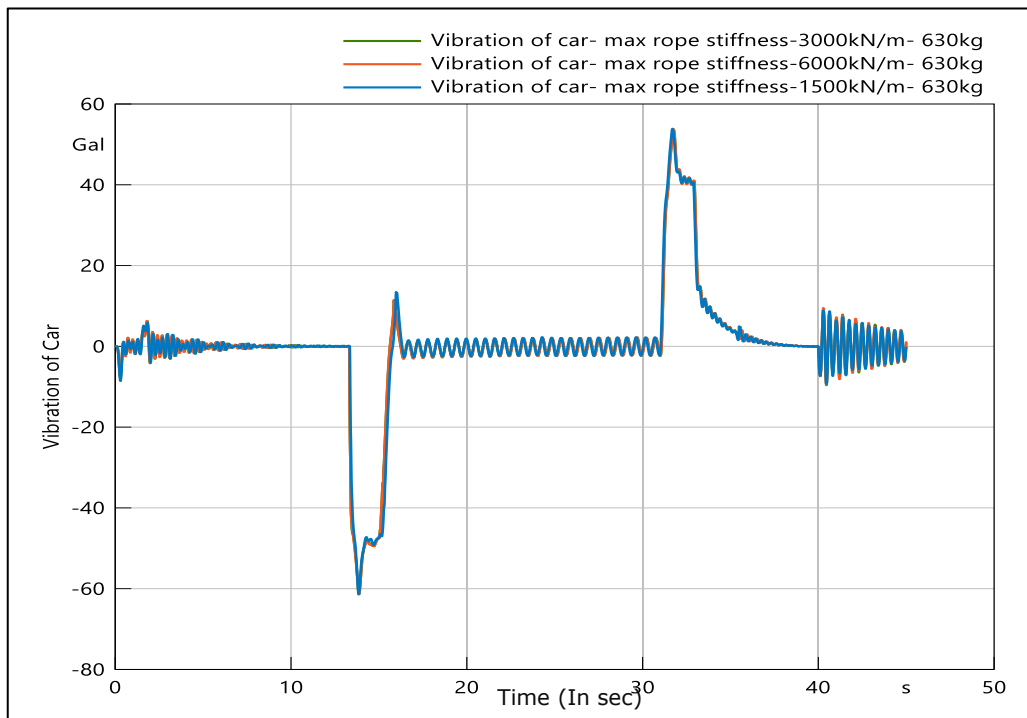
Figure 49. Effect on car vibration of different rope stiffness.

The elevator auto together with its counterweight undergo a significant upright vibration simultaneously immediately the brake is applied at the traction machine as a result of unusual behaviours. The oscillation also invokes the erect movement that opposes the compensating sheave. The requiting sheave's vertical displacement is assessed at each car movement and position. The sheave goes down during the deceleration and acceleration period [132]. The tabling rope's stiffness at the auto surface is at its maximum when the auto halts at the apex most flooring. Car loading state does not seem to affect the vertical movement of the sheave at the shaft' top.

It has been observed when the pulley beam stiffness is 1500 kN/m in LHS then the peak to the peak value of car vibration is 15,96 Gal. Also, at 3000 kN/m and 6000 kN/m, the peak to peak values of car vibrations are 14,21 Gal and 14,463 Gal, respectively, so peak to peak value is decreasing while increasing the rope stiffness.

The sheave's vertical position is determined by the tabling strand's stretch at the car's top-tonnage surface. However, when the car is stopped at the bottom while empty, the sheave rises to the peak flooring's level. This is as a result of the tabling strand's stretch at the motor surface being smaller due to the motor's lightness align its counterweight.

The sheave receives significant vibration when the brake is applied. The elevator car and its counterweight work against the braking force, hence rendering a vertical vibration that continues as the car decelerates [133]. When it terminates, the sheave gets twin opposing power and then invokes another oscillation.

If both vibrations are concurrent at the motor stoppage time, the second oscillation magnifies resulting in a bigger one after the auto stops. The static exclusion relies on the motor loading state and position. The maximum erect oscillation invoked by the traction machine control is equal to the structure's elevation. Simply expressed formulas regarding static displacement and maximum vertical vibration can be implemented to obtain the elevator's optimal plan.

SAG 1D MODEL

Elevator passengers may sometimes perceive the oscillation as undesirable or uncomfortable regarding the dynamic car movement [36]. The load-bearing components have a length and construction that invokes the elevator car sagging, bouncing or oscillating effect when the car is positioned at desired floor levels.

The formulae for stepping in and step out have been defined in chapter 3. The subject matter demonstrated in Figure 50 generally involves an elevator system, particularly the system's rope dynamic sag initiated from different initial floors. A roping arrangement in a traction-based elevator system includes more than one roping component suspending the elevator car's weight and the counterweight [35]. Sag, i.e. the difference between unloaded and loaded car position, i.e. 1.38 mm as shown in Figure 50. Negative sign just shows the downward direction of the car. The effect is as demonstrated in the graph above, shows the simulated sag is only 1.38 mm while the measured sag with real elevator had 2 to 3 mm, simultaneously.
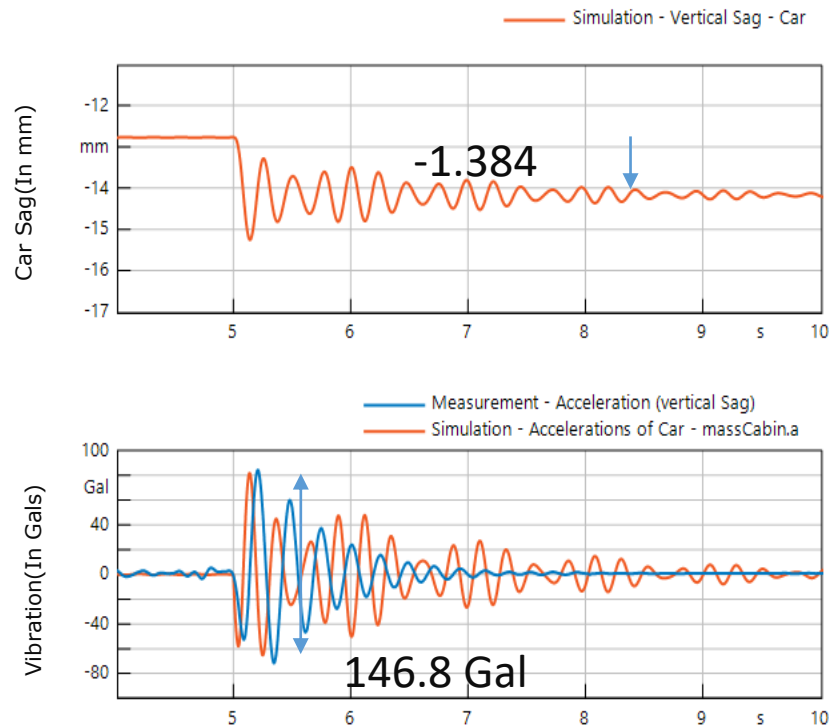
Figure 50. Sag and its Vibration.

The measured vibration peak to peak value was 155.3 Gal and maximum vibration was 84 Gal However, in the simulated virtual model. The peak to peak value is only 146.8 Gal and the observed vibration on the first floor is 81.6 Gal. Using this approach, the EA value is changing depending on the position, decreases to approx, 60 % of the nominal value that shows more strain.

Where, $EA = 16084.95 \, kN > 9650.97 \, kN$

$$\varepsilon = 0.000201 < 0.000335$$

All excitations were investigated using equations 3.36 to 3.40, which were calculated using mass excitation and Hermite interpolation, as described in chapter 3.

Validation with default configuration gives a good correlation for car sag due to some real physics element; the measured sag improvement in the MBS model has been improved. Physics element is tuned for real-time with accurate re-levelling that has solved the sag and bouncing problem, it will not only make the ride Comfortable and faster, but it will also be very safer for its user.

7.2 HIL validation

7.2.1 Car sag

Figure 51, shows the on HIL and off HIL car sag vibration that has been compared and investigated after HIL deployment and testing and it shows the better and smooth result on HIL. The off-HIL 1D simulation uses the step-in load calculation approach. Refinement of the parameterisation assumable will show an even better result. The sag has test has been done where the load has been varied from 0 to 80 kg.
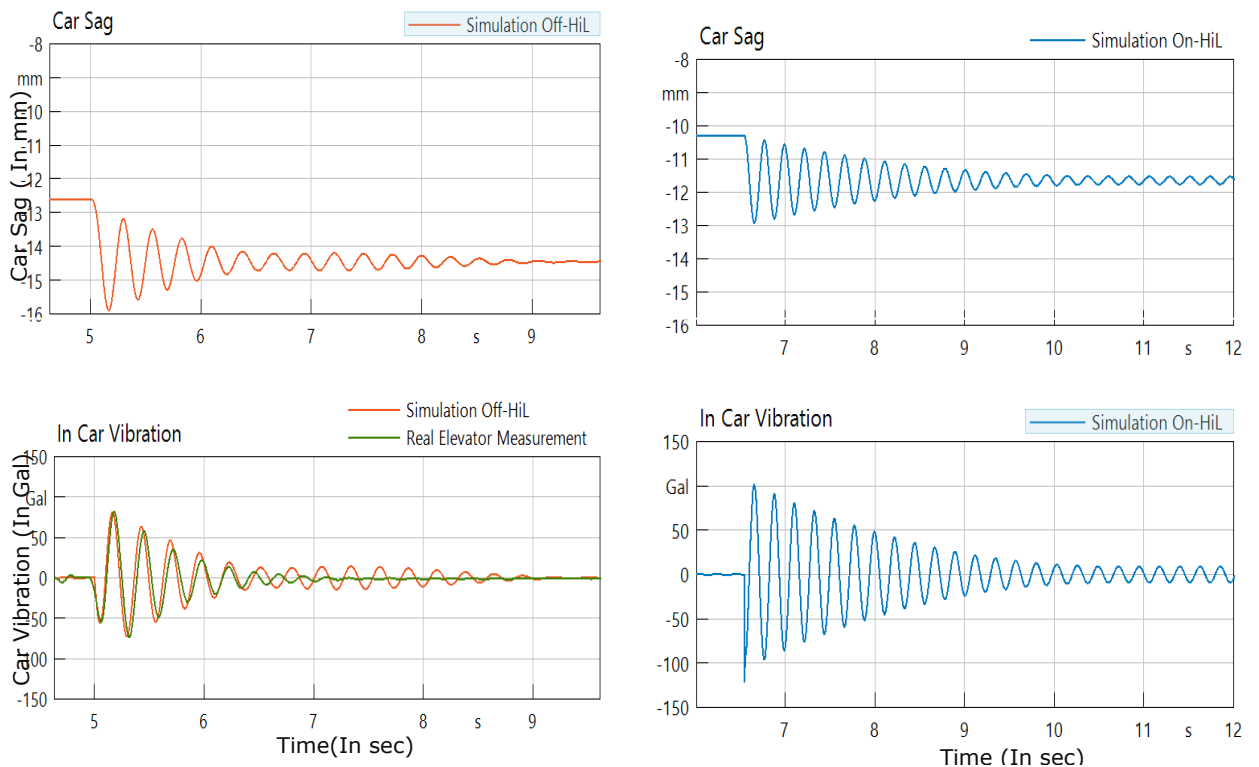
Figure 51. Car sag and Vibration Off HIL and on HIL.

In Off HIL approx. 3 mm while on HIL, the car sag was found to be only 2 mm and it is smoother, earlier off HIL car sag was starting later at approx.-13 mm but on HIL, it started early but with less sag. Similarly, the vibration due to sag is also found to be quite better.

The first graph (LHS) at Figure 51, where green indicated the real car vibration due to sag and red line Indicates sag in the virtual elevator model. Earlier car sag vibration was more frequent but now on HIL, it was not smoother; It is possible to decrease the car sag and vibration more and the author is working on making it more feasible.

7.2.2 Car position and velocity

Figure 52 shows the impact of on HIL and Off HIL on Car position and vertical velocity, where it is shown how the result of on HIL provides the better position as compared to real elevator position and SimulationX position although there is a need to shift the signal by working on Beckhoff. Similarly, LHS of Figure 52, the Greenline shows the real elevator position and the red line shows the SimulationX elevator model. As stated above in a general elevator measurement had some human error and it had a big difference in the target landing position. Here all the measurement was done with the guide roller.
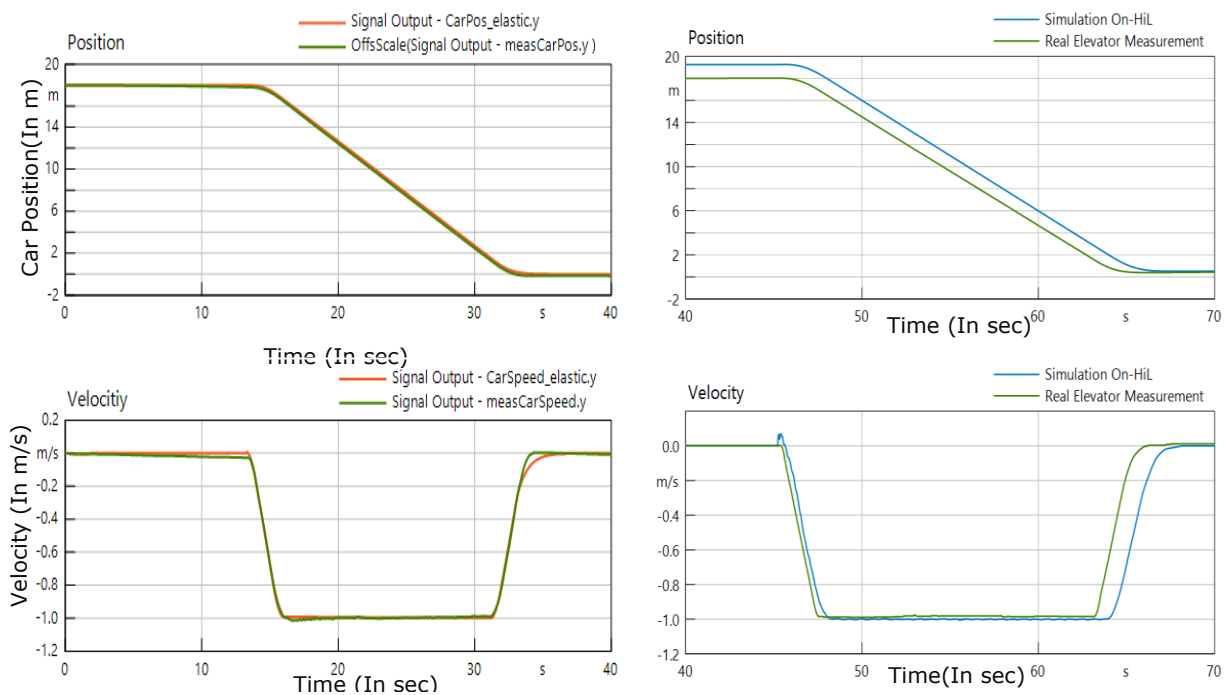
Figure 52. Position and velocity [Left] Off-HIL(SimulationX) and [Right] On HIL.

7.2.3 Car Vibration comparison on HIL and Off HIL

The number of discrete mass points refers to the system's DOF as well as the number of natural frequencies and mode shapes that are considered. By updating the models at each time level, this method allows for the simulation of vertical vibration during travel. Figure 53 shows the Car vibration comparison on and off HIL, where the L.H.S graph of Figure 53 indicates vibration without HIL, where the green line shows the real elevator measured vibration while the red line shows the simulation vibration. In Off- HIL, since

111

the drive frequency excitation was limited, SimulationX had very narrow frequency bandwidth and no torque ripple as compared to measured acceleration.

HIL vibration on the other hand in the R.H.S graph of Figure 53, was caused by a shift in frequency spectrum caused by real drive that has not been set up properly by SimulationX, as the drive has not been changed and it is causing extra frequency on the overall system that leads to torque ripple also.
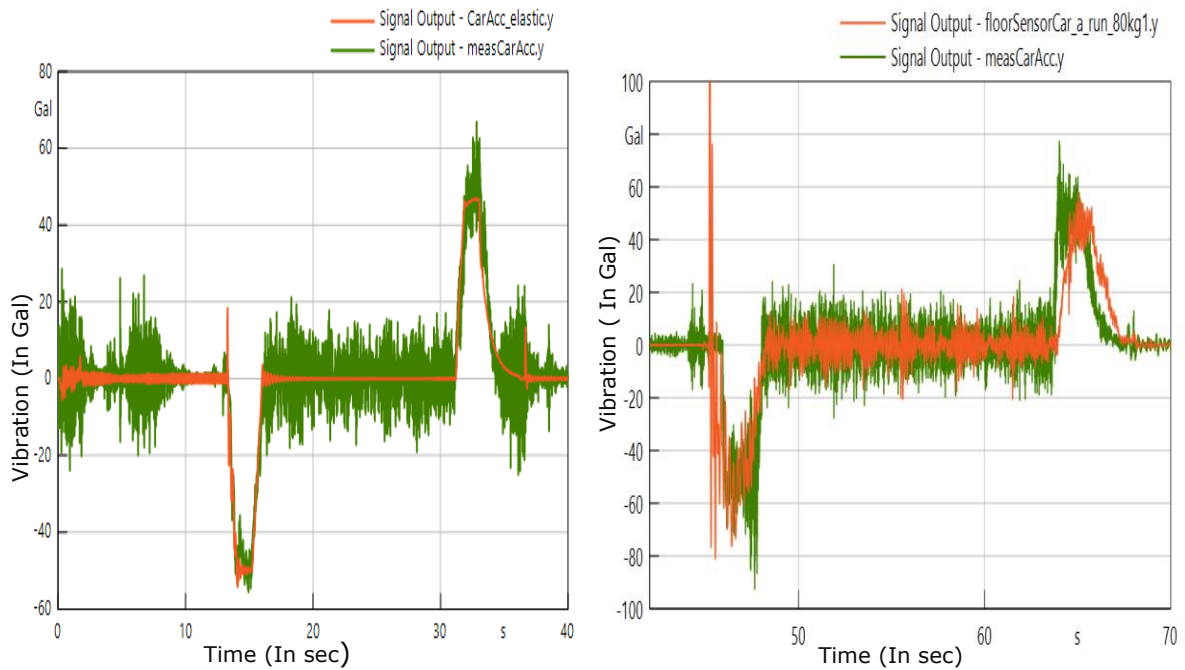
Figure 53. Car Vibration off-HIL[Left] (SimulationX) and Right On HIL.

Higher excitation and peak at t- 45 s different profile due to controller setting In on HIL Vibration, nonetheless, a good co-relation between the vibration level on and off HIL was established.

7.2.4 FFT analysis on HIL and OFF HIL

Frequency varies according to lateral modes of car, rope and suspension according to the position of the elevator car in the hoist way measured from the bottom landing level. In Figure 54 left side shows the off HIL FFT and Vibration and the right-side figure shows the on HIL FFT and vibration. the left-hand side of Figure 54, off HIL where orange line represents the variation of frequency on SimulationX and Blue line shows the general elevator measurement which has a higher peak at higher frequency (at 68 Hz and 75 Hz), It also shows detail vibration Higher peaks in low frequency between 0 to 1 Hz due

112

to change in velocity. There is also some more sudden peak Similarly on the right-hand side of Figure 54, the orange line represents a variety of frequency and vibration on HIL, where on HIL there is no peak of vibration at higher frequencies, peaks are only at lower frequencies till 10 Hz. Both the above graph shows the detailed vibration between 0 to 5 Hz.
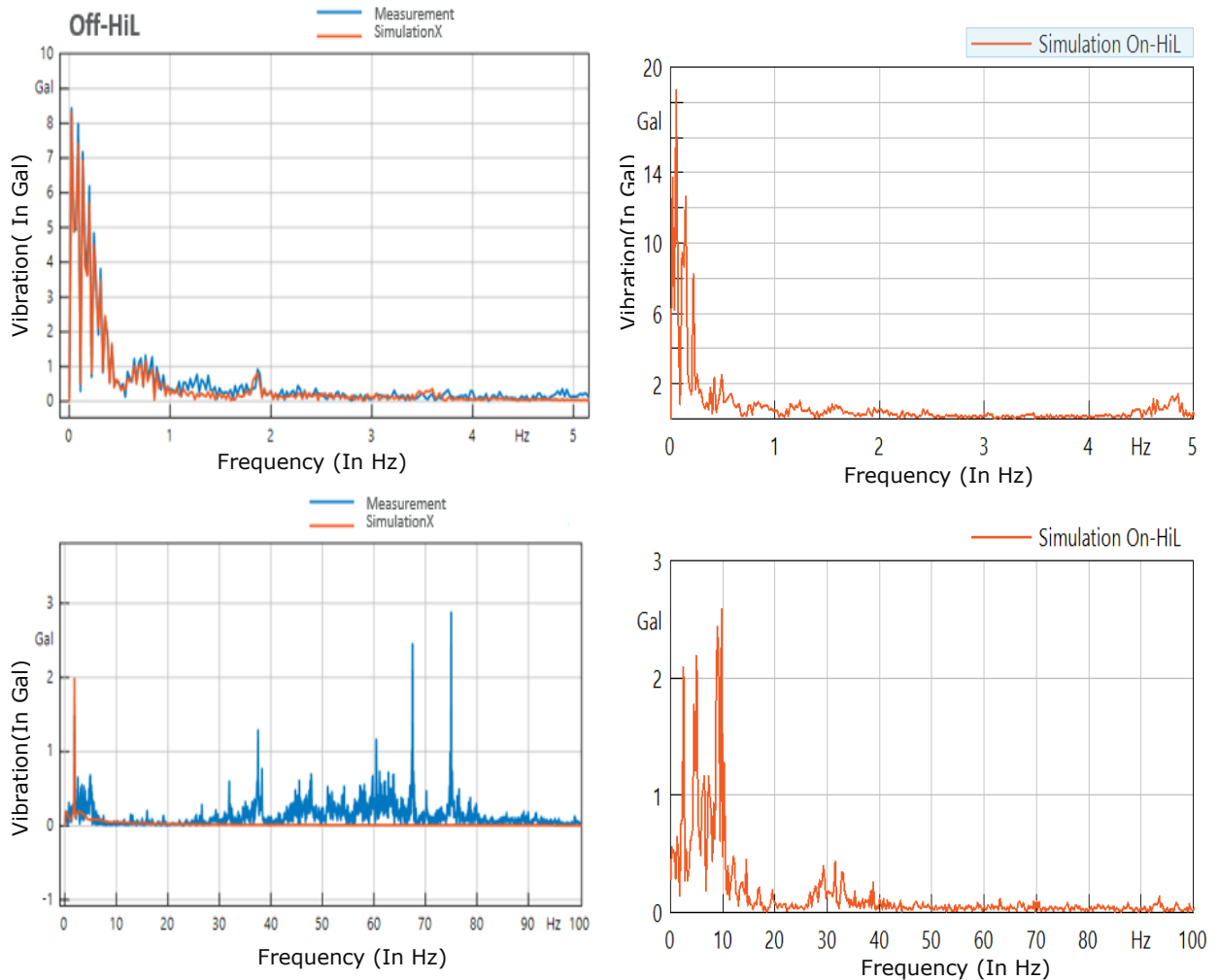
Figure 54. FFT comparison On HIL and Off HIL.

Based on the car vibration values, the graph shows that vibration waves corresponding to frequencies where the amplitude is approx 8 Gal measured while in simulation X vibration shows 2 Gal and the subsequent one are started getting slightly smaller as frequency increases, In both the graph frequencies have been analysed till 5 Hz for more detailed insight, due to drive excitation on HIL, it is possible to get the more detailed vibration at the time of the constant velocity section. The factor that can cause the higher peak is velocity, compensating ropes and suspension [28]. As drive-system borne excitation frequencies close to the elevator system natural frequencies [29], When the car-to-hoistway interface is considered static and the car mass is taken into account,

lateral movements are not permitted. As The input to the model is the encoder increment over time i.e., input signal can excite certain eigenfrequencies inside the model and test setup limits the mapping of higher frequency phenomena from the encoder input into the model due to the interior of coupled motor and signal delays from an inverter. Test of the load motor's response to a torque step through step response test.

The natural frequency is higher at fundamental frequency in simulation at the same time the real elevator has a natural frequency at somewhere around 75 Hz. The compensating ropes can be excited at the fundamental natural frequency if the car is positioned at a certain height that has some special frequency. The first natural frequency in the longitudinal direction is twice the fundamental natural frequency of the elevator car, suspension, and compensating ropes at the car side when the elevator car vibrations are approximately 8 Gal. When the elevator car is located at a height of 18 m, the external excitation of the car direction was set at the fundamental natural frequency of the elevator car, suspension, and compensating ropes at the car side. In Appendix 6, various energy, power losses at different natural frequencies with the exact value have been depicted.

Benefit on the HIL:
1. Using the more realistic oscillating position for the landing sensors will result in an enhancement of the landing and releveling procedure.
2. On-HIL the load excitation was applied as a hard step, showing response with higher altitude.
3. The results show a good correlation between oscillation and damping behaviour.

Conclusion

Modelling an elevator car system's dynamic performance forms a complex but important task in the system's design procedure. The requirement to assess the elevator passenger behaviour makes the modelling endeavour more complicated. The results are meant to evaluate the impact of the elevator car dynamics by comparing its damping and stiffness characteristics [134]. The experimental procedure is simplified by decreasing transmissibility measurements using the vibration frequency range. Damping and stiffness coefficients are evaluated based on measurements and analysis using a loaded and empty elevator car model. The model facilitates an optimal standard

of the stiffness and damping elevator system traits after assessing its mechanical behaviour while accounting for the dynamic loading effects.

All results are listed above especially rope forces, car velocity, car vibration, torque and velocity of motor has been calculated and plotted through the help of SimulationX software. The result has been performed by considering Eight people (passenger can very in an Asian country like Asia and China where average weight is considered as lower than European countries) where maximum mass could be $630\,\mathrm{Kg}$, Considering some constant values for maximum vertical acceleration, vertical velocity and the total height of the elevator I.e. $0,5\,\mathrm{m/s^2}$, $1\,\mathrm{m/s}$ and $18\,\mathrm{m}$ respectively. where the elevator is moving from the seventh to the first floor.

From all these graphs, it has been concluded that decreasing in mounting motor stiffness and decreasing the number of rope increasing the peak to peak value. decreasing the rope elastic modulus giving some sudden large oscillation at the time of landing and the author is working on it to remove that large vibration.

The peak to peak value was 55 Gal in a general elevator but the Virtual model is giving only approx 20 Gal which is quite lower than a real elevator, that part still needs to work on. Peak to peak value is about 14 Gal , increasing by two-parameter Rope and mounting motor stiffness. By decreasing the number of ropes (2), Peak to peak value becomes 19,9 Gal, and that is the maximum that has been achieved) and peak to peak value is also increasing by reducing the mounting motor stiffness (where at 321 $\mathrm{N/mm}$, peak to peak value is 17,41 Gal). Also, the result is better after HIL deployment.

8 SUMMARY

The aim of the thesis was to develop an elevator model's virtual prototype inside the Beckhoff unit (CXxxxx) to deliver more accurate software testing for drive-by using hardware in the loop (HIL). The presented work proves to be feasible and applicable, which is necessary for the future design of high quality and safe vertical transportation system (VTS). A general multibody approach to analyse an elevator system that consists of rigid bodies and wire ropes has been described in the thesis; SimulationX software inbuilt Modelica has made it simple to design a model and simulate the system-. System simulation enables faster drive software testing that will decrease the release time and provide more comprehensive testing that is safe, reliable, flexible, and repeatable.

It is known HIL simulation is one of the high-tech approaches that combine theory, numerical simulation, software, hardware devices, digital communications, data acquisition, and control to give a complete mechatronic system [135]. Such a system-level approach can simplify the development and design processes for complex systems and their testing and validation at a low cost. While the Automotive Industry has implemented HILS widely in their research projects and investigations.

In this thesis, the simulation was performed in numerous ways to get an optimised output. PLC logic was used to achieve the results and validated by comparing the available studies; in-depth research is being conducted in various fields such as elevator mechanics, which helps install, maintain, or fix the elevator in the required position, SimulationX software was used, which has some fundamental physics element that allows the user to develop and analyse virtual prototypes for testing at various stages, Hardware PMSM has been used to provide some motion, and Beckhoff hardware embedded P.C. was used for control, within the embedded P.C., Beckhoff Twin CAT PLC was used via Microsoft visual studio, which is responsible for executing the command.

For automation, the Jenkins open source automation server was used to automate software development segments related to infrastructure, testing, and deploying various commands for obtaining continuous delivery with integration. This resulted in a high detailed elevator model, which runs on the Beckhoff PLC, & In-the-loop interaction between model, load drive and drive-under-test. This HIL is being used in the MONO500 model of the residential elevator. It will also be used in another elevator model in the future.

For the elevator's proper functioning, a HIL technique has been used that can help in testing and designing how the elevator should work. Alternatively, system simulation can help apply various technologies using computers for the system's efficiency and accuracy. The HIL testing technique is essential as it ensures the elevator system's reliability and testing the interdependence and connectivity between the various parts of the system. The simulation of the system is required as it ensures the safety of the system. Without simulation, the elevator may have safety problems that can be harmful.

Validation result show advances in testing, re-levelling and controller accuracy of car position. Sensor functionality in-car vertical vibration in the future will be scaled to another elevator. As such, there is no need to invest in a more powerful motor as HIL increases test coverage with sag and bouncing releases control pulley eccentricity.

Due to Multibody dynamics and high stiffness, HIL testing was a challenging task. As far as author knowledge, no one has developed HIL testing in the elevator system yet. The challenging part of the work was modelling, balance, accuracy, performance and HIL deployment where currently available HIL equipment limit the simulation performance. However, the sensor was used all around the elevator model to detect every component's fault and behaviour. Most importantly, more than 450 automatic tests are lasting only some hours. Customer safety and comfort has also been considered by removing sag, bounce and by providing accurate releveling.

In the future, it will be possible to change the motor with SimulationX, and its drive effectiveness could be verified by simulation results at different operating conditions [22]; it will also have a possibility to be scaled to another elevator also. In addition, it will also be possible to do the Customer problem troubleshooting, which can make a similar setup that the customer has. Model-based systems engineering is the key to understanding how a holistic system will perform.

-The current system simulation with the HIL technique is the landmark step in the field of automated testing. It has helped to solve the problems associated with testing, such as, due to increase of test coverage the HIL technique not only assists the elevator industry but is extremely beneficial in any automotive industry also. Its contribution to the automotive industry field has been good, and it can help solve many problems that the Industry faces concerning the equipment it manufactures as it will decrease the testing cost. The author believes that the elevator industry will have a new design and technique that has fewer faults and has increased the elevator's overall life. It will take

the quality of elevator experiences several notches higher for builder, architect, developer and the end-user.

This thesis contribution includes:

1) Improvement in the Software quality.
2) Wider testing.
3) Enabled fully automatic testing.
4) Enabled the testing of the actual elevator cycle.
5) Enabled to test elevator commissioning /fault behaviour.
6) Enabled to test with a different kind of elevator shaft.
7) Enabled to test of different elevator components and running parameters.
8) Increased the pace of drive software development.
9) Less testing time.
10) High ride comfort by decreasing vibration from the motor.
11) Less power consumption by optimizing demanded torque.
12) Safer ride by removing sag and bounce.
13) Faster landing by more accurate positioning.
14) Virtual mechanical system allows changing any configuration.

The testing approach can be further improved by introducing a more detailed description of testing and debugging. The approach can be tailored for more real-time applications by using the simplified 3D model that is slow at the moment, but as the parameter is the same for 3D and 1D; The work will be done continuously to make the 3D model run.

The comparison between the results obtained with the proposed approach and the original hardware site results in a "real system" that confirms the effectiveness of the approach, even in the presence of relevant sensor noise and modelling errors, the effects of which have been extensively investigated through a sensitivity analysis. Finally, the proposed approach's small amount of computational time assures implementing it in a real-time environment.

Kokkuvõte

Lõputöö eesmärk oli arendada Beckhoffi seadme (CXxxxx) sees oleva liftimudeli virtuaalne prototüüp, et pakkuda rohkem ajami täpsem tarkvara testimine on teostatud läbi riistvara silmuse. Esitatav töö osutub teostatavaks ja rakendatavaks, mis on vajalik kvaliteetse ja ohutu vertikaalse transpordisüsteemi (VTS) edaspidiseks disainimiseks. Lõputöös on kirjeldatud üldist mitmikkehaga lähenemist jäikadest keredest ja trossidest koosneva liftisüsteemi analüüsimiseks; SimulationX tarkvara sisseehitatud Modelica on lihtsustanud mudeli kujundamise ja süsteemi simuleerimise. Süsteemi simulatsioon võimaldab kiiremat ajamitarkvara testimist, mis vähendab väljaandmise aega ja pakub ulatuslikumat, turvalisemat, usaldusväärsemat, paindlikkuma ja korratavamat testimist.

On teada, et riistvaralise silmuse simulatsioon (HILS) on kõrgtehnoloogiline lähenemisviis, mis ühendab teooria, numbrilise simulatsiooni, tarkvara, riistvaraseadmed, digitaalse suhtluse, andmete hankimise ja juhtimise, et saada täielik mehhatrooniline süsteem [135]. Selline süsteemitasandi lähenemisviis võib lihtsustada keerukate süsteemide väljatöötamise ja kujundamise protsesse ning nende testimist ja valideerimist väikeste kuludega. Autotööstus on HILSi juba oma uurimisprojektidesse ja uurimistesse laialdaselt rakendanud.

Optimeeritud väljatuleku jaoks viidi selles lõputöös simulatsioon läbi mitmel viisil. Tulemuste saavutamiseks kasutati PLC loogikat ning selle kinnitamiseks võrreldi seda olemasolevate uuringutega; põhjalikke uuringuid viiakse läbi erinevates valdkondades, näiteks liftimehaanikas, mis aitab lifti vajalikus asendis paigaldada, hooldada või fikseerida, tarkvara SimulationX-i, millel on mõni põhiline füüsikaelement, kasutati võimaldamaks kasutajal arendada ja analüüsida virtuaalseid prototüüpe testimiseks erinevates etappides, liikumise tagamiseks on kasutatud riistvara PMSM-i ja juhtimiseks Beckhoffi sisseehitatud riistvara, sisseehitatud PC-s kasutati Microsofti visuaalstuudio kaudu Beckhoff TwinCAT PLC-d, mis vastutab käsu täitmise eest.

Automatiseerimiseks kasutati Jenkinsi avatud lähtekoodiga automatiseerimisserverit, et automatiseerida tarkvaraarenduse segmente, mis on seotud infrastruktuuri, testimise ja mitmesuguste käskude juurutamisega pideva edastuse saamiseks koos integreerimisega. Selle tulemuseks oli üksikasjalik liftimudel, mis töötab Beckhoffi PLC-I, ja mudeli, koormusajami ja testitava ajami vaheline in-the-loop koostoime. Seda HIL-i kasutatakse elamu lifti mudelis MONO500 ja tulevikus ka mõnes teises lifti mudelis.

Lifti nõuetekohaseks toimimiseks on kasutatud HIL-tehnikat, mis aitab katsetada ja kavandada, kuidas lift peaks töötama. Alternatiivina võib süsteemi simulatsioon aidata süsteemi tõhususe ja täpsuse huvides rakendada arvuteid kasutades erinevaid tehnoloogiaid. HIL-i testimistehnika on hädavajalik, kuna see tagab liftisüsteemi töökindluse ning süsteemi erinevate osade vastastikuse sõltuvuse ja ühenduvuse testimise. Süsteemi simulatsiooni on vaja, kuna see tagab süsteemi ohutuse. Ilma simulatsioonita võib liftil olla ohutusprobleeme, mis võivad osutuda ohtlikuks.

Valideerimise tulemus näitab edusamme liftikabiini asukoha testimisel, tasandamisel ja kontrolleri täpsusel. Anduri funktsionaalsus liftikabiinis vertikaalse vibratsiooni korral laieneb tulevikus edasi teisele liftile. Iseenesest pole vaja investeerida võimsamasse mootorisse, kuna HIL suurendab testi ulatust vajumisega ja vabastab põrgatades rihmaratta ekstsentrilisuse.

Mitmikkeha dünaamika ja kõrge jäikuse tõttu oli HIL-testimine keeruline ülesanne. Autori teada pole keegi veel HIL-testimist liftisüsteemis välja töötanud. Töö väljakutsuv osa oli modelleerimine, tasakaal, täpsus, jõudlus ja HIL-i kasutuselevõtt seal, kus praegu saadaval olevad HIL-seadmed piiravad simulatsiooni jõudlust. Andurit kasutati aga kogu lifti mudeli ümbruses, et tuvastada iga komponendi viga ja käitumine. Kõige tähtsam on see, et rohkem kui 450 automaatset testi kestavad vaid mõned tunnid. Kliendi ohutust ja mugavust on kaalutud ka vajumise ja põrgatuse eemaldamise ja täpsema tasanduse tagamise abil.

Tulevikus on võimalik mootorit vahetada SimulationX-iga ja selle ajami efektiivsust saab erinevates töötingimustes kontrollida simulatsioonitulemuste abil [22]; seda on võimalik laiendada ka teise lifti. Lisaks on võimalik läbi viia kliendi probleemide tõrkeotsing, tehes sarnase seade nagu kliendil. Mudelipõhine süsteemitehnika on terviku süsteemi toimimise mõistmise võti.

-Praegune süsteemi simulatsioon HIL-tehnika abil on teetähiseks sammuks automatiseeritud testimise valdkonnas. See on aidanud lahendada testimisega seotud probleeme, näiteks testimise ulatuse suurendamise tõttu ei aita HIL-tehnika mitte ainult liftitööstust, vaid on äärmiselt kasulik ka mis tahes autotööstuses. Selle panus autotööstuse valdkonda on olnud hea ja see võib aidata lahendada paljusid probleeme, millega tööstus seisab silmitsi seoses tema toodetud seadmetega. Autor usub, et liftitööstus saab uue konstruktsiooni ja tehnika, millel on vähem vigu ja mis on

suurendanud lifti üldist elutsüklit. See tõstab liftikogemuste kvaliteeti mitu astet kõrgemale nii ehitaja, arhitekti, arendaja kui ka lõppkasutajate jaoks.

See lõputöö sisaldab:

1) Tarkvara kvaliteedi paranemist.

2) Laiemat testimist.

3) Lubatud täisautomaatset testimist.

4) Lubatud tegeliku liftitsükli testimist.

5) Lubatud lifti kasutuselevõtu / rikke käitumise testimist.

6) Lubatud teist tüüpi liftišahtiga katsetamist.

7) Lubatud lifti erinevate komponentide ja sõiduparameetrite testimist.

8) Suurendas ajami tarkvara uuendamise tempot.

9) Vähem testimisaega.

10) Kõrgemat sõidumugavust, vähendades mootori vibratsiooni.

11) Vähemat energiatarvet, optimeerides nõutavat pöördemomenti.

12) Ohutumat sõitu eemaldades lõtvumise ja põrutuse.

13) Kiiremat maandumist täpsema positsioneerimisega.

14) Virtuaalne mehaaniline süsteem võimaldab muuta mis tahes konfiguratsiooni.

Testimisviisi saab veelgi parandada, lisades testimise ja silumise üksikasjalikuma kirjelduse. Lähenemist saab kohandada rohkem reaalajas rakendamiseks, kasutades lihtsustatud 3D-mudelit, mis on hetkel aeglane, kuid kuna parameeter on sama 3D ja 1D puhul; tööd tehakse pidevalt 3D-mudeli käivitamiseks.

Kavandatud meetodi ja algse riistvaraga saadud tulemuste võrdlus "reaalse süsteemi" tulemusel kinnitab meetodi tõhusust isegi asjakohase andurimüra ja modelleerimisvigade olemasolu korral, mille mõju on põhjalikult uuritud tundlikkusanalüüsi abil. Lõpuks tagab pakutud lähenemisviisi väike arvutusaeg selle rakendamise reaalajas.

LIST OF REFERENCES

[1]   P. Pillay and R. Krishnan, 'Modeling, Simulation, and Analysis of Permanent-Magnet Motor Drives,Part I: The Permanent-Magnet Synchronous Motor Drive', *IEEE Trans. Ind. Appl.*, vol. 25, no. 2, pp. 265–273, 1989, doi: 10.1109/28.25541.

[2]   Z. Haigang, Q. Weiguo, Y. Wu, G. Shihong, and Y. Yuan, 'Modeling and simulation of the permanent-magnet synchronous motor drive', in *Proceedings of the International Conference on Uncertainty Reasoning and Knowledge Engineering, URKE 2011*, 2011, vol. 2, pp. 256–260, doi: 10.1109/URKE.2011.6007882.

[3]   M. F. N. Henriques, A. A. C. Vieira, L. M. S. Dias, G. A. B. Pereira, and J. A. Oliveira, 'Analysis of an elevator system using discrete event simulation: Case study', *Int. J. Qual. Res.*, vol. 13, no. 4, pp. 823–836, Dec. 2019, doi: 10.24874/IJQR13.04-05.

[4]   Modelling of elevator car Dynamics with simulationX, 'Pilot Project', Aalto, 2018.

[5]   G. Schupp, C. Weidemann, and L. Mauer, 'Modelling the contact between wheel and rail within multibody system simulation', *Veh. Syst. Dyn.*, vol. 41, no. 5, pp. 349–364, 2004, doi: 10.1080/00423110412331300326.

[6]   O. Gietelink, J. Ploeg, B. De Schutter, M. Verhaegen, and B. DE Schutter, 'Vehicle System Dynamics Development of advanced driver assistance systems with vehicle hardware-in-the-loop simulations Development of advanced driver assistance systems with vehicle hardware-in-the-loop simulations', *Veh. Syst. Dyn.*, vol. 44, no. 7, pp. 569–590, Jul. 2006, doi: 10.1080/00423110600563338.

[7]   A. Schreiber, 'Acoustic Optimization of elevator cars using A hybrid simulation Approach', Freiberg University of Mining and Technology, 2015.

[8]   M. Pijorr, 'Digital Transformation in the Elevator Industry Moving from Physical Testing to Simulation', 2019.

[9]   'Form Follows Function - thyssenkrupp AG - Reinventing the Elevator Concept'. https://www.altair.com/resource/form-follows-function-thyssenkrupp-ag-reinventing-the-elevator-concept (accessed Nov. 14, 2020).

[10]   W. Ren, M. Steurer, T. B.-I. T. on Industry, and undefined 2008, 'Improve the stability and the accuracy of power hardware-in-the-loop simulation by selecting appropriate interface algorithms', *ieeexplore.ieee.org*, Accessed: Oct. 18, 2020. [Online]. Available: https://ieeexplore.ieee.org/abstract/document/4578805/.

[11]   M. Pokharel and C. N. M. Ho, 'Stability study of power hardware in the loop (PHIL)simulations with a real solar inverter', in *Proceedings IECON 2017 - 43rd Annual Conference of the IEEE Industrial Electronics Society*, Dec. 2017, vol. 2017-January, pp. 2701–2706, doi: 10.1109/IECON.2017.8216454.

[12]   S. Wang, Z. Xu, B. Li, and D. Xu, 'Stability Evaluation of Power Hardware-in-the-

loop Simulation for DC System', Dec. 2018, doi: 10.1109/PEAC.2018.8590411.

[13] M. Park, S. Ha, H. S. Lee, Y. K. Choi, H. Kim, and S. Han, 'Lifting demand-based zoning for minimizing worker vertical transportation time in high-rise building construction', *Autom. Constr.*, vol. 32, pp. 88–95, 2013, doi: 10.1016/j.autcon.2013.01.010.

[14] G. Bonney, B. Paffen, and M. Schuba, 'ICS / SCADA Security Analysis of a Beckhoff CX5020 PLC', 2014.

[15] T. Meen and W. Zhao, 'Selected Papers from IEEE ICKII 2018', 2019, Accessed: Oct. 18, 2020. [Online]. Available: https://www.mdpi.com/books/pdfdownload/book/1468.

[16] T. I. Strasser, S. Rohjans, and G. M. Burt, 'Methods and Concepts for Designing and Validating Smart Grid Systems', *Energies*, vol. 12, no. 10, p. 1861, May 2019, doi: 10.3390/en12101861.

[17] D. Jung and P. Tsiotras, 'Modeling and hardware-in-the-loop simulation for a small unmanned aerial vehicle', in *Collection of Technical Papers - 2007 AIAA InfoTech at Aerospace Conference*, 2007, vol. 1, pp. 581–593, doi: 10.2514/6.2007-2768.

[18] 'ADAS HiL Test in Real-Time - ADAS iiT'. https://www.adas-iit.com/hardware-in-the-loop/expertise/adas-hil-test-in-real-time/ (accessed Jan. 01, 2021).

[19] S. V. Vaseghi, 'Noise and Distortion', in *Advanced Digital Signal Processing and Noise Reduction*, John Wiley & Sons, Ltd, 2009, pp. 35–50.

[20] S. V. Vaseghi, *Advanced Digital Signal Processing and Noise Reduction*. Chichester, UK: John Wiley & Sons, Ltd, 2008.

[21] M. Jung, J. Moon, M. Park, H. S. Lee, S. U. Joo, and K. P. Lee, 'Construction worker hoisting simulation for sky-lobby lifting system', *Autom. Constr.*, vol. 73, pp. 166–174, Jan. 2017, doi: 10.1016/j.autcon.2016.10.002.

[22] A. Saghafinia, H. W. Ping, M. N. Uddin, and A. Amindoust, 'Teaching of Simulation an Adjustable Speed Drive of Induction Motor Using MATLAB/Simulink in Advanced Electrical Machine Laboratory', *Procedia - Soc. Behav. Sci.*, vol. 103, pp. 912–921, Nov. 2013, doi: 10.1016/j.sbspro.2013.10.413.

[23] X. Arrasate *et al.*, 'The modeling and experimental testing of the vertical dynamic response of an elevator system with a 2:1 roping configuration. Modelling of Elevator Installations View project Modelling and Simulation of a nonstationary high-rise elevator system to predict the dynamic interactions between its components View project The modelling and experimental testing of the vertical dynamic response of an elevator system with a 2:1 roping configuration', 2012. Accessed: Apr. 05, 2021. [Online]. Available: https://www.researchgate.net/publication/261759084.

[24] X. Arrasate, S. Kaczmarczyk, G. Almandoz, J. M. Abete, and I. Isasa,

'Measurement and Simulation of Machine-Borne Vertical Vibration in Elevator Systems', *11th Int. Conf. Vib. Probl.*, no. September, pp. 1–10, 2013.

[25] 'Hamilton's Principle'. https://galileoandeinstein.phys.virginia.edu/7010/CM_04_HamiltonsPrinciple.ht ml (accessed May 03, 2021).

[26] '(No Title)'. http://www.unishivaji.ac.in/uploads/distedu/SIM2013/M. Sc. Maths Classifical Mechanics/Chapter III.pdf (accessed May 03, 2021).

[27] R. S. Crespo, S. Kaczmarczyk, P. Picton, and H. Su, 'Modelling and simulation of a stationary high-rise elevator system to predict the dynamic interactions between its components', *Int. J. Mech. Sci.*, vol. 137, no. October 2017, pp. 24–45, 2018, doi: 10.1016/j.ijmecsci.2018.01.011.

[28] R. S. Crespo, S. Kaczmarczyk, P. Picton, and H. Su, 'Modelling and simulation of a stationary high-rise elevator system to predict the dynamic interactions between its components', *Int. J. Mech. Sci.*, vol. 137, pp. 24–45, Mar. 2018, doi: 10.1016/j.ijmecsci.2018.01.011.

[29] X. Arrasate, S. Kaczmarczyk, G. Almandoz, J. Abete, and I. Isasa, 'MEASUREMENT AND SIMULATION OF MACHINE-BORNE VERTICAL VIBRATION IN ELEVATOR SYSTEMS', 2013.

[30] D. Supervised, K. L. Date, T. S. Fulfillment, T. Requirements, T. Msceng, and D. Engineering, *A Travelling Cable System: Apparatus Development, System Modeling, and Vibration Control*. 2005.

[31] Q. Peng, A. Jiang, H. Yuan, G. Huang, S. He, and S. Li, 'Study on Theoretical Model and Test Method of Vertical Vibration of Elevator Traction System', *Math. Probl. Eng.*, vol. 2020, 2020, doi: 10.1155/2020/8518024.

[32] V. Lubarda, 'The mechanics of belt friction revisited', *Int. J. Mech. Eng. Educ.*, vol. 42, no. 2, pp. 97–112, 2014, doi: 10.7227/IJMEE.0002.

[33] A. Metzger, A. Konyukhov, and K. Schweizerhof, 'Finite Element implementation for the EULER-EYTELWEIN-problem and further use in FEM-simulation of common nautical knots', *PAMM*, vol. 11, no. 1, pp. 249–250, Dec. 2011, doi: 10.1002/pamm.201110116.

[34] S. Kaczmarczyk and P. Andrew, 'The systems analysis and design of lifts (elevators): the models and assumptions appraised', pp. 1–10.

[35] 'APPROVAL SHEET Title of Dissertation: Accurate Simulation of the Dynamics of Elevator Systems'.

[36] 'System and method for damping vibrations in elevator cables', Nov. 2004.

[37] 'Hermite Interpolation - an overview | ScienceDirect Topics'. https://www.sciencedirect.com/topics/mathematics/hermite-interpolation (accessed May 07, 2021).

[38] 'Noise of Polyphase Electric Motors - Jacek F. Gieras, Chong Wang, Joseph Cho Lai - Google Books'. https://books.google.ee/books?hl=en&lr=&id=SUVuBwAAQBAJ&oi=fnd&pg=PP1&dq=J.+F.+Gieras,+C.+Wang,+J.+C.+Lai.+Noise+of+polyphase+Electric+Motors.+Taylor+%26+Francis+Group,+LLC,+2006&ots=D8E4JtbuCc&sig=6sTSXJt2zF9ON4O-BucBgWEPGgw&redir_esc=y#v=onepage&q&f=false (accessed Apr. 05, 2021).

[39] R. H. PARK, 'Two-Reaction Theory of Synchronous Machines: Generalized Method of Analysis-Part I', *Trans. Am. Inst. Electr. Eng.*, vol. 48, no. 3, pp. 716–727, 1929, doi: 10.1109/T-AIEE.1929.5055275.

[40] U. Lugrís, J. L. Escalona, D. Dopico, and J. Cuadrado, 'Efficient and accurate simulation of the rope–sheave interaction in weight-lifting machines', *Proc. Inst. Mech. Eng. Part K J. Multi-body Dyn.*, vol. 225, no. 4, pp. 331–343, Dec. 2011, doi: 10.1177/1464419311403224.

[41] J. L. Escalona, G. Orzechowski, and A. M. Mikkola, 'Flexible multibody modeling of reeving systems including transverse vibrations', *Multibody Syst. Dyn.*, vol. 44, no. 2, pp. 107–133, Oct. 2018, doi: 10.1007/s11044-018-9619-6.

[42] 'Vibration analysis of elevator ropes | Request PDF'. https://www.researchgate.net/publication/295723956_Vibration_analysis_of_elevator_ropes (accessed Apr. 29, 2021).

[43] D. Baimel, J. Belikov, J. M. Guerrero, and Y. Levron, 'Dynamic Modeling of Networks, Microgrids, and Renewable Sources in the dq0 Reference Frame: A Survey', *IEEE Access*, vol. 5, pp. 21323–21335, 2017, doi: 10.1109/ACCESS.2017.2758523.

[44] '(PDF) Variable Speed Drives in Lift Systems'. https://www.researchgate.net/publication/279193580_Variable_Speed_Drives_in_Lift_Systems (accessed Mar. 27, 2021).

[45] KONE, 'Kone MONOSPACE 500 configuration', 2019.

[46] K. Monospace, 'A BRAND-NEW ELEVATOR FOR YOUR BUILDING AN INVESTMENT IN YOUR BUILDING ' S FUTURE'.

[47] KONE, 'Architectural Planning Guide Kone Offers Solutions for Each Phase of the Building'sLife Cycle'.

[48] P. Guide, 'KONE MonoSpace700', no. 8.

[49] 'Construction & Architecture Update'. https://online.fliphtml5.com/dysdc/wdpi/?fbclid=IwAR05liP1-tqa7H5CSQi8p8t8MNxlLCmrewkA12GIzDf9FeY-QwrzpJAbHTI#p=26 (accessed Apr. 30, 2021).

[50] W. J. Karplus, 'SPECTRUM OF MATHEMATICAL MODELING AND SYSTEMS

SIMULATION.', in *ACM SIGSIM Simulation Digest*, Sep. 1977, vol. 9, no. 1, pp. 5–13, doi: 10.1145/1102505.1102522.

[51] '9 Using Modeling and Simulation in Test Design and Evaluation | Statistics, Testing, and Defense Acquisition: New Approaches and Methodological Improvements | The National Academies Press'. https://www.nap.edu/read/6037/chapter/11 (accessed Apr. 05, 2021).

[52] 'Modeling and Simulation'. http://home.ubalt.edu/ntsbarsh/simulation/sim.htm (accessed Apr. 05, 2021).

[53] 'Simcenter System Simulation | Siemens Digital Industries Software'. https://www.plm.automation.siemens.com/global/en/products/simcenter/simcenter-system-simulation.html (accessed Apr. 05, 2021).

[54] D. SimulationX, 'SimulationX: Simulation Software for Modeling | ESI ITI'. https://www.simulationx.com/simulation-software.html (accessed Nov. 08, 2020).

[55] 'System Simulation Software'. https://www.esi-group.com/products/system-simulation (accessed Apr. 05, 2021).

[56] M. Description, 'Modelica Language — Modelica Association'. https://www.modelica.org/modelicalanguage (accessed Nov. 08, 2020).

[57] 'Systems Modeling and Simulation Software | Modelon'. https://www.modelon.com/ (accessed Feb. 25, 2021).

[58] 'Why Simulation: Possibilities, Advantages, Benefits | ESI ITI'. https://www.simulationx.com/system-simulation/benefits.html (accessed Mar. 27, 2021).

[59] J. K. Hosam Fathy, Z. S. Filipi, J. Hagena, J. L. Stein, and H. K. Fathy, 'Review of hardware-in-the-loop simulation and its prospects in the automotive area United States Downloaded From: https://www.spiedigitallibrary.org/conference-proceedings-of-spie on 18 Oct 2020 Terms of Use: https://www.spiedigitallibrary.org/terms-of-use Review of Hardware-in-the-Loop Simulation and Its Prospects in the Automotive Area', *spiedigitallibrary.org*, no. 22, 2006, doi: 10.1117/12.667794.

[60] 'Hardware-in-the-Loop (HIL) Simulation - MATLAB & Simulink'. https://es.mathworks.com/discovery/hardware-in-the-loop-hil.html (accessed Jan. 01, 2021).

[61] S. Köhl and D. Jegminat, 'How to do hardware-in - The-loop simulation right', 2005, doi: 10.4271/2005-01-1657.

[62] B. Scherer and G. Horváth, 'Microcontroller tracing in Hardware in the Loop tests: Integrating trace port measurement capability into NI VeriStand', *Proc. 2014 15th Int. Carpathian Control Conf. ICCC 2014*, no. October, pp. 522–526, 2014, doi:

10.1109/CarpathianCC.2014.6843660.

[63] 'Simulation - Home'. https://www.systemstech.com/research-engineering/ground-vehicle-engineering-2/ (accessed Apr. 05, 2021).

[64] 'Hardware in the loop | HIL simulation | OPAL-RT'. https://www.opal-rt.com/hardware-in-the-loop/ (accessed Apr. 05, 2021).

[65] 'Automotive Hardware-in-the-Loop (HIL) Test - National Instruments - NI'. https://www.ni.com/en-us/innovations/automotive/hardware-in-the-loop.html (accessed Apr. 05, 2021).

[66] 'Hardware-in-the-Loop | TAMA Systems India'. https://tama.systems/hardware-in-the-loop (accessed Apr. 05, 2021).

[67] 'Home Page - Typhoon HIL'. https://www.typhoon-hil.com/ (accessed Apr. 05, 2021).

[68] A. Wagener, T. Schulte, P. Waeltermann, and H. Schuette, 'Hardware-in-the-loop test systems for electric motors in advanced powertrain applications', 2007, doi: 10.4271/2007-01-0498.

[69] 'VFDs with integrated PLCs for motion and machine controls: Programming and setup considerations'. https://www.motioncontroltips.com/vfds-with-integrated-plcs-for-motion-and-machine-controls-programming-and-setup-considerations/ (accessed Jan. 27, 2021).

[70] O. Kouhei, M. Shibata, and T. Murakami, 'Motion control for advanced mechatronics', *IEEE/ASME Trans. Mechatronics*, vol. 1, no. 1, pp. 56–67, 1996, doi: 10.1109/3516.491410.

[71] W. K. Chung, L. C. Fu, and T. Kröger, 'Motion control', in *Springer Handbook of Robotics*, Springer International Publishing, 2016, pp. 163–194.

[72] 'SwipeGuide'. https://drives-abb.swipeguide.com/guide/acs580-user-guide/setting-up-your-drive/setting-up-embedded-modbus-rtu (accessed Apr. 05, 2021).

[73] 'ACS580 - Effortless process automation for a broad range of applications - General purpose drives - cover your control and energy savings options wisely (Low voltage AC) | ABB'. https://new.abb.com/drives/low-voltage-ac/general-purpose/acs580 (accessed Apr. 05, 2021).

[74] 'Engineering learning path - Channel'. https://kone.sharepoint.com/portals/hub/_layouts/15/PointPublishing.aspx?app=video&p=c&chid=84083c56-000a-43d8-9633-791b41db4c48&s=0&t=pfb (accessed Feb. 02, 2021).

[75] D. Chenumalla, V. Kishore Garimella, and A. Gangavarapu, 'Modelling and simulation of synchro and synchro-to-digital converter for electrical motor drives', *IET Sci. Meas. Technol.*, vol. 10, no. 1, pp. 58–68, Jan. 2016, doi: 10.1049/iet-

smt.2014.0288.

[76] H. Al Ghossini, T. T. Dang, and S. Duchesne, 'A New Concept for Deeper Integration of Converters and Drives in Electrical Machines: Simulation and Experimental Investigations', *Open Phys.*, vol. 17, no. 1, pp. 809–815, Jan. 2019, doi: 10.1515/phys-2019-0084.

[77] 'Kone EcoDisc | Elevator Wiki | Fandom'. https://elevation.fandom.com/wiki/Kone_EcoDisc#NMX_11 (accessed Jan. 31, 2021).

[78] 'Switched Reluctance Motor Drives: Modeling, Simulation, Analysis, Desi'. https://www.routledge.com/Switched-Reluctance-Motor-Drives-Modeling-Simulation-Analysis-Design/Krishnan/p/book/9780849308383 (accessed Feb. 28, 2021).

[79] 'Encoder vs. Resolver-Based Servo Systems'. Accessed: Feb. 28, 2021. [Online]. Available: www.ormec.com.

[80] I. I. Incze, C. Szabó, and M. Imecs, 'Incremental encoder in electrical drives: Modeling and simulation', *Stud. Comput. Intell.*, vol. 313, pp. 287–300, 2010, doi: 10.1007/978-3-642-15220-7_23.

[81] 'Industrial PC - PC Control for all applications | Beckhoff Sverige'. https://www.beckhoff.com/sv-se/products/ipc/ (accessed Apr. 12, 2021).

[82] 'Industrial Computers | Allen-Bradley'. https://www.rockwellautomation.com/en-dk/products/hardware/allen-bradley/industrial-computers-monitors/industrial-computers.html (accessed Apr. 12, 2021).

[83] 'Industrial PC, Inc. | Industrial Embedded, Rackmount, and Panel PCs'. https://industrialpc.com/ (accessed Apr. 12, 2021).

[84] 'Beckhoff | New Automation Technology | Beckhoff Eesti'. https://www.beckhoff.com/et-ee/index.html (accessed Apr. 05, 2021).

[85] B. C. series Documention of, 'CX51x0', 2020.

[86] 'TwinCAT | Automation software | Beckhoff India'. https://www.beckhoff.com/hi-in/products/automation/twincat/ (accessed Feb. 26, 2021).

[87] 'Jenkins'. https://www.jenkins.io/ (accessed Apr. 05, 2021).

[88] N. Seth and R. Khare, 'ACI (automated Continuous Integration) using Jenkins: Key for successful embedded Software development', Apr. 2016, doi: 10.1109/RAECS.2015.7453279.

[89] J. Hembrink and P.-G. Stenberg, 'Continuous Integration with Jenkins Coaching of Programming Teams (EDA270)', 2013.

[90] 'Jenkins continuous integration cookbook : over 90 recipes to produce great results from Jenkins using pro-level practices, techniques, and solutions - Royal Holloway, University of London'. https://librarysearch.royalholloway.ac.uk/primo-

explore/fulldisplay/44ROY_ALMA_DS5188223770002671/44ROY_VU2 (accessed Mar. 21, 2021).

[91] 'Duvall, Matyas & Glover, Continuous Integration: Improving Software Quality and Reducing Risk | Pearson'. https://www.pearson.com/us/higher-education/program/Duvall-Continuous-Integration-Improving-Software-Quality-and-Reducing-Risk/PGM157751.html (accessed Mar. 21, 2021).

[92] H. Spieker, A. Gotlieb, D. Marijan, and M. Mossige, 'Reinforcement learning for automatic test case prioritization and selection in continuous integration', in *ISSTA 2017 - Proceedings of the 26th ACM SIGSOFT International Symposium on Software Testing and Analysis*, Jul. 2017, pp. 12–22, doi: 10.1145/3092703.3092709.

[93] 'Continuous Integration'. https://www.martinfowler.com/articles/continuousIntegration.html (accessed Mar. 21, 2021).

[94] 'Systems Engineering of Elevators - NECTAR'. http://nectar.northampton.ac.uk/4293/ (accessed Mar. 14, 2021).

[95] 'Simulation model of a gear synchronisation unit for application in a real-time HiL environment - NASA/ADS'. https://ui.adsabs.harvard.edu/abs/2017VSD....55..668K/abstract (accessed Feb. 26, 2021).

[96] 'Two to One Roping (2:1) | Classroom on demand'. https://www.thyssenkruppelevator.com/webapps/classroom-on-demand/LessonViewer.aspx?lesson=16338 (accessed Apr. 29, 2021).

[97] O. V. Kruglikov, 'Low-speed induction motors for directly driven elevator machines', *Russ. Electr. Eng.*, vol. 86, no. 3, pp. 118–124, Mar. 2015, doi: 10.3103/S1068371215030050.

[98] E. L. Carrillo Arroyo, 'MODELING AND SIMULATION OF PERMANENT MAGNET SYNCHRONOUS MOTOR DRIVE SYSTEM'.

[99] 'MULTIPHYSICS SIMULATION BY DESIGN FOR ELECTRICAL MACHINES, POWER ELECTRONICS, AND DRIVES'.

[100] L. Qingyun, J. Tiantian, Y. Chunhuizi, L. Tao, W. Quanxian, and Y. Xiaoliu, 'Research on electromagnetic field simulation of permanent magnet synchronous motor', *J. Softw. Eng.*, vol. 10, no. 1, pp. 99–108, 2016, doi: 10.3923/jse.2016.99.108.

[101] 'Elevators & Escalators - MITSUBISHI ELECTRIC'. https://www.mitsubishielectric.com/elevator/modernization/elevator_index.html (accessed Apr. 29, 2021).

[102] K. Stefan, G. Almandoz, and J. M. Abete, 'The Modelling, Simulation and

Experimental Testing of Vertical Vibrations in an Elevator System with 1:1 Roping Configuration', 2012. Accessed: Apr. 05, 2021. [Online]. Available: https://www.researchgate.net/publication/261759104.

[103] A. O'Dwyer, *Handbook of PI and PID controller tuning rules*. Imperial College Press, 2009.

[104] 'Time domain simulation models for inverter-cable-motor Systems in Electrical drives - IEEE Conference Publication'. https://ieeexplore.ieee.org/document/5279148 (accessed Mar. 02, 2021).

[105] M. S. Zaky, 'A self-tuning PI controller for the speed control of electrical motor drives', *Electr. Power Syst. Res.*, vol. 119, pp. 293–303, Feb. 2015, doi: 10.1016/j.epsr.2014.10.004.

[106] H. Prasad and T. Maity, 'Real-time simulation for performance evaluation of bidirectional quasi z-source inverter based medium voltage drives', *COMPEL - Int. J. Comput. Math. Electr. Electron. Eng.*, vol. 35, no. 3, pp. 1123–1135, May 2016, doi: 10.1108/COMPEL-06-2015-0224.

[107] S. Umashankar, M. Bhalekar, S. Chandra, D. Vijayakumar, and D. P. Kothari, 'Development of a new research platform for electrical drive system modelling for real-time digital simulation applications', *Adv. Power Electron.*, vol. 2013, 2013, doi: 10.1155/2013/719847.

[108] C. Nguyen, 'Bachelor Degree Project Priority automation engineering Evaluating a tool for automatic code generation and configuration of PLC-Applications', 2018. Accessed: Feb. 27, 2021. [Online]. Available: http://urn.kb.se/resolve?urn=urn:nbn:se:lnu:diva-85797.

[109] K. Hee, 'Object-Oriented Modeling, Simulation and Automatic Generation of PLC Ladder Logic', in *Programmable Logic Controller*, InTech, 2010.

[110] C. Y. Cho, Y. Lee, M. Y. Cho, S. Kwon, Y. Shin, and J. Lee, 'An optimal algorithm of the multi-lifting operating simulation for super-tall building construction', *Autom. Constr.*, vol. 35, pp. 595–607, Nov. 2013, doi: 10.1016/j.autcon.2013.01.003.

[111] Z. Yang, P. Iravani, A. Plummer, and M. Pan, 'Investigation of hardware-in-the-loop walking/running test with spring mass system', in *Lecture Notes in Computer Science (including subseries Lecture Notes in Artificial Intelligence and Lecture Notes in Bioinformatics)*, 2017, vol. 10454 LNAI, pp. 126–133, doi: 10.1007/978-3-319-64107-2_11.

[112] A. R. Plummer, 'Model-in-the-Loop Testing', *Proc. Inst. Mech. Eng. Part I J. Syst. Control Eng.*, vol. 220, no. 3, pp. 183–199, May 2006, doi: 10.1243/09596518JSCE207.

[113] A. Shawky, A. Bayoumy, A. Nashar, and M. Elsayed, 'Hardware-in-the-loop

simulation for a small unmanned aerial vehicle', 2016, doi: 10.21608/asat.2015.22923.

[114] A. Soltani and F. Assadian, 'A Hardware-in-the-Loop Facility for Integrated Vehicle Dynamics Control System Design and Validation', *IFAC-PapersOnLine*, vol. 49, no. 21, pp. 32–38, Jan. 2016, doi: 10.1016/j.ifacol.2016.10.507.

[115] O. Tremblay, H. Fortin-Blanchette, R. Gagnon, and Y. Brissette, 'Contribution to stability analysis of power hardware-in-the-loop simulators', *IET Gener. Transm. Distrib.*, vol. 11, no. 12, pp. 3073–3079, Aug. 2017, doi: 10.1049/iet-gtd.2016.1574.

[116] W. Pawlus, F. Liland, N. Nilsen, S. Øydna, G. Hovland, and T. K. Wroldsen, 'Modeling and simulation of a cylinder hoisting system for real-time hardware-in-the-loop testing', *SPE Drill. Complet.*, vol. 32, no. 1, pp. 69–78, Mar. 2017, doi: 10.2118/184406-PA.

[117] R. S. Kaarthik, K. S. Amitkumar, and P. Pillay, 'Emulation of a permanent-magnet synchronous generator in real-time using power hardware-in-the-loop', *IEEE Trans. Transp. Electrif.*, vol. 4, no. 2, pp. 474–482, 2018, doi: 10.1109/TTE.2017.2778149.

[118] D. Hauf, S. Sus, A. Strahilov, and J. Franke, 'Multifunctional use of functional mock-up units for application in production engineering', *Proc. - 2017 IEEE 15th Int. Conf. Ind. Informatics, INDIN 2017*, pp. 1090–1095, 2017, doi: 10.1109/INDIN.2017.8104925.

[119] W. Zeng, Y. Huang, X. Zheng, and W. Zhao, 'Study on engine control software testing based on hardware-in-the-loop simulation platform', in *Lecture Notes in Electrical Engineering*, vol. 486, Springer Verlag, 2019, pp. 995–1014.

[120] E. Breck, S. Cai, E. Nielsen, M. Salib, and D. Sculley, 'What's your ML Test Score? A rubric for ML production systems'.

[121] 'Downloads | Functional Mock-up Interface'. https://fmi-standard.org/downloads/ (accessed Apr. 12, 2021).

[122] 'Testing for Developers- Unit Testing Fundamentals'. https://www.automatetheplanet.com/unit-testing-fundamentals/ (accessed Apr. 12, 2021).

[123] 'Unit Testing - SOFTWARE TESTING Fundamentals'. https://softwaretestingfundamentals.com/unit-testing/ (accessed Apr. 12, 2021).

[124] S. C. Park and M. Chang, 'Hardware-in-the-loop simulation for a production system', *Int. J. Prod. Res.*, vol. 50, no. 8, pp. 2321–2330, Apr. 2012, doi: 10.1080/00207543.2011.575097.

[125] S. Salmelin, S. Vatanen, and H. Tonteri, 'Life Cycle Assessment of an Elevator', *Sustain. Build. Conf. 2002*, p. 157, 2002.

[126] D. Nakazawa *et al.*, 'LATERAL VIBRATION ANALYSIS FOR ELEVATOR COMPENSATION ROPE', 2013.

[127] L. Qiu, Z. Wang, S. Zhang, L. Zhang, and J. Chen, 'A Vibration-Related Design Parameter Optimization Method for High-Speed Elevator Horizontal Vibration Reduction', *Shock Vib.*, vol. 2020, 2020, doi: 10.1155/2020/1269170.

[128] C. Li, C. Hua, J. Qin, and Z. Zhu, 'Research on the Dynamic Characteristics of High-Speed Elevator System', Mar. 2019, pp. 105–109, doi: 10.2991/ice2me-19.2019.23.

[129] S. Watanabe, T. Okawa, D. Nakazawa, and D. Fukui, 'Vertical vibration analysis for elevator compensating sheave', in *Journal of Physics: Conference Series*, 2013, vol. 448, no. 1, doi: 10.1088/1742-6596/448/1/012007.

[130] I. Craciun, M. Ungureanu, and D. Stoicovici, 'An analysis of the oscillatory movements of the suspension ropes for an elevator with parabolic speed modeling and continuous deceleration', in *IOP Conference Series: Materials Science and Engineering*, May 2017, vol. 200, no. 1, p. 012016, doi: 10.1088/1757-899X/200/1/012016.

[131] P. Wolszczak, P. Lonkwic, A. Cunha, G. Litak, and S. Molski, 'Robust optimization and uncertainty quantification in the nonlinear mechanics of an elevator brake system', *Meccanica*, vol. 54, no. 7, pp. 1057–1069, May 2019, doi: 10.1007/s11012-019-00992-7.

[132] M. Otsuki, K. Yoshida, K. Nagata, S. Fujimoto, and T. Nakagawa, 'Experimental study on vibration control for rope-sway of elevator of high-rise building', *Proc. Am. Control Conf.*, vol. 1, pp. 238–243, 2002, doi: 10.1109/ACC.2002.1024810.

[133] S. Watanabe and T. Okawa, 'Vertical vibration of elevator compensating sheave due to brake activation of traction machine', in *Journal of Physics: Conference Series*, Jul. 2018, vol. 1048, no. 1, doi: 10.1088/1742-6596/1048/1/012012.

[134] I. Herrera, H. Su, and S. Kaczmarczyk, 'Investigation into the damping and stiffness characteristics of an elevator car system', in *Applied Mechanics and Materials*, 2010, vol. 24–25, pp. 77–82, doi: 10.4028/www.scientific.net/AMM.24-25.77.

[135] M. Spiryagin and C. Cole, 'Hardware-in-the-loop simulations for railway research', *Vehicle System Dynamics*, vol. 51, no. 4. pp. 497–498, 2013, doi: 10.1080/00423114.2013.777495.

APPENDICES

Appendix 1 Result and properties windows in SimulationX

Figure A1.1 Result window to get the simulation result.
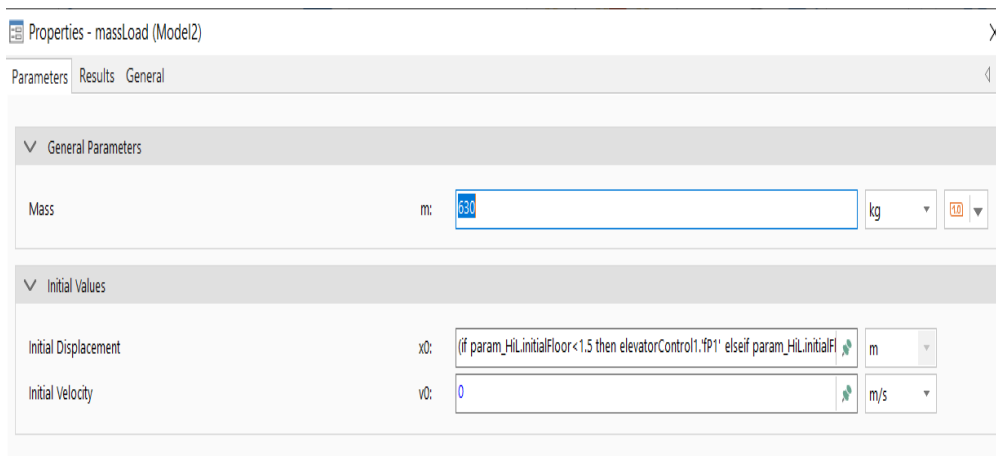
Figure A1.2 Properties and parameter of Carload.

Initial displacement - (if param_HiL.initialFloor<1.5 then elevatorControl1.'fP1'

elseif param_HiL.initialFloor<2.5 then elevatorControl1.'fP2'

elseif param_HiL.initialFloor<3.5 then elevatorControl1.'fP3'

elseif param_HiL.initialFloor<4.5 then elevatorControl1.'fP4'

elseif param_HiL.initialFloor<5.5 then elevatorControl1.'fP5'

elseif param_HiL.initialFloor<6.5 then elevatorControl1.'fP6'

elseif param_HiL.initialFloor<7.5 then elevatorControl1.'fP7'

elseif param_HiL.initialFloor<8.5 then elevatorControl1.'fP8'

else elevatorControl1.'fP9')+0*param_HiL.carSensor
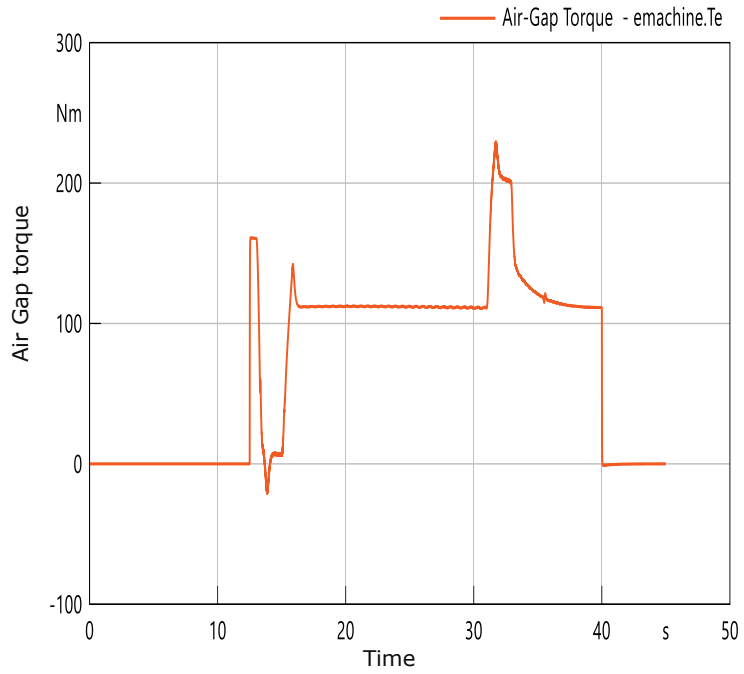
Figure A2.1 Normal Air Gap torque at default value
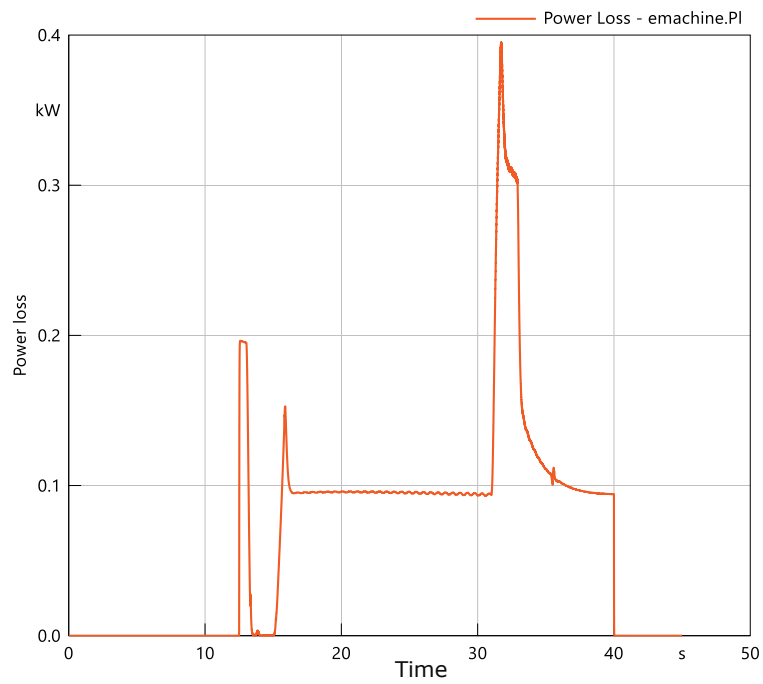
Figure A2.2 (Normal)Power loss at default value

Table 5. Element of Hoisting machine.

S.NO	Parameters	Component in SimulationX
1	Total height of elevator travel/Sh Nominal Torque/nomMT Many General parameters	
2	Motor mounts/Mount motor	
3	Motor/emachine	
4	Pulley Beam	
5	ControllerFMU1	CTRL
6	Car	
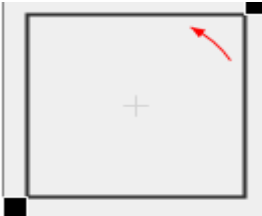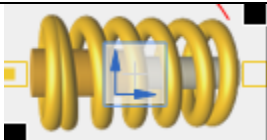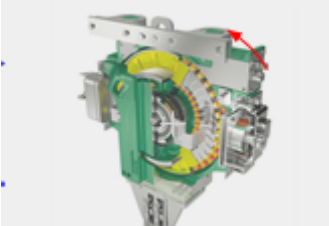
7	Frame Elevator Car	
8	Dummy car/Dummy C.W , there are two dummy has been used one for car and one for C.W	
9	CarMounts	
10	Rope compressor There are two dummy has been used one for car and one for C.W	
11	Guiderail Shoes It has been used both the side(Car and C.W side)	
12	Counterweight/cW	
13	CW -> FrameCW	
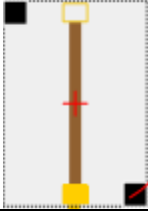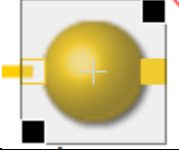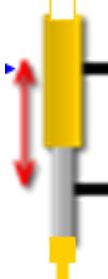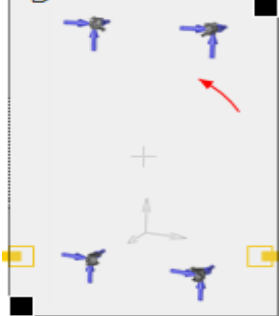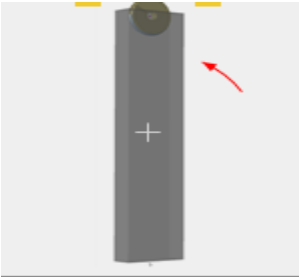
14	ropeFixCar there are two fixing element on both the side of the pulley	
15	Rope element(RopeFixCW, Rope motorCW and RopeMotorsling) has been used for for fixing CW, motor and sling	
16	Rope Compression SpringR	
17	Pulley in 1 D	
18	Release Brake	
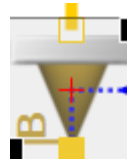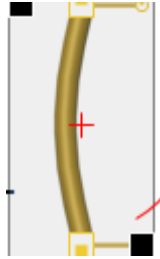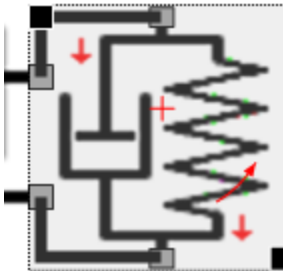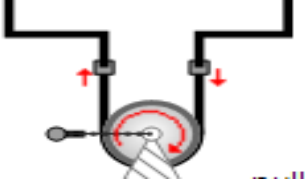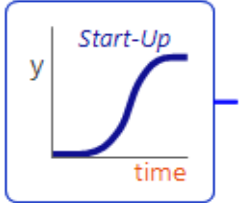
Effect on car vibration due to the cange in mounting motor stiffness.
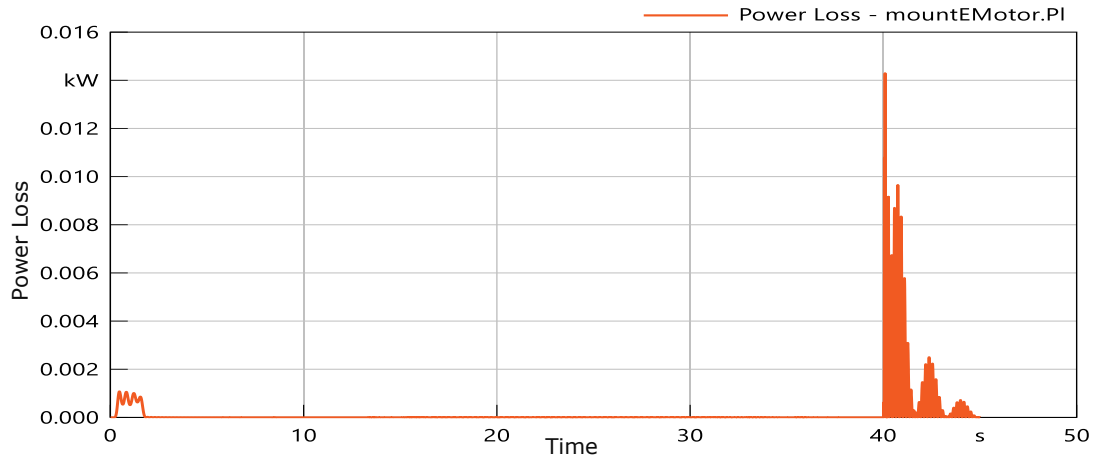
Figure A4.1 Power loss due to mounting motor stiffness at 321 N/mm
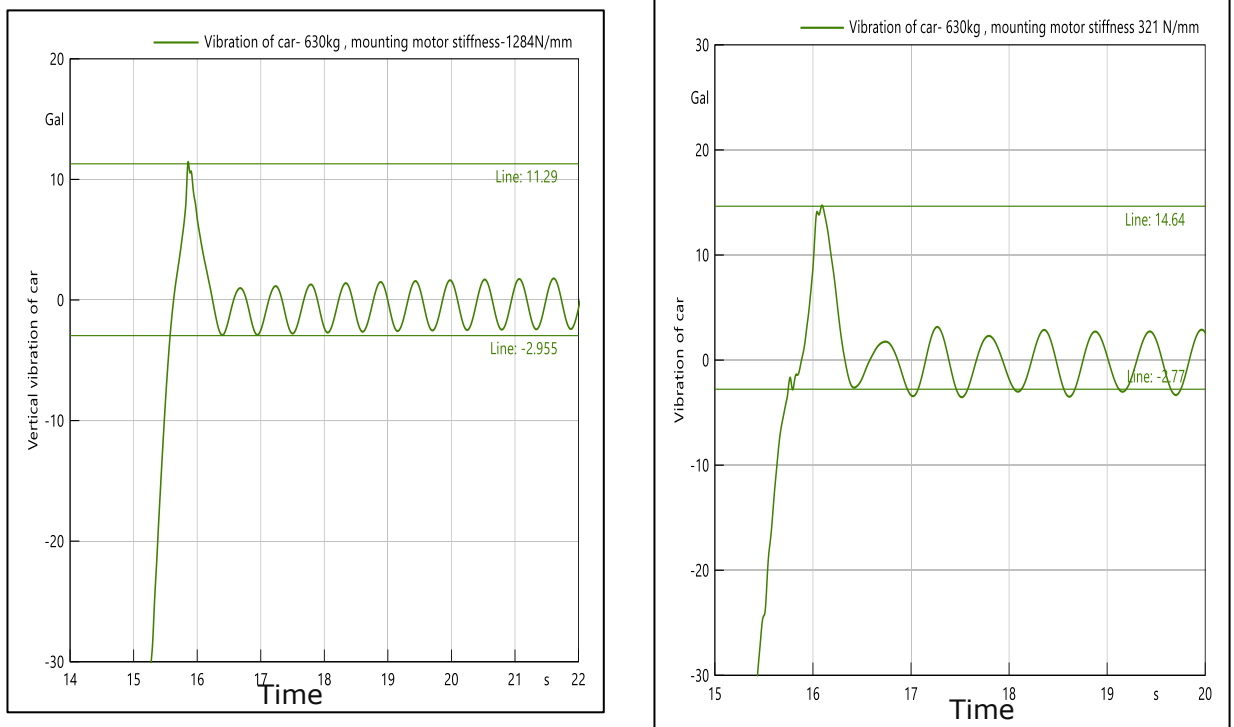
Figure A4.2 Peak to peak value at different mounting motor stiffness (left 321 N/mm, Right 1284 N/mm.

Figure A5.1 Power loss due to car elastic modulus 60,000 N/mm2
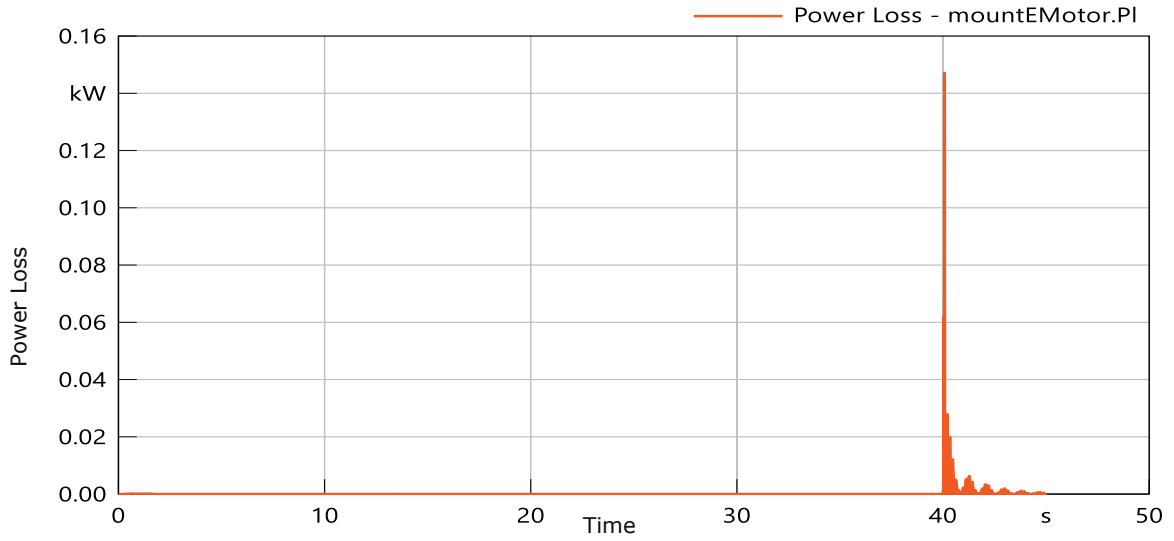
Figure A5.1 Power loss due to car elastic modulus 60,000 N/mm^2.
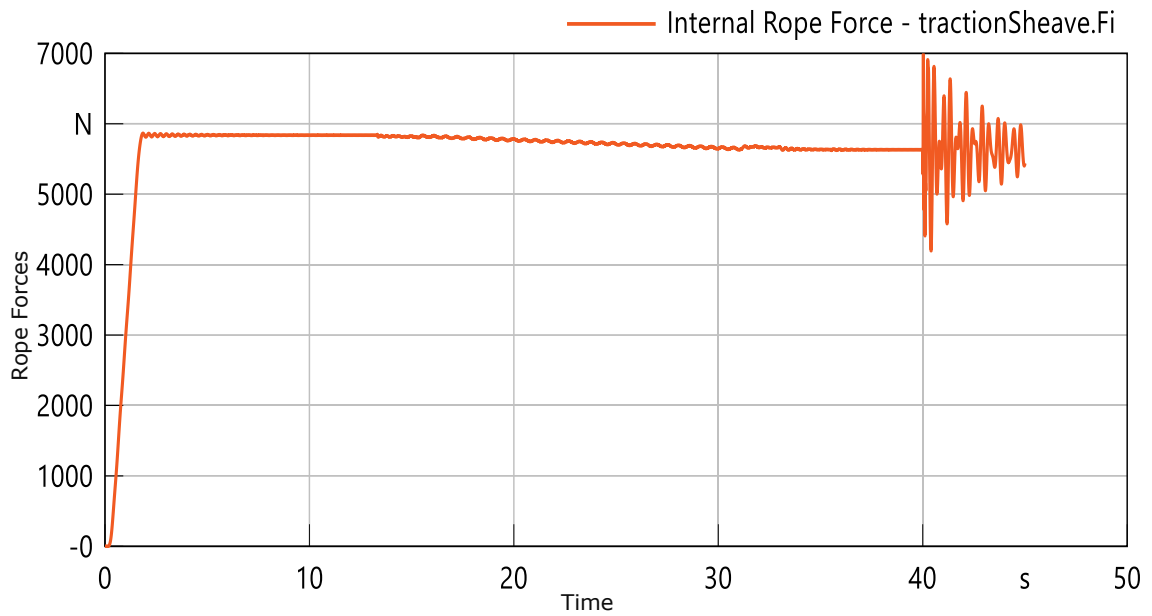
Figure A5.2 Internal Rope force due to car elastic modulus 60,000 N/mm^2.
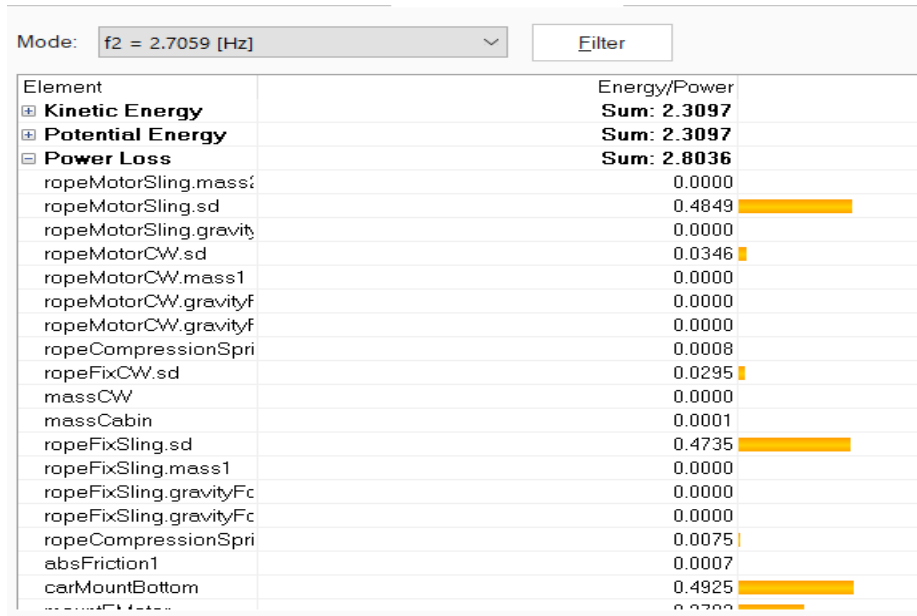
Figure A6.1 FFT value at F2 mode 2.7 Hz
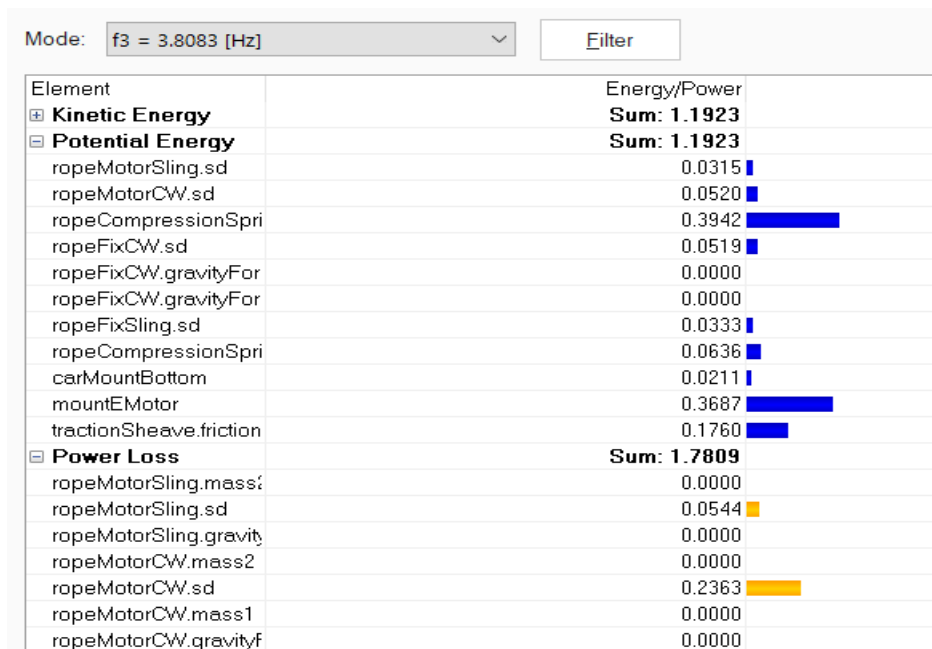
Figure A6.2 FFT value at F3 mode 3.8 Hz.
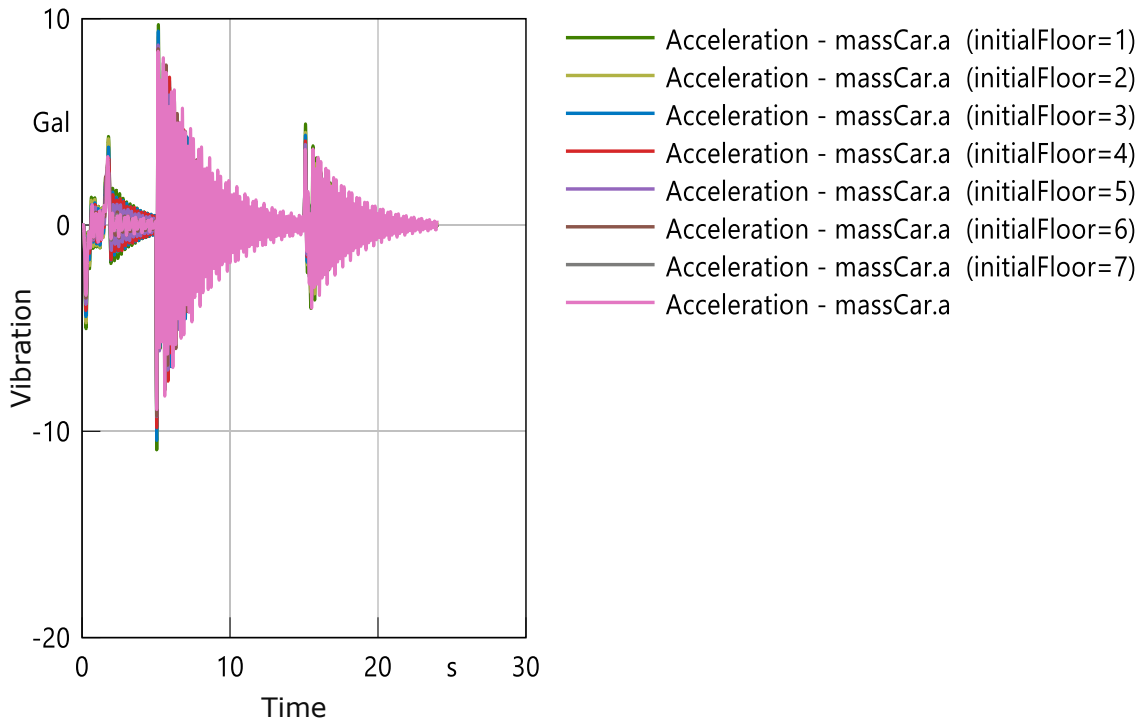
Figure A7.1 Car Vibration at different floor.
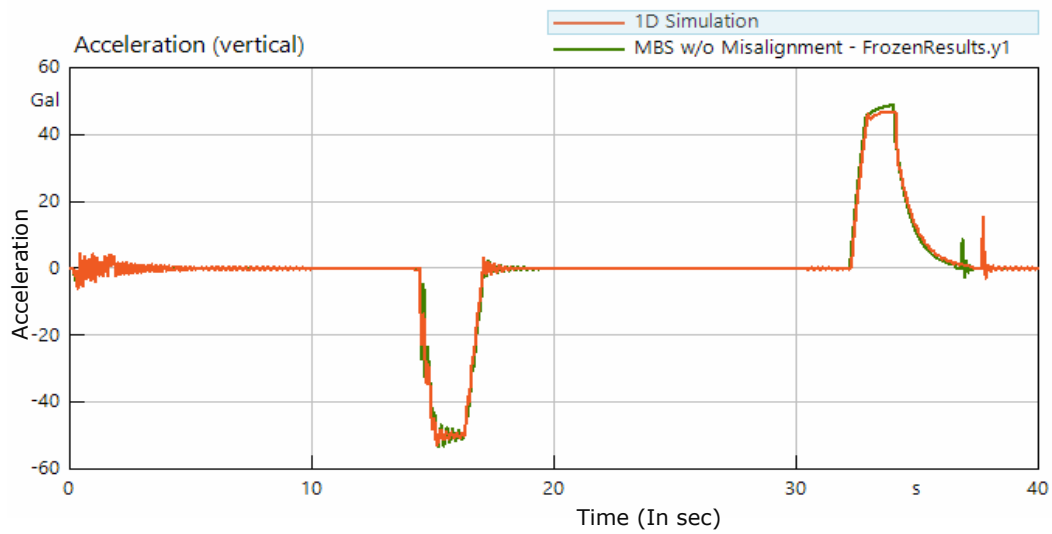
Figure A7.2 Acceleration comparison of different 1D and 3D model.